8-2019

Trout Habitat in an Altered Gravel-Bed River with an Augmented Flow Regime

Jacob B. Stout
Utah State University

TROUT HABITAT IN AN ALTERED GRAVEL-BED RIVER WITH AN AUGMENTED FLOW REGIME

by

Jacob B. Stout

A thesis submitted in partial fulfillment
of the requirements for the degree

of

MASTER OF SCIENCE

in

Watershed Science

Approved:

_____	_____
Peter Wilcock, Ph.D. Major Professor	Patrick Belmont, Ph.D. Committee Member
_____	_____
Jereme Gaeta, Ph.D. Committee Member	Richard S. Inouye, Ph.D. Vice Provost for Graduate Studies

UTAH STATE UNIVERSITY
Logan, Utah

2019

ABSTRACT

Trout Habitat in an Altered Gravel-Bed River with an

Augmented Flow Regime

by

Jacob Stout, Master of Science

Utah State University, 2019

Major Professors: Dr. Peter Wilcock, Dr. Patrick Belmont
Department: Watershed Science

The Diamond Fork River, and it's tributary Sixth Water Creek, has been highly altered both geomorphically and ecologically due to substantial, trans-basin flow augmentation for irrigation starting in the early 1900s. Flows were exceptionally large for 80 years, after which they were reduced in 2004. Larger than natural, minimum instream flow mandates were then imposed in an effort to improve ecosystem health and recreational fishing opportunities. Since the prescription of minimum instream flows, the river channel has undergone further change, most noticeably in the form of narrowing under the different controls for each of the eight distinct process domains that have been identified for the system (Jones, 2018). With the channel change that has occurred over the past decade, it has been suggested that the prescribed instream flow mandates, which augment baseflows, are too large and that key habitat elements, particularly pools, are lacking throughout the river.

We evaluated trout habitat throughout the altered reaches of the Diamond Fork

River and Sixth Water Creek which are still subject to flow augmentation. We used a drift-forage model, also known as a net rate of energy intake (NREI) model, to evaluate the effect of an augment flow regime on trout habitat quality. We found by modeling an array of scenarios that the current summer baseflows of 80 cfs for the lower Diamond Fork and 32 cfs for Sixth Water Creek are less than desirable and that flows less than 40 cfs for the lower Diamond Fork and flows between 20 cfs and 30 cfs for Sixth Water Creek would increase the quality of trout habitat.

We also evaluated the size and number of pools throughout the system and identified that pools are generally lacking both in size and number relative to standard trout requirements and fluvial geomorphic fundamentals. We documented a reduction in channel habitat complexity as the channel narrowed over the last decade. Sediment starvation and the limited number of sediment mobilizing flows were identified as key causes of the channel simplification and loss of pool habitat. Crucial components of future pool formation and maintenance are i) an active, coarse grained, sediment supply and ii) frequent sediment mobilizing flows. If the baseflow regime were to be lowered, we predict that the channel would narrow, which would increase the effectiveness of floods, increase sediment transport, and overall increase pool habitat. This research, as part of a larger, interdisciplinary project, lays the foundation for proposing an instream flow regime for the Diamond Fork River that targets ecological goals identified by stakeholders as well as providing information for future habitat restoration projects.

(170 pages)

PUBLIC ABSTRACT

Trout Habitat in an Altered Gravel-Bed River with an Augmented Flow Regime

Jacob B. Stout

The Diamond Fork River, and it's tributary Sixth Water Creek, has been highly altered in terms of shape, function, and ecologicaly due to large, trans-basin flows additions to the system for irrigation starting in the early 1900s. Flows were exceptionally large for 80 years, after which they were reduced in 2004. Larger than natural flows during the low flow season were then added to the river in an effort to improve ecosystem health and recreational fishing opportunities. Since the prescription additional flow during low flow seasons, the river channel has undergone further change, most noticeably in the form of narrowing. With the channel change that has occurred over the past decade, it has been suggested that the additional flows, which augment baseflows, are too large and that key habitat elements, particularly pools, are lacking throughout the river.

We evaluated trout habitat throughout the altered reaches of the Diamond Fork River and Sixth Water Creek which are still subject to flow additions. We used a model to estimate the number of fish a reach can support at a given flow in order to evaluate which flow produces the highest quality trout habitat. We found that the current summer baseflows of 80 cfs for the lower Diamond Fork and 32 cfs for Sixth Water Creek are less than desirable and that flows less than 40 cfs for the lower Diamond Fork and flows between 20 cfs and 30 cfs for Sixth Water Creek would increase the quality of trout habitat.

We also evaluated the size and number of pools throughout the system and

identified that pools are generally lacking both in size and number relative to standard requirements for trout success. We documented that as the channel narrowed, the number of pools/deep water disappeared. The lack of sediment and the limited number of flows capable of moving sediment were identified as key causes of the channel simplification and loss of pool habitat. Crucial components of future pool formation and maintenance are i) active sediment availability and ii) frequent sediment mobilizing flows. If the baseflow regime were to be lowered, we predict that the channel would narrow, which would increase the effectiveness of floods, increase mobility of sediment, and overall increase pool habitat. This research, as part of a larger, interdisciplinary project, lays the foundation for proposing new flows for the Diamond Fork River that targets ecological goals identified by stakeholders as well as providing information for future habitat restoration projects.

ACKNOWLEDGMENTS

This work was funded by the Utah Reclamation, Mitigation and Conservation Commission (UMRCC), who engaged with Utah State University (USU) scientists in order to research the altered flow regime of Diamond Fork River system. This research project would not have been possible without their support.

I would like to thank my co-advisors, Dr. Peter Wilcock and Dr. Patrick Belmont, for their patience, support, and guidance throughout my time at USU. They taught me to never stop asking questions and to always think critically. Their insight and expertise has been a valued resource and has been an important factor in developing my skills as a scientist, hydrologist, and geomorphologist.

I would also like to thank the other members of the Diamond Fork project – Dr. Jereme Gaeta, Dr. Edd Hammill, Dr. Trisha Atwood, Jabari Jones, Josh Epperly, Hannah Moore, and the many field and lab technicians. The countless hours of collaborative research across the multiple disciplines within the project has been inspiring and motivating. I am particularly grateful for Jabari, with whom I spent countless hours in the field picking up rocks, wading through floods, and discussing the dynamics of the Diamond Fork. His perspective to both things of science and the world were greatly appreciated.

Lastly, I would like to thank the Belmont Lab, my friends, and my family for all the love and support. To my family, thank you for instilling in me a love for the outdoors and a desire to understand and better the world. To Sidney, thank you for your great support and encouragement.

Jacob B. Stout

CONTENTS

Page

LIST OF TABLES

LIST OF FIGURES

Figure Page

CHAPTER 1

INTRODUCTION

The health of a river ecosystem depends on the interactions of many factors such as hydrology, geomorphology, water quality, biology, and connectivity (Annear et al. 2004). Hydrology, or the flow regime, is considered the master variable because it directly affects all other factors in the riverine system (Poff et al. 1997). Thus, alterations in flow regime are often a key factor when evaluating river ecosystems and management. Water diversions to or from a stream can have large impacts on the other components of the system in the form of channel adjustment, degraded ecology, and loss of biodiversity (Lane 1955; Richter et al. 1997; Pringle et al., 2000; Richter et al., 2003; Postel and Carpenter 1997; Naiman et al. 2002). As the channel adjusts to changes in flow and sediment, important instream habitat features are influenced.

Considerable research has been conducted on those elements of a site's hydrologic record that are needed to maintain or re-establish essential ecological functions (Poff et al. 2010, Arthington et al. 2006, Richter et al. 2003). Those critical characteristics of the flow regime include timing, magnitude, frequency, and duration of flows. Thus, alterations in one or more of those characteristics may influence ecological processes and interactions (Lytle and Poff, 2004). In some cases, restoration of a natural flow regime may be difficult or impossible, due to water storage requirements, water rights, and climate change. Other times, restoring a natural flow regime may be unrealistic or undesirable due to different, possibly conflicting, objectives involved in water management decisions. In such cases, improving ecosystem health through the implementation of instream flow mandates can be oriented towards meeting specific

ecological goals as identified by stakeholders instead of returning to natural conditions. To achieve this, there is a need to create and understand the relations between flow alterations and ecological responses (Poff et al. 2010).

There are well over 200 methods to evaluate the design of instream flows (Dyson et al., 2003; Tharme, 2003). Integral to the Instream Flow Incremental Methodology (IFIM) are habitat simulation models, which link the physical elements of river habitat, such as depth, velocity, substrate, and cover (Tonina and Jorde, 2013), to ecological requirements by quantifying the weighted usable area (WUA) for a single species. Drift-feeding salmonids are often the target of such methods. Although WUA can be used to evaluate how instream habitat changes with flow, it neglects the effects of flow on basal resources (i.e., primary production, macroinvertebrate drift) and how the flux of energy (drift) is delivered to available habitat (Rosenfeld and Ptolemy, 2012).

Drift-forage models, also known as net rate of energy intake (NREI) models simulate interactions of depth, velocity, temperature, and energy flux (drift). These models calculate the spatial distribution of energy for a drift-feeding salmonid as well as a reach carrying capacity. Hayes et al. (2016) found that NREI models are better at evaluating the instream flow requirements for drift-feeding salmonids because they provide more realistic representations of stream habitat dynamics than WUA methods, which tend to underestimate flow needs.

Pools are important habitat features for trout, crucial to the success of multiple life stages (Hickman and Raleigh, 1982). Many studies have shown trout preference for deeper channel units (Rosenfeld and Boss, 2001; Glova, 1984; Heggenes et al., 1991; Lonzarich and Quinn 1995) and that trout populations can be limited by the narrow

stream width and lack of deep pools (Harig and Fausch, 2002). Pools favor trout growth via low swimming costs associated with slower velocities. When adjacent or downstream of riffles, pools offer high energy consumption via nearby food delivery (Rosenfeld and Boss, 2001). Understanding crucial elements of flow convergence (Thompson, 2011) and sediment supply constraints (Buffington et al., 2002) and how they play a role in pool maintenance and formation, is crucial for determining the long term trout habitat availability in a stream.

The Diamond Fork River and its tributary, Sixth Water Creek, are mountainous streams located in central Utah, have been highly altered both geomorphically and ecologically due to substantial, trans-basin flow augmentation for irrigation starting in the early 1900s. Exceptionally large flows of 200-500+cfs were delivered from Strawberry Reservoir to Sixth Water Creek and Diamond Fork River during the irrigation season for nearly 80 years. In the 1990s and early 2000s, a series of tunnels and pipelines were constructed so that all irrigation flows could bypass the river. In 2004, with the completion of the irrigation infrastructure, larger than natural, minimum instream flow mandates were then imposed in an effort to improve ecosystem health and recreational fishing opportunities. These flows were approximately 3-4 times larger than the natural baseflow of these streams. Since the prescription of minimum instream flows, the river channel has undergone further change, most noticeably in the form of narrowing, especially in the partially confined and unconfined reaches of the river (Jones, 2018). With the channel change that has occurred over the past decade, it has been suggested that the prescribed instream flow mandates, which augment baseflows, are too large and that key habitat elements, particularly pools, are lacking throughout the river.

In this thesis, we analyze the interactions of flow and sediment and their effect on the habitat quality throughout the Diamond Fork River and its tributary, Sixth Water Creek. This research is part of a broader, interdisciplinary project intended to provide recommendations for a revised instream flow regime that targets ecological goals identified by stakeholders. Re-establishing the natural flow regime has been determined to be undesirable because of the intense channel alteration that has taken place, and the desire for a medium size fishery, which are relatively uncommon in Utah. This study is therefore novel in its approach, diverging from current practices focused on restoring a natural flow regime, and instead focusing on changing the flow to meet specific ecological goals.

In Chapter 2, we evaluate the augmented baseflow regime of the Diamond Fork system and its effect on habitat quality for trout through the use of a drift-forage, or NREI, model. This model was used to 1) test the hypothesis that the current instream flow mandates are too high for supporting a healthy trout population and 2) identify a range of viable flows at which the carrying capacity for trout is maximized.

In Chapter 3, we evaluate the hydraulic and geomorphic conditions of trout habitat and how they differ throughout the eight process domains that have been delineated for the Diamond Fork system. We use a combination of field mapping techniques, statistical analysis with Random Forest multivariate regression modeling, and aerial image analysis to quantify and describe trout habitat. In particular, we investigate 1) the size and distribution of pools throughout the system and 2) the roles of flow and sediment in promoting pool formation and maintenance.

References

Annear, T., Chisholm, I., Beecher, H., Locke, A., Aarrestad, P., Burkhart, N., Coomer, C., Estes, C., Hunt, J., Jacobson, R. and Jobsis, G. (2004). *Instream flows for riverine resource stewardship*. Revised edition. Instream Flow Council, Cheyenne, Wyoming.

Arthington, A. H., Bunn, S. E., Poff, N. L., & Naiman, R. J. (2006). The challenge of providing environmental flow rules to sustain river ecosystems. *Ecological applications*, *16*(4), 1311-1318.

Buffington, J. M., Lisle, T. E., Woodsmith, R. D., & Hilton, S. (2002). Controls on the size and occurrence of pools in coarse-grained forest rivers. *River Research and Applications*, *18*(6), 507-531.

Dyson, M., Bergkamp, G., & Scanlon, J. (2003). Flow: the essentials of environmental flows. *IUCN, Gland, Switzerland and Cambridge, UK*, 20-87.

Glova, G. J. (1984). Management implications of the distribution and diet of sympatric populations of juvenile coho salmon and coastal cutthroat trout in small streams in British Columbia, Canada. *The Progressive Fish-Culturist*, *46*(4), 269-277.

Harig, A. L., & Fausch, K. D. (2002). Minimum habitat requirements for establishing translocated cutthroat trout populations. *Ecological Applications*, *12*(2), 535-551.

Hayes, J. W., Goodwin, E., Shearer, K. A., Hay, J., & Kelly, L. (2016). Can weighted useable area predict flow requirements of drift-feeding salmonids? Comparison with a net rate of energy intake model incorporating drift–flow processes. *Transactions of the American Fisheries Society*, *145*(3), 589-609.

Heggenes, J., Northcote, T. G., & Peter, A. (1991). Seasonal habitat selection and preferences by cutthroat trout (Oncorhynchus clarki) in a small coastal stream. *Canadian Journal of Fisheries and Aquatic Sciences*, *48*(8), 1364-1370.

Hickman, T. J., & Raleigh, R. F. (1982). *Habitat suitability index models: cutthroat trout* (No. 82/10.5). US Fish and Wildlife Service.

Jones, Jabari C., "Historical Channel Change Caused by a Century of Flow Alteration on Sixth Water Creek and Diamond Fork River, UT" (2018). *All Graduate Theses and Dissertations*. 7353.
https://digitalcommons.usu.edu/etd/7353

Lane, E. W. (1955). Importance of fluvial morphology in hydraulic engineering. *Proceedings (American Society of Civil Engineers); v. 81, paper no. 745*.

Lonzarich, D. G., & Quinn, T. P. (1995). Experimental evidence for the effect of depth and structure on the distribution, growth, and survival of stream fishes. *Canadian Journal of Zoology*, *73*(12), 2223-2230.

Lytle, D. A., & Poff, N. L. (2004). Adaptation to natural flow regimes. *Trends in ecology & evolution*, *19*(2), 94-100.

Naiman, R. J., Bunn, S. E., Nilsson, C., Petts, G. E., Pinay, G., & Thompson, L. C. (2002). Legitimizing fluvial ecosystems as users of water: an overview. *Environmental management*, *30*(4), 455-467.

Poff, N. L., Allan, J. D., Bain, M. B., Karr, J. R., Prestegaard, K. L., Richter, B. D., ... & Stromberg, J. C. (1997). The natural flow regime. *BioScience*, *47*(11), 769-784.

Poff, N. L., & Zimmerman, J. K. (2010). Ecological responses to altered flow regimes: a literature review to inform the science and management of environmental flows. *Freshwater Biology*, *55*(1), 194-205.

Postel, S., & Carpenter, S. (1997). Freshwater ecosystem services. *Nature's services: Societal dependence on natural ecosystems*, 195.

Pringle, C. M., Freeman, M. C., & Freeman, B. J. (2000). Regional effects of hydrologic alterations on riverine macrobiota in the new world: tropical-temperate comparisons: the massive scope of large dams and other hydrologic modifications in the temperate New World has resulted in distinct regional trends of biotic impoverishment. While neotropical rivers have fewer dams and limited data upon which to make regional generalizations, they are ecologically vulnerable to increasing hydropower development and biotic patterns are emerging. *AIBS Bulletin*, *50*(9), 807-823.

Richter, B., Baumgartner, J., Wigington, R., & Braun, D. (1997). How much water does a river need?. *Freshwater biology*, *37*(1), 231-249.

Richter, B. D., Mathews, R., Harrison, D. L., & Wigington, R. (2003). Ecologically sustainable water management: managing river flows for ecological integrity. *Ecological applications*, *13*(1), 206-224.

Rosenfeld, J. S., & Boss, S. (2001). Fitness consequences of habitat use for juvenile cutthroat trout: energetic costs and benefits in pools and riffles. *Canadian Journal of Fisheries and Aquatic Sciences*, *58*(3), 585-593.

Rosenfeld, J. S., & Ptolemy, R. (2012). Modelling available habitat versus available energy flux: do PHABSIM applications that neglect prey abundance underestimate optimal flows for juvenile salmonids?. *Canadian journal of fisheries and aquatic sciences*, *69*(12), 1920-1934.

Tharme, R. E. (2003). A global perspective on environmental flow assessment: emerging trends in the development and application of environmental flow methodologies for rivers. *River research and applications*, *19*(5-6), 397-441.

Thompson, D. M. (2011). The velocity-reversal hypothesis revisited. *Progress in Physical Geography*, *35*(1), 123-132.

Tonina, D., & Jorde, K. (2013). Hydraulic modelling approaches for ecohydraulic studies: 3D, 2D, 1D and non-numerical models. *Ecohydraulics: An integrated approach*, 31-74.

CHAPTER 2

USE OF A DRIFT-FORAGE MODEL TO EVALUATE AN AUGMENTED BASEFLOW REGIME AND ITS EFFECTS ON AVAILABLE TROUT HABITAT

2.1 Introduction

Water resources development for hydropower, irrigated agriculture, industry, and domestic use often causes adverse impact on riverine ecosystems through the alteration of the magnitude, timing, frequency, duration and predictability of natural flow regimes (Rosenberg et al., 2000; Poff et al., 1997). There have been many studies that show that organisms have evolved to depend and thrive within the patterns of temporal variation of the natural flow regime (Poff et al., 1997; Richter et al., 1996; Lytle and Poff, 2004, and references therein). As flows diverge from their natural regime, ecological degradation and loss of biological diversity become an increasing concern (Poff et al., 1997; Bunn and Arthington, 2002; Lloyd et al., 2003; Poff and Zimmerman, 2010). It is now widely accepted, and seen as beneficial to society, that rivers need allocated water that either restores or mimics the natural flow regime in order to support important environmental needs (Arthington et al., 2006; Naiman et al., 2002; Postel and Richter, 2003; Petts, 2009).

In the late 1940's, methods designed to support fish populations appeared in the form of minimum in-stream flows (Arthington et al., 2006). Increasing concern about the adverse environmental impacts produced by flow alterations led to the science of instream flows (Penaz et al., 1968; Gill, 1971; Davies et al., 1975; Armitage, 1976; Ward, 1976; Hynes 1970; Stalnaker, 1994; Orsborn and Allman, 1976; Petts, 2009). Instream

flows, also known as environmental flows or e-flows, were generally based on the professional judgement of scientists and engineers up until the late 1970's (Fraser, 1972; Petts, 2009). Subsequent environmental flow research has led to over 200 methods for specifying instream flows and can be grouped into four categories: hydrological rules, hydraulic rating methods, habitat simulation methods, and holistic methods (Dyson et al. 2003; Tharme 2003). Of these four categories, habitat simulation methods have been widely applied for estimating instream flow requirements for single species of fish or invertebrates.

Since the development of the instream flow incremental methodology (IFIM) framework in the 1970s, hydraulic-habitat simulation modeling, particularly the Physical Habitat Simulation Model (PHABSIM), has become the most widely used and accepted way to determine flow requirements for maintaining and improving fish populations (Stalnaker et al. 1995; Tharme 1996; Dunbar et al. 1998; Tharme 2003; Annear et al. 2004). These models combine hydraulic models with habitat suitability curves (HSC), which are developed by observing fish occupancy relative to physical habitat variables (e.g., water depth, velocity, substrate, etc.). These curves define the weighted usable area (WUA) of habitat at a given flow. These types of models are limited by assuming that physical habitat alone predicts habitat selection, especially for drift feeding fishes (Hayes et al. 2016). There have been many critiques surrounding the use of WUA, as it is often misinterpreted as an index of fish abundance instead of habitat availability (Mathur et al., 1985; Shirvel, 1986; Orth, 1987; Scott and Shirvel, 1987). Although WUA can be used to evaluate how habitat changes with flow, it neglects the effects of flow on basal resources and how the flux of energy (drift) is delivered to available habitat (Rosenfeld and

Ptolemy, 2012).

Drift-foraging models extend instream flow predictions by integrating the available physical habitat (velocity and depth) with prey abundance (drift) (Anderson et. al., 2006; Rosenfeld et al., 2014). Drift-foraging models estimate the gross rate of energy intake of a fish as well as the energy expended due to swimming, in order to calculate an estimated net rate of energy intake (NREI) for fish at given locations within a stream. Originally, drift-foraging models were created to better understand habitat selection of drift-feeding fish (Fausch, 1984; Hughes and Dill, 1990). These models were quickly recognized for their potential applications in evaluating stream habitat quality (Rosenfeld et al. 2014). Studies such as Jenkins and Keeley (2010) and Urabe et al. (2010) showed positive correlations between predicted NREI and observed fish biomass. These studies suggested that NREI models are suitable for evaluating the habitat quality of drift-feeding fish.

Hayes et al. (2007) developed a drift-foraging, or NREI, model combining hydraulic and drift dynamics to estimate spatially explicit NREI values within a reach and, with an estimate of territory size, fish carrying capacity. Their model, referred to hereafter as the Hayes NREI model, provides a platform to estimate habitat selection and carrying capacity and to evaluate how those are affected by changes in flow, temperature and prey availability. The model uses the depth and velocity outputs from a 2D hydraulic model as inputs to a stream tubes model; which divides flow vertically and laterally into tubes of equal discharge separated by longitudinal cross sections. This three-dimensional simulation of the flow field is used to model the spatial distribution of drift, a fish's ability to capture prey, and the energy required to maintain a foraging location; resulting

in more biologically realistic outputs of NREI and carrying capacity. Rosenfeld et al. (2014) argued that the Hayes NREI model was the most comprehensive drift-forage model to date. Wall et al. (2015) used this approach to evaluate the habitat of steelhead (*Oncorhynchus mykiss*) as part of the Columbia River Habitat Monitoring Program (CHaMP). Due to model complexity, they used the assumption that there was uniform drift density throughout the reach. They did not find a correlation between NREI and fish biomass as did Jenkins and Keeley (2010) and Urabe et al. (2010). However, they did observe a positive correlation between predicted carrying capacity and the observed fish densities. Although there was a positive correlation, the Hayes NREI model over predicted carrying capacity when compared to observed fish density. They attributed this to the likelihood of under recruitment of steelhead and argued that carrying capacity provides a useful habitat metric. Jensen (2017) used a modified version of the Hayes NREI model, employing a 3D grid of velocities and depths instead of stream tubes, in order to evaluate a system with an abundant population of Bonneville Cutthroat Trout. Her results indicated that the NREI model predicted more fish within a reach than observed, consistent with the results of Wall et al. (2015). She concluded that the Hayes NREI model was useful in predicting fish locations as well as evaluating the potential carrying capacity of a reach.

In a study comparing a process based drift-foraging model to a traditional hydraulic-habitat model (RHYHABSIM, River Hydraulics and Habitat Simulation), Hayes et al. (2016) evaluated the baseflow regime of a New Zealand river to test which method produced the most biologically realistic instream flow predictions. They found that the traditional WUA-flow relations tended to underestimate the flow needs for drift-

feeding salmonids. As part of their analysis, they modeled drift with scenarios of constant drift density and flow-varying drift density. Constant drift density scenarios produced asymptotic or linear curves with only modest increase in fish number with flow. Flow-varying drift produced more pronounced, non-linear logistic-type curves indicating that the number of trout was small at the flow with maximum WUA and greatly increased at higher flows. The NREI model showed that predicting beneficial instream flows for drift feeding salmonids is far more complex than can be represented by WUA-flow relations. Specifically, WUA-flow analyses cannot capture the interaction between available energy flux (drift) and physical habitat (depth, velocity, temperature). They identified drift as a key component supporting the accuracy and applicability of the NREI model. Where WUA-flow relations are often used to identify a single optimum discharge, they argue that NREI is best used to select a range of flows that produce the greatest potential carrying capacity and that the effects of flow are best addressed as relative, not absolute, with regards to the change in fish abundance (i.e., percent change in carrying capacity). They concluded that the use of an NREI model produced more biologically realistic results and urged that the principles and predictions from drift-foraging models be used in the assessment of instream flow needs for drift-feeding fish.

The Diamond Fork River and its tributary, Sixth Water Creek, have been subject to flow alteration since the early 1900s. Trans-basin flows of 200 – 500 cfs were introduced throughout the irrigation season to Sixth Water Creek and routed through lower Diamond Fork to provide agricultural irrigation supply along the Wasatch Front in Utah. These augmented flows exceeded most natural floods and caused extensive channel change in the form of incision in Sixth Water Creek and active channel migration on

lower Diamond Fork. In 1996 and 2004, infrastructure was completed to have diversion flows completely bypass the river. In an effort to mitigate the effects of the irrigation flows, minimum instream flows about 3-4 times larger than natural baseflows were prescribed in the hopes of maximizing the amount of available fish habitat. Since 2004, mandated base flows on the lower Diamond Fork River are 80 cfs in summer and 60 cfs in winter. Mandated base flows on Sixth Water Creek are 32 cfs in summer and 25 cfs in winter. Since removal of the full trans-basin diversion flows and implementation of base flows, Sixth Water Creek has experienced minimal changes as the channel from the 20th century has largely remained intact due to an exhausted sediment supply. The lower Diamond Fork on the other hand has narrowed considerably and increased in sinuosity as alluvial deposits from the trans-basin diversions era have been reworked.

To evaluate the effect of baseflow regime on the trout population, we use a net rate of energy intake (NREI) model to predict trout carrying capacity within two reaches of the Diamond Fork Watershed. Bonneville cutthroat trout (*Oncorhynchus clarkii utah*) and brown trout (*Salmo trutta*) are the two major sport fishes of concern within this watershed. Like other streams, brown trout dominate the lower portions of the river while the cutthroat trout are present in the headwaters (Raleigh et al. 1984). We modeled one reach in Sixth Water Creek for cutthroat trout, and another reach in the lower Diamond Fork for brown trout. For model simplicity, and for lack of data to the contrary, we assume spatially-uniform, flow-constant drift. We model an array of scenarios to constrain the variation in carrying capacity with fish size, discharge, drift density, and temperature change. We use the model to evaluate summer instream flows because the summer months are a crucial growing period for trout (Cattanéo et al., 2002). Our main

questions are: 1) Are summer flows lower than the mandated 80 cfs for lower Diamond Fork and 32 cfs for Sixth Water Creek more favorable for trout? 2) What is the optimal flow, or range of flows that results in the highest trout carrying capacity?

2.2 Study Area

The Diamond Fork River, located in Utah County, Utah, drains approximately 400 km^2 of the Wasatch Mountains (Figure 2.2.1). It empties into Spanish Fork River which terminates at Utah Lake. It is a mountainous watershed, primarily underlain by Mesozoic sedimentary rocks, and ranges in elevation from 1500 meters to approximately 3100 meters. In the lower elevations, juniper, gamble oak, mountain maple, and grasses and shrubs dominate the hillslopes. Higher elevations transition to coniferous forests with intermingled stands of aspen. Riparian areas are characterized by several species of willow, grasses, sedges, forbs, rushes, narrowleaf cottonwoods, and water birches. Mean annual precipitation is 678 mm (PRISM Climate Group, 2004), the majority of which falls as snow during winter months. Like most streams and rivers in Northern Utah, Diamond Fork River has a snow-melt dominated hydrograph and is an important source of water for agriculture in downstream communities. The system is prone to flash floods from micro-burst storms in the headwaters during the monsoon season.

Sixth Water Creek and Diamond Fork River represent an important sport fishery in Utah, supporting self-sustaining populations of Bonneville cutthroat trout (*Oncorhynchus clarkii utah*) and brown trout (*Salmo trutta*). Historically, the watershed has been used for livestock grazing, agriculture, timber harvesting and recreation. Currently, it is used primarily for livestock grazing and recreation. Most of the watershed is part of the Uinta National Forest and is managed by the U.S. Forest Service (BIO-

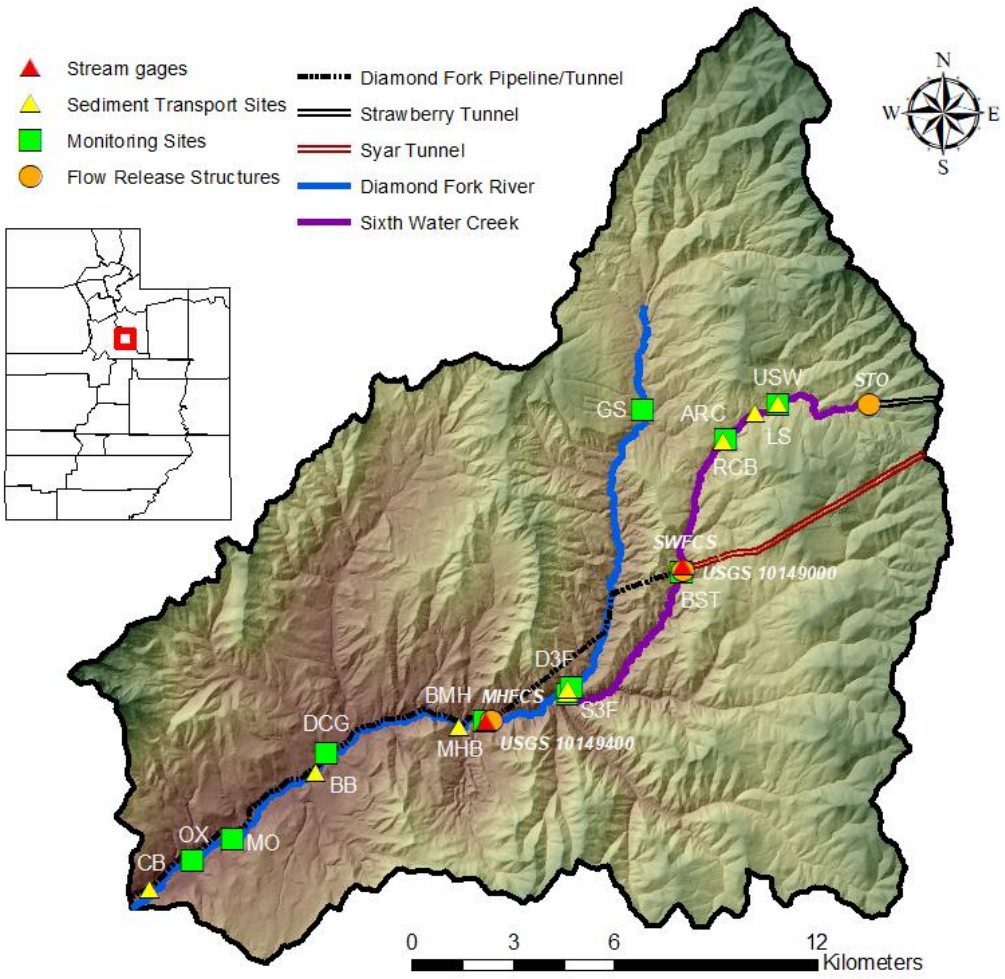

Figure 2.2.1. Locations of monitoring and sediment transport sites, flow release structures, and stream gages within the Diamond Fork River and Sixth Water Creek. Monitoring sites are: OX – Oxbow, MO – Motherlode, DCG – Diamond Campground, BMH – Below Monks Hollow, S3F – Sixth Water 3 Forks, BST – Below Syar Tunnel, ARC – Above Rays Crossing, USW – Upper Sixth Water, D3F – Diamond Fork 3 Forks, GS – Guard Station. Sediment Transport sites are CB – Childs Bridge, BB – Brimhall Bridge, MHB – Monks Hollow Bridge, D3F, S3F, RCB – Rays Crossing Bridge, LS – Landslide, USW. Flow release structures are: STO – Strawberry Tunnel Outlet (also known as West Portal), SWFCS – Sixth Water Flow Control Structure, MHFCS – Monks Hollow Flow Control Structure. The locations of Strawberry Tunnel, Syar Tunnel and the Diamond Fork Pipeline are approximations.

WEST, Inc., 2007).

The Diamond Fork River, and its largest tributary, Sixth Water Creek have experienced flow alterations in the form of trans-basin diversions for the past century. One of the first Bureau of Reclamation projects in the early 1900s was the Strawberry Valley Project. This project brings water from the Colorado River Basin through Strawberry Tunnel to the Wasatch Front to support and sustain agricultural practices. Strawberry Tunnel was completed in 1913 and irrigation releases began in 1915. Average flows of 200+ cubic feet per second (cfs), with peaks well above 400 – 500 cfs, occurred during the irrigation season (May to September). These flows were diverted into the headwaters of Sixth Water Creek and routed downstream, through the lower Diamond Fork (the reach between the confluence of Sixth Water Creek and the Diamond Fork River to the confluence of the Diamond Fork River with the Spanish Fork River), where they were then diverted into a canal. For Sixth Water Creek, these flows well exceeded the 100-year flood, and perhaps even the 500-year flood (Figure 2.2.2; Kenney et al., 2007). For lower Diamond Fork, these flows were the equivalent of the 10-year flood (Figure 2.2.3; Kenney et al., 2007). Irrigation flows were generally not released from the months of October to April, so flows during that time frame were largely natural flows. The sustained augmented flow regime caused the channel to incise in Sixth Water Creek up to 6 meters or more in places (Jones, 2018).

The natural baseflow regime of the Diamond Fork was such that summer and winter flows ranged from 15 to 25 cfs, whereas for Sixth Water Creek they were between 5 and 10 cfs. During the irrigation flows of the 20th century, summer flows were on average over 200 cfs. These effectively exceeded most natural floods. The current flow

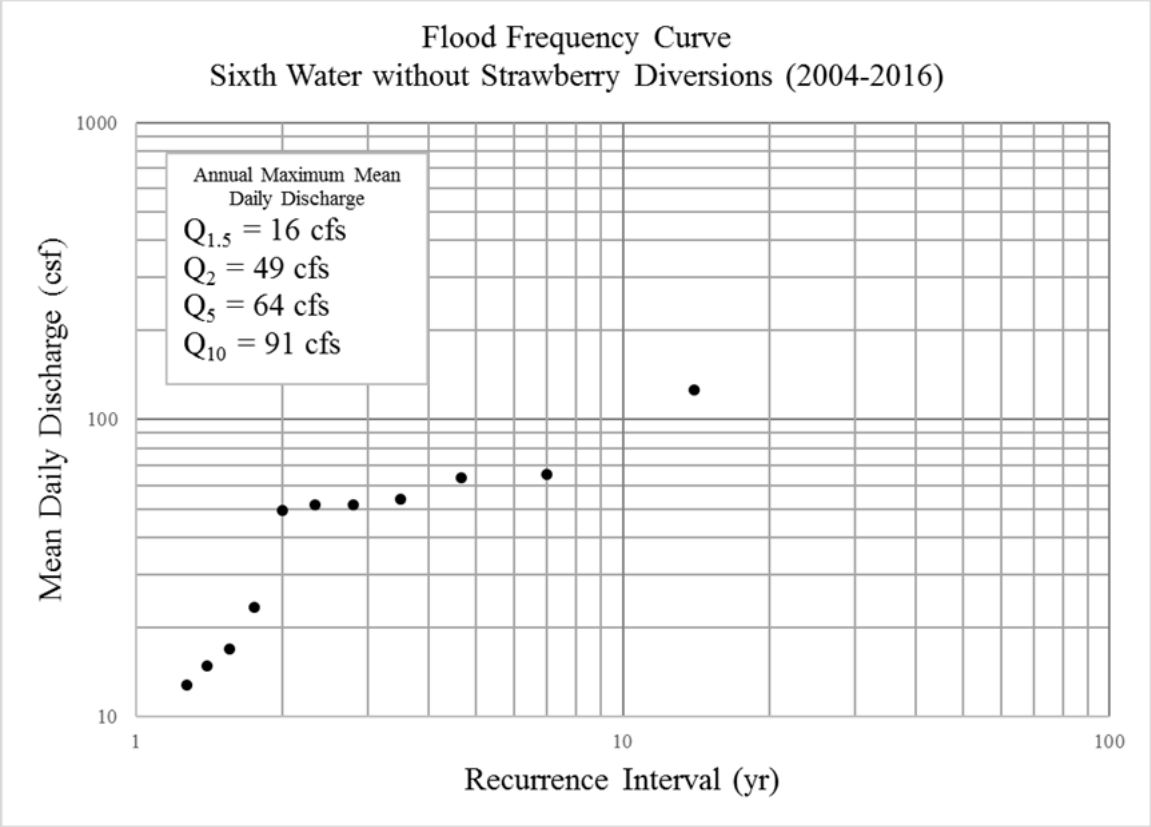

Figure 2.2.2. Estimated natural flood frequency (Wiebull distribution) for Sixth Water Creek by subtracting mean daily Strawberry Diversion flows from the mean daily discharge as measured at the USGS gage on Sixth Water Creek (Station ID: 1049000) from 2004 to 2016.

regime (2004 to the present) is more uniform, with the natural floods only being slightly higher relative to the sustained baseflows (Figure 2.2.4).

The lower Diamond Fork was first described by Father Escalante and Father Dominguez in their 1776 expedition as a meandering stream with “pretty bends” and flat adjacent meadows (Vâelez de Escalante and Warner, 1995, p. 62-63). The diversion flows, in combination with several exceptionally large flood years (1952, 1954, 1983, 1984) converted the lower Diamond Fork into a wide, braided river. Jones (2018) documented cycles of channel widening and narrowing throughout the 20th century, from

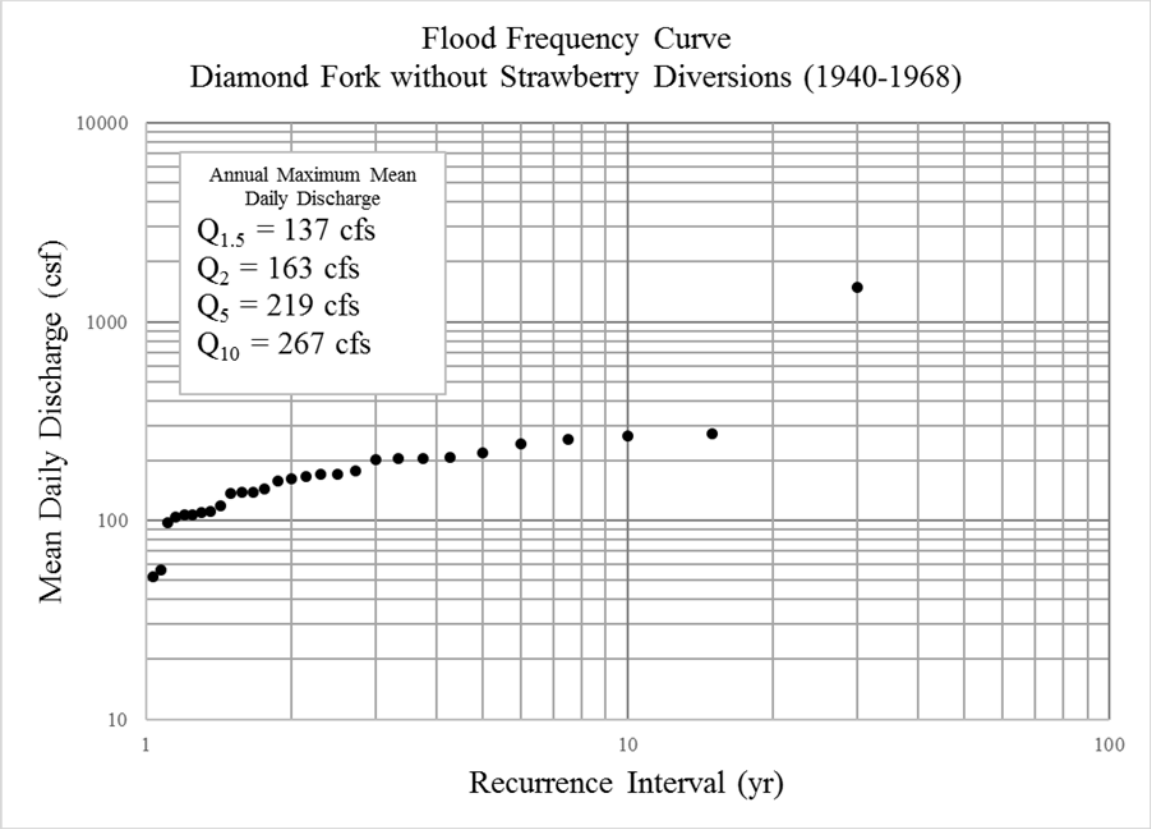

Figure 2.2.3. Estimated natural flood frequency (Wiebull distribution) for the Diamond Fork River by subtracting mean daily Strawberry Diversion flows from the mean daily discharge as measured at the USGS gage on the Diamond Fork (Station ID: 10150000) from 1940 to 1968.

historical air photos. The combination of increased flow and sediment supply made the lower Diamond Fork a highly dynamic system.

As part of the Central Utah Project Completion Act (CUPCA), legislation which transferred the responsibility of planning and construction activities to the Central Utah Water Conservancy Distract as overseen by the Department of Interior, a series of pipelines and tunnels were constructed — effectively removing all trans-basin diversion flows from Sixth Water Creek and Diamond Fork River (U.S. Congress, 1992). In 1996, Syar Tunnel, located ~10 km downstream of Strawberry Tunnel, was the first phase to be

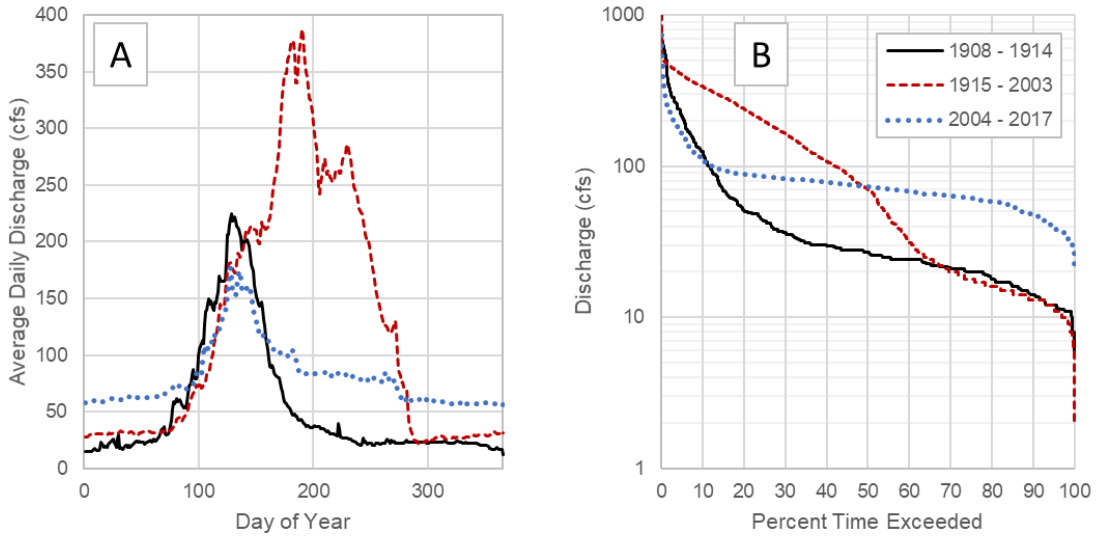

Figure 2.2.4. Discharge statistics for three periods of gage data on the lower Diamond Fork. A) Average daily discharge and B) flow duration curve. The three time periods represent pre-diversion flows (1908-1914), the irrigation flows (1915-2003), and current flow regime (2004-2017).

completed; allowing irrigation flows to bypass the upper portions of Sixth Water Creek. The lower Diamond Fork channel narrowed considerably after 1996 (Jones, 2018). This was attributed to a decrease in sediment supply because the Syar Tunnel release point bypasses the more erodible shale and limestone lithology located in the headwaters. In 2004, the Diamond Fork Tunnel and Pipeline were completed, making it possible to bypass the entire river. Two flow control structures were built, one at Syar Tunnel on Sixth Water Creek, and the other at Monks Hollow, located approximately 12 km upstream of the mouth of the Diamond Fork River (Figure 2.2.1).

In an effort to mitigate the effects of the 20th century flows, and as part of the environmental commitments associated with the Central Utah Project Completion Act

(U.S. Congress, 1992), minimum instream flows were released from Strawberry Tunnel, Syar Tunnel, and Monks Hollow. The purpose of these flows is primarily to maximize the amount of available habitat for trout. Minimum instream flows are 80 cfs during summer months (May-1 to September-30) and 60 cfs during winter months (October-1 to April-30) for the lower Diamond Fork. For Sixth Water Creek, minimum instream flows are 32 cfs during summer months and 25 cfs during winter months. These flows requirements are measured at the two USGS gages on the streams: 10149400 Diamond Fork River above Red Hollow near Thistle, UT; 10149000 Sixth Water Creek above Syar Tunnel near Springville, UT (Figure 2.2.1).

Since 2004, the channel has continued to adjust, primarily in the form of channel narrowing in the unconfined and partially-confined valleys along lower Diamond Fork (Jones, 2018). The decrease in flow, along with an exhausted sediment supply was determined as the primary cause for the channel narrowing. The reworking of local sediment, along with the establishment of vegetation on banks and floodplains have also contributed to the narrowing. As a result of the narrowing, channel simplification and habitat degradation was observed throughout much of the lower Diamond Fork.

2.2.1 Process Domains and Channel Change

Jones (2018) identified eight distinct process domains using the River Styles Framework (Brierley and Fryirs, 2005) throughout the lower Diamond Fork and Sixth Water Creek (Figure 2.2.5). Process domains were characterized by valley setting, floodplain composition, hillslope and channel gradient, bedrock type, tributary junctions, and channel substrate. Process domains were generally steep and confined (Upper Sixth Water Canyon, Lower Sixth Water Canyon); moderately steep and partially unconfined

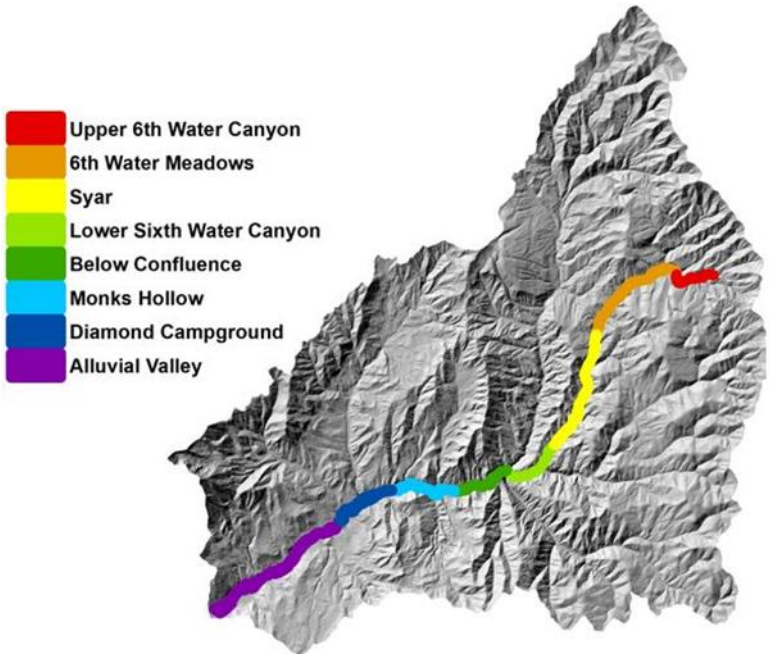

Figure 2.2.5. Location of process domains on Sixth Water and Diamond Fork (Jones, 2018).

(Sixth Water Meadow, Syar, Below Confluence, Monks Hollow, Diamond Campground); and unconfined (Alluvial Valley). General characteristics for each process domain are summarized in Table 2.2.1, with detailed descriptions found in Jones (2018).

Each of the process domains have responded differently to changes in flow and sediment. Jones (2018) observed that in the Upper and Lower Sixth Water Canyons process domain active widths were generally wider during the 20th century diversion flows (10 to 12 meters for Upper Sixth Water Canyon; 11 to 15 meters for Lower Sixth Water Canyon), and narrowed to and remained at approximately 8 to 10 meters after Syar tunnel was completed in 1996. Less confined Sixth Water Meadows and Syar process domains were wide in the 1950s (27 meters and 23 meters) and narrowed to approximately 10 meters by the late 1990s. Since the completion of Syar Tunnel and the

Diamond Fork pipeline, these two process domains have narrowed to approximately 8 meters. During the 20th century flows, the uppermost portions of Sixth Water Creek were greatly incised, with some reaches having incised up to an estimated 10+ meters. Since the exclusion of large diversion flows from Sixth Water Creek, the channel has adjusted very minimally.

For the lower Diamond Fork, active widths in all process domains were very wide (13 – 40 + meters). Active widths increased in correlation with large floods from the 1980s and 1950s as sediment was flushed from the headwaters and re-activated from banks and floodplains. For Below Confluence and Monks Hollow process domains, active channel widths narrowed to approximately 10 and 12 meters by 2004 and have remained relatively stable. The Diamond Campground and Alluvial Valley process domain active widths narrowed to approximately 15 and 17 meters by 2004, and since have narrowed to approximately 11 and 12 meters. In accordance with channel narrowing, Jones (2018) observed increased sinuosity, reductions in active channel width variability, and vegetation encroachment. He suggested that if summer baseflows were to be decreased further that previously inundated areas (i.e., inundated bars) may be exposed, allowing vegetation so establish.

2.2.3 Study Reaches

We surveyed two stream reaches within the Diamond Fork Watershed: Below Monks Hollow (BMH) on lower Diamond Fork and Above Rays Crossing (ARC) on Sixth Water Creek (Figure 2.2.1). The BMH site is located within a partially confined valley immediately downstream of the Diamond Fork above Red Hollow USGS gage (station ID: 101494000) and the Monks Hollow flow release structure. The BMH site is

103 meters long, contains two pools, two runs, one riffle and has a drainage area of 251 km^2. The ARC site is also located in a partially confined valley a few kilometers upstream of the Above Syar Tunnel USGS gage (station ID: 10149000) on Sixth Water Creek. The ARC site has one pool, two runs, and a riffle, and drains an area of 28 km^2. Table 2.2.2 summarizes general characteristics for each site.

Table 2.2.1. Attributes of process domains on Diamond Fork and Sixth Water (Jones, 2018).

Process domain	Percent confinement	Confining material	Slope (%)	Substrate	Geomorphic units	Length (km)
Upper Sixth Water Canyon	73	Shale mudstone	5.3	Bedrock boulder cobble	Bedrock scour pools cascades	2.1
Sixth Water Meadows	30	Shale mudstone active landslide	4.8	Cobble boulder gravel	Long runs broken up by beaver dams	3.4
Syar	64	Limestone sandstone	3.1	Cobble boulder gravel	Runs, few pools and riffles	6
Lower Sixth Water Canyon	87	Conglomerate	4	Boulder bedrock cobble gravel	Bedrock scour pools cascades	3
Below Confluence	26	Alluvial fans sandstone roads	1.5	Cobble boulder gravel, bedrock	Long runs pool/riffle sequences woody debris	2.9
Monks Hollow	33	Sandstone alluvial fans, roads	1.1	Cobble gravel boulder	Point bars pool/riffle/run sequences woody debris	3.5
Diamond Campground	26	Terraces alluvial fans	0.92	Gravel cobble sand	Point bars pool/riffle/run sequences	3.4
Alluvial Valley	22	Alluvial fans, terraces	0.69	Gravel cobble sand	Point bars instream bars	8.1

Table 2.2.2. Site characteristics of reaches used to build net rate of energy intake models.

Site	Site Length (m)	Valley Confinement (m)	Average Valley Width (m)	Average Bankfull Width (m)	D_{50} (mm)	D_{84} (mm)	Reach Average Slope	Drainage Area (km^2)
Below Monks Hollow	103	Partially Confined	151	7.2	64	111	.008	251
Above Rays Crossing	75	Partially Confined	54	6.4	79	170	.019	28

2.3 Methods

2.3.1 Field Data Collection

The stream channel, wetted perimeter, banks and floodplains of each reach were mapped by collecting topographic (XYZ) points with an rtk GPS. Topography was characterized by capturing all major breaks in slope, with more points collected in areas of complexity and less points collected in simple areas. This resulted in an average point density of 0.7 points/m^2 for BMH and 1.1 points/m^2 for ARC. A water surface elevation profile was surveyed for four different discharges (Table 2.4.2), facilitated by a step flow experiment conducted in September 2017. Discharge was stable throughout each of the days on which the surveys were conducted, recorded as 57.7 cfs, 81.8 cfs, 97.9 cfs, 168 cfs at BMH (mean daily discharge from the Diamond Fork USGS gage, 10149400), and 20.1 cfs, 29.7 cfs, 50.9 cfs, and 98 cfs at ARC (mean daily discharge, estimated using methods outlined in Appendix 2). An unmanned aerial vehicle (UAV) was used on August 11th, 2017 to capture an aerial image of the BMH site (mean daily discharge 82.9 cfs). We quantified the substrate composition of the riffle/run at each site using Wolman pebble counts (Wolman, 1954) during sampling campaigns in the months of April, June, August, and October of both 2016 and 2017.

We calculated the 25th, 50th, and 75th percentile temperatures for the months of August and September from instream temperature loggers recording each 10 minutes. BMH temperatures were calculated from 2016 and 2017 data and ARC temperatures were calculated using 2016 data (no 2017 data collected at ARC).

Drift data were collected and processed by Epperly (2018). He collected drift by deploying two 300 mm x 300 mm, 150-micron mesh drift nets at approximately 1/3 the width of the wetted channel. The drift nets were placed at the upstream end of the reach for a period of two hours during daylight hours of August 2016 and 2017. The two drift samples were combined and oven dried to estimate total drift biomass in grams. Only aquatic organisms were processed, excluding any emergent and/or terrestrial macroinvertebrates. The volume of water filtered by the nets was estimated from the 2D hydraulic model (discussed later) by retrieving the values of depth and velocity at the locations where drift nets were placed because no field measurements of these variables were made. It was noted that due to the duration of the sampling period, drift nets often became blocked with suspended debris and invertebrates. Such clogging has been shown to decrease the amount of water filtered within a drift sample, leading to an underestimation of drift density (Slack et al. 1991; Muehlbauer et al. 2017; Mureithi et al. 2018). Therefore, our estimations for the volume of water filtered are likely too large and produce low estimations of total drift biomass concentrations. To compensate for the effects of net clogging and potentially low drift density estimations, we multiplied the drift biomass by factors of 2, 5, and 10 to use in different drift scenarios within the NREI model. The total drift biomass concentration of aquatic individuals in grams per meter cubed of water (TBC) was estimated by using equations 2.1 and 2.2,

$$TBC = TB/(b_n*h*v)/t \quad (2.1)$$

where TB is the total biomass, b_n is the net width, h is the water depth, v is water velocity, and t is sampling time. For water depths that exceeded the net heights, we used Equation 2.2,

$$TBC = TB/(b_n*h_n*v)/t \quad (2.2)$$

where h_n is the height of the net.

Because these drift measurements include only aquatic macroinvertebrates, and therefore represent only a fraction of drift available for consumption by fish, we analyzed the biomass proportions of aquatic and non-aquatic (terrestrial and emergent) macroinvertebrates from drift samples collected during the month of August from the Logan River, a productive stream in Utah (Jensen, 2017). Aquatic macroinvertebrates represented on average 55% (range of 34% to 70%) of the total biomass for the five sites sampled on the Logan River. We assumed that the measured aquatic macroinvertebrate drift samples from BMH and ARC represent approximately 55% of the total drift biomass and estimated total drift biomass concentration by dividing each drift sample by 0.55.

Estimated total drift biomass concentrations (ETBC) were converted into an estimated drift density (DD), by dividing ETBC by the dry weight of a mayfly with a length equal to the average taxa length of each site (Smock, 1980). The average taxa length was determined as 5 mm from a drift sample collected in April 2016 from a site upstream of ARC. No taxa lengths were recorded for the August samples, and because studies have shown that dry weights of invertebrate biomass can be as much as 3 orders

of magnitude smaller in August than in April (Vannote and Sweeney, 1980), we assumed the average prey length would be smaller than 5mm. We assumed a modest average taxa length of 3 mm (Wall et al., 2015, used 4 mm), resulting in an estimated drift density represented as the number of 3 mm mayfly individuals in a cubic meter of water, no/m^3. Drift densities from here on refer to the estimated drift densities for both aquatic, emergent, and terrestrial individuals as described above.

As part of the interdisciplinary study for the Diamond Fork, fish were surveyed across the nine monitoring sites via backpack electrofishing in 2016 and 2017 through the months of April to October (Wilcock et al., 2019). Block nets were placed at the top and bottom of each monitoring site so that no fish could escape or enter the sampling reach during the sampling period. The number of passes at the different sites ranged from 1 to 3. The length (mm: total length) and weight (grams) was recorded for up to the first 50 individuals of each species. A length-weight relation for brown trout was developed using data from sites in the lower Diamond Fork while the length-weight relation for Bonneville cutthroat trout was developed using data from sites on Sixth Water Creek (Figure 2.3.1).

Population estimates for all drift-feeding salmonids at ARC and BMH were derived from samples taken during August 2016 and 2017 using the methods of Carle and Strub (1978). For ARC, the estimate was 703 fish/km in 2016 and 845 fish/km in 2017. For BMH, the estimate was 878 fish/km in 2016. We evaluated all drift-feeding salmonids at each site in order to get a best estimate of observed carrying capacity for each reach. Bonneville cutthroat trout, brown trout, and rainbow trout were evaluated in the population estimate for ARC, while Bonneville cutthroat trout and brown trout were

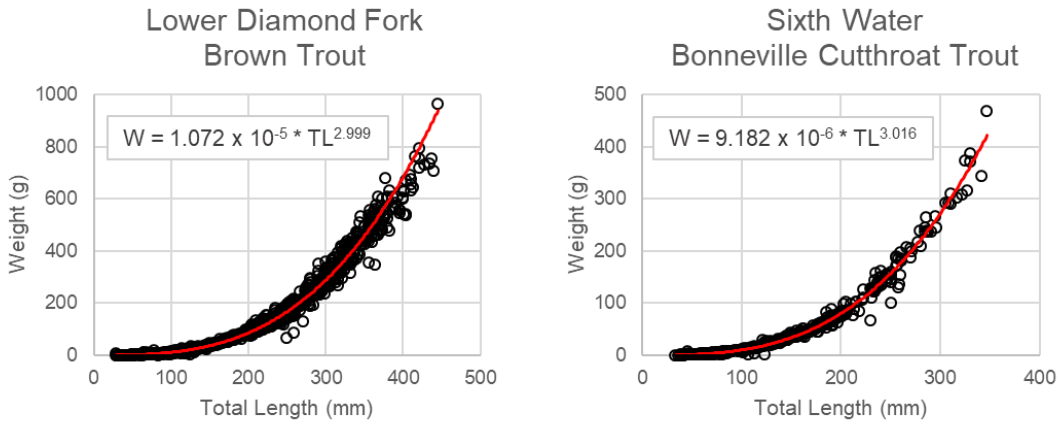

Figure 2.3.1. Length-weight relations for brown trout sampled from sites within the lower Diamond Fork (n = 1429), and Bonneville cutthroat trout sampled from sites within Sixth Water Creek (n = 532). Erroneous data points were removed to improve regression. Data was collected between 2016 and 2017.

evaluated for BMH. The approximate length of young of year (YoY) were estimated from length distributions (ARC: 63 mm; BMH: 100mm). The mean length of fish at each site was estimated using all drift-feeding salmonids (ARC: 162 mm; BMH: 167); the mean length of Bonneville cutthroat trout at ARC was 164 mm; the mean length of brown trout at BMH was 167 mm.

2.3.2 Hydraulic Modeling

We used GIS software to process topographic data and create 10 cm digital elevation models (DEMs) for channel and water surface elevations at each site. We expanded the BMH reach by 15 meters, in order to incorporate a large pool that was sampled for fish, by georeferencing a UAV aerial image with a second-order polynomial transformation and using spectral depth retrieval methods from Legleiter et al. (2009) to estimate bed topography. Because the aerial image was collected at a time when the flow was 82.9 cfs, we used the water surface profile surveyed at 81.8 cfs to estimate the

elevation of the water surface for the aerial image. Out-of-channel features were based on the slope and elevation of measured floodplains and banks. Because the study is only investigating low flow conditions, accuracy of topography outside of the channel was not necessary.

We used the DEMs to build two-dimensional hydraulic models using HEC-RAS 5.0.1. Bruner (2016) described the robust and flexible capabilities of HEC-RAS (Hydrologic Engineering Center – River Analysis System) that were added so that it could perform 2D or combined 1D/2D modeling. Users have the option to use the 2D Saint Venant equations or the 2D Diffusion Wave equations. The 2D Saint Venant equations are applicable to more situations and generally produce better results. However, the 2D Diffusion Wave equations can accurately model many situations while allowing the software to run faster and have greater stability properties (Bruner, 2016). The 2D unsteady flow equations use an Implicit Finite Volume algorithm which allows for larger computational time steps and provides improved stability and robustness when compared to other finite element techniques. In particular, it appropriately handles the wetting and drying of 2D cells and can be used for subcritical, supercritical, and mixed flow regimes.

Brunner (2016) further explains that the software was designed to operate with structured or unstructured computational meshes where computational cells can be a mixture of shapes and sizes with up to eight sides. An important attribute of HEC-RAS is a “high resolution subgrid model” (Casulli, 2008) that uses computational cells defined using the topography of the underlying terrain. The elevation-volume relations for each cell allows water to move between cells based on the underlying terrain instead of the

computational mesh size. This allows for a coarser computational mesh, resulting in faster run times without compromising the detail of the final output. The RAS Mapper graphical user interface (GUI) allows for multiple file types (shapefiles, rasters, aerial images) to be viewed and processed, making it easy to visualize results and calibrate the model.

We modeled unsteady conditions using the Diffusion Wave equations within HEC-RAS. We considered these equations to be appropriate for our case of stable flow at a single discharge for four hours, incrementally increasing to the next higher discharge. Each two-dimensional model was calibrated using a uniform Manning's n, as all modeled flows were retained within the channel and the size distribution of bed substrate was relatively uniform throughout. We assume that local increases or decreases of Manning's n values produced by roughness elements such as bed features (bars, width constrictions, bends) are resolved through the elevation-volume relations computed in each cell of the 2D computational mesh. During calibration, we used a 0.5-meter structured computational mesh in order to decrease computational time during iterations of Manning's n.

Downstream boundary conditions were specified by using the downstream slope to calculate the normal depth while the upstream boundary conditions were specified by a stepped flow hydrograph. Manning's n was initially chosen by comparing our site to sites described in Barnes (1967). Manning's n was then modified iteratively until the mean modeled water surface elevation matched the surveyed water elevation corresponding to the mandated summer flows (81.8 cfs for BMH, 29.7 cfs for ARC). We validated the model using three other discharges for which there were corresponding surveyed water

elevations.

Once an appropriate roughness coefficient was derived and validated, the computational mesh was reduced to 0.2 meters and the computational time step was reduced to 0.2 seconds in order to satisfy the Courant number condition for the diffusion wave equations (Brunner, 2016). We chose this mesh size because it provided a balance between computational time and a hydraulic solution with a resolution relevant to trout (Wall et al. 2015). We modeled 10 discharges per site by increasing discharge in steps over a 40-hour period (4 hours per each magnitude of discharge) (Table 2.4.1). This approach allowed the discharge for each step to stabilize and produce a steady state solution.

2.3.3 NREI Modeling

We modeled NREI and carrying capacity for 10 separate discharges at each site using an adaptation of the Hayes NREI model used by Jensen (2017) and McHugh et al. (2017). The 2D hydraulic outputs from HEC-RAS were used to estimate the water velocity at depths spaced 0.05 m throughout the water column by applying a logarithmic velocity profile (Gordon et al., 1992). The logarithmic velocity profile, which is calculated using depth, depth-averaged velocity, and a roughness height, allows for the flow to be slower near the bed and faster near the surface. If negative velocity values are calculated near the bed, the roughness height is incrementally decreased until there are no negative velocity values within the reach. The average D84 from the Wolman pebble counts was used as the roughness height (Bouwes et al., 2011; Jensen, 2017). The output is considered a 2.5D representation of the channel hydraulics because a 3D solution was not explicitly solved. Instead we used the logarithmic velocity profile equation in order to

create a 3D grid of depth and velocity (scalars). The 3D grid is used in the subsequent foraging and swimming cost models to calculate the capture area, gross rate of energy intake, and swimming costs of a fish associated with each node of the 3D grid.

NREI is calculated by estimating the gross rate of energy intake (GREI) and subtracting energy losses due to waste and swimming. We assume that energy due to waste losses is 30% of the GREI (Hughes et al., 2003), so that NREI = (GREI x 0.7) – Swimming Costs. To estimate GREI, a prey capture area is calculated for each node (i.e., fish position) of the 3D grid. The area is delineated by the foraging radii of 36 foraging radials that emanate from the fish position (based on the reactive distance to prey and local velocity). The foraging radials define the prey capture area due to the varying velocities that surround a fish's location (Hughes et al., 2003). The foraging area is used to calculate the volume of water a fish can filter for drifting prey under constraints of successful prey encounters (Figures 2.3.2, 2.3.3).

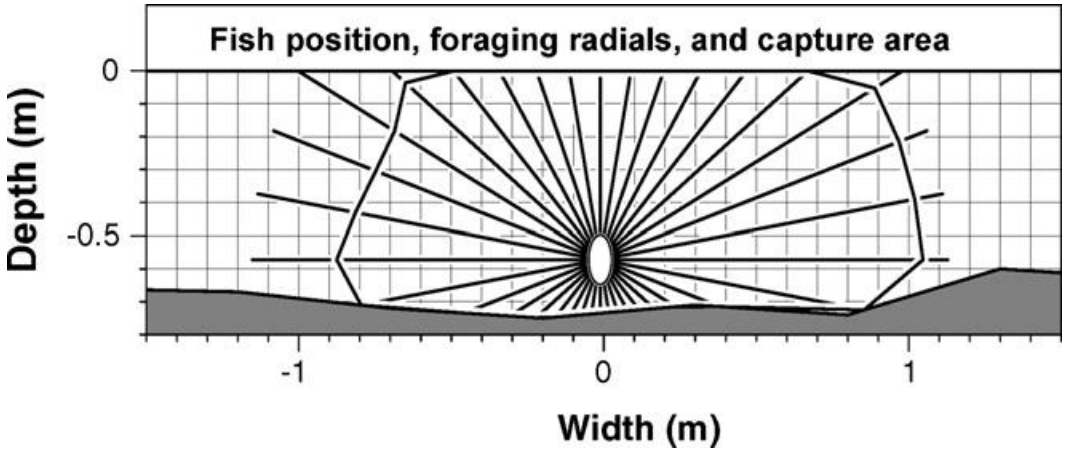

Figure 2.3.2. Cross-sectional view of the drift-foraging model showing: fish position; computational foraging radials; and predicted prey capture area interpolated from predicted foraging radius along each foraging radial (based on prey reaction distance and velocity). Foraging radials facilitate computation of capture distance where velocity varies around the fish's position (cf. Hughes et al., 2003).

Foraging success is the proportion of prey consumed relative to the number or individuals a fish encounters. We assume a foraging success of 55% for both cutthroat and brown trout, which is the success rate Hughes et al. (2003) observed for brown trout (*Salmo trutta*). Drift density scenarios were based on the estimated total drift density (DD) from measurements made in August 2016 and 2017 at both BMH and ARC sites and are summarized in Table 2.4.1. For BMH, scenarios were 1x, 2x, 5x, and 10x that of DD for August 2016. For ARC, scenarios were 1x, 2x, and 5x that of DD for August 2016, as well as DD from August 2017. We assume a uniform drift density for the reach as it is a common approach in estimating NREI (Hughes et al. 2003; Railsback et al. 2009; Jenkins and Keeley 2010; Urabe et al. 2010; Rosenfeld and Ptolemy 2012, McHugh et al., 2017) and helps decrease model complexity (Wall et al. 2015). Hayes et al. (2007) used a more robust and complex drift dispersion model to replicate drift dynamics (Rosenfeld et al., 2014), however, that approach requires a level parameterization, data collection, and modeling beyond that available for this work.

Fish were assumed to hold a foraging position at least 5 cm above the streambed (Wall et al. 2015). Swimming costs were calculated from the velocity at those locations. Physiological traits in fish are size- and temperature-dependent (Jobling, 1995; Hayes et al., 2007) therefore we used length-weight relations (equations 2.3 and 2.4) from the lower Diamond Fork for brown trout and Sixth Water Creek for Bonneville cutthroat trout:

$$W = 1.072 \times 10^{-5} * TL^{2.999} \text{ (brown trout)} \quad (2.3)$$

$$W = 9.182 \times 10^{-6} TL^{3.016} \text{ (Bonneville cutthroat trout)} \quad (2.4)$$

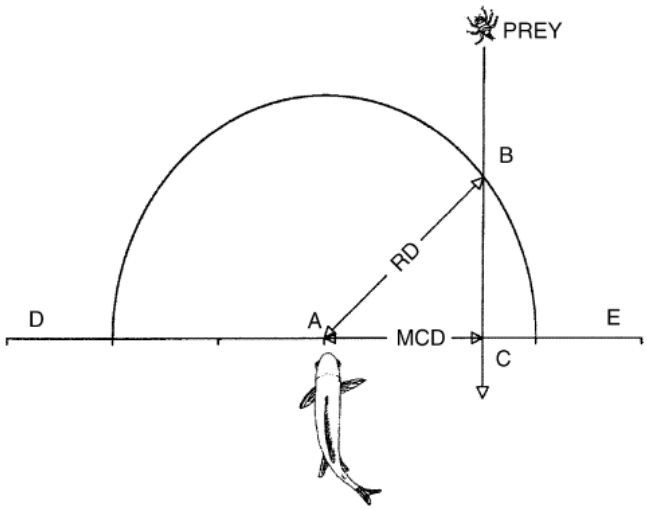

Figure 2.3.3. Plan view of the foraging model showing the geometry of prey interception. The fish is assumed to detect prey as they hit the surface of the hemispherical reaction volume with a radius equal to its reaction distance (RD) to the length class of the prey in question. The fish intercepts prey at its maximum sustainable swimming speed (Vmax) and may only capture prey that it is able to intercept before they cross the line D–E. Under these conditions, when water velocity is V, the maximum lateral capture distance (MCD) is: $MCD = (RD2 - (V \cdot RD/Vmax)2)^{0.5}$ (cf. Hughes et al., 2003).

where W is the wet weight (g) and TL is the total length (mm). These length-weight relations were derived from data collect during 2016 and 2017 (Figure 2.3.1).

At BMH, we modeled brown trout lengths of 100 mm (a representative length for YoY observed in August 2016), 150 mm (stock length), and 300 mm (preferred length) (Milewski and Brown, 1994). We used bioenergetics parameters from Dieterman and Anderson (2004) and the swimming cost model from Hayes et al. (2000). At ARC, we modeled cutthroat trout lengths of 63 mm (average YoY length during September/October for 2016, 2017), 150 mm (stock length), and 300 mm (preferred length). Length categories for cutthroat were assumed to be the same as brown trout categories from Milewski and Brown (1994). For GREI calculations, we used parameters

defined for cutthroat trout from Beauchamp et al. (1995). We used the swimming cost model and steelhead parameters from Railsback and Rose (1999) to calculate swimming costs because steelhead and cutthroat trout are similar species and swimming cost parameters have yet to be determined for cutthroat trout. The drift-foraging period was set at 15.5 hours, a time interval used in Hayes et al., (2016). Temperature scenarios were the 25^{th}, 50^{th}, and 75^{th} percentile temperatures from August-September of 2016 and 2017. Table 2.4.1 summarizes all parameters used in the different NREI scenarios. Each site totaled 360 individual scenarios of varying discharge, drift density, temperature, and fish length.

The model calculates NREI and a fish carrying capacity for each scenario using approaches adapted from Hayes et al. (2007) and Kelly et al. (2012). It uses a fish placement algorithm to predict fish locations by selecting those locations that are favorable for foraging (i.e., positive NREI) and not allowing other fish placement within a territory based on an allometric body size-territory size relation (Imre et al. 2004), which is multiplied by 2 to ensure no overlap. We used a NREI value of 0.0 Joules per hour (J/h) as a threshold to warrant fish placement. This threshold is used because it is a value at which a fish is neither gaining or losing weight (Wall et al., 2015). A threshold for a p-value, the proportion of energy allotted to growth relative to the maximum energy consumed, was used as a secondary threshold, where fish could not be placed at a node if the p-value was less than 0.4. The algorithm begins by placing fish at the node with the highest NREI, then placing subsequent fish at the node with the next highest NREI that is not within the territory of another fish. This continues until the reach is “filled”, or there are no more locations that have an NREI value above 0.0 J/s or a p-value greater than 0.4,

and do not intersect with the territory of another fish. The predicted carrying capacity of trout in each reach is reported as a density of trout/km or fish/km.

2.3.3.1 Sensitivity Analysis

We conducted a simple sensitivity analysis for a 150 mm size fish at each site by varying discharge (BMH = 50 cfs, ARC = 25 cfs) by 20%, and temperature (50^{th} percentile temperature: BMH = 13.9° C, ARC = 12.8° C), drift (BMH = 1.4 no/m^3, ARC = 1.8 no/m^3), and drift-foraging period (15.5 hours) by 10% and 20%. The discharges at each site were selected to permit 20% changes in discharge using existing model runs.

2.3.4 Stream Width as a Function of Discharge

Jones (2018) suggested that the augmented baseflow regime may act as a control on channel width by inundating bars and other features that would otherwise establish vegetation and collect sediment at a lower discharge, potentially causing the channel to narrow even further. In order to understand how the channel might respond under different scenarios of flow, we developed a stream wetted width-discharge relation for the lower Diamond Fork using wetted width data from discharge measurements taken at CB and BB sediment transport sites and reach averaged wetted width data (wetted area divided by reach length) from BMH (HEC-RAS modeling results), DCG, MO, and OX (surveyed water extent) monitoring sites. The sediment transport sites and surveys for other monitoring sites are covered in more detail in Jones (2018).

2.3.5 Diamond Fork System Compared to Blue Ribbon Fisheries and Reference Streams

We compared the current flow regime (2004-2017) of the Diamond Fork River and Sixth Water Creek to the flow regimes of streams listed as Blue Ribbon fisheries for

brown trout and cutthroat trout in the state of Utah, and reference streams with similar basin characteristics within 400 km of the USGS gage located on the Diamond Fork (Stout, 2017). Blue Ribbon fisheries for the state of Utah are those streams and lakes that contain good fish habitat and a healthy fish population that results in a quality fishing experience. Blue Ribbon streams where streamflow was monitored were identified from the Utah Division of Wildlife Resources website (Blue Ribbon Fisheries) and were included in this analysis because the majority of these streams are influenced by dams and diversions but provide insight to flow regimes that produce healthy brown and cutthroat trout populations. Reference streams were identified by Stout (2017) and included in this analysis to demonstrate the Diamond Fork system's deviation from reference conditions. Stout (2017) was part of a class project and contains provisional results which are subject to change. The comparison between these streams and the Diamond Fork River and Sixth Water Creek is preliminary and only evaluated for a few flow metrics at annual and seasonal scales. The annual hydrographs for these streams are included as part of this thesis as they sufficiently portray the differences between flow regimes in lieu of a detailed hydrologic analysis.

2.4 Results

2.4.1 Field Surveys

The upstream site (Above Rays Crossing, ARC) was generally coarser, cooler, and had higher macroinvertebrate drift than the lower site (Below Monks Hollow, BMH). The median grain size (D_{50}), estimated from pebble counts was 79 mm for ARC and 64 mm for BMH. The 84th percentile grain size (D_{84}) was estimated as 170 mm for ARC and 111 mm for BMH. Thus, the channel bed at the upstream site is somewhat coarser,

but both are characterized as coarse gravel to cobble beds. The 25th, 50th, and 75th percentiles of temperature at ARC, derived from August and September of 2016, were 11.1° C, 12.8° C, and 15.1° C. For BMH, the 25th, 50th, and 75th, percentiles of temperature at BMH, derived from August and September of 2016 and 2017, were 12.9° C, 13.9° C, and 15.6° C.

Drift density for August 2017 at ARC was estimated as 1.1 no/m^3, and 1.8 no/m^3 for August 2016. Because of the potential effects caused by net clogging, the August 2016 drift density was multiplied by 2 and 5, resulting in additional drift density scenarios of 3.6 no/m^3 and 8.9 no/^{3}. Drift density at BMH for August 2016 was estimated as 0.7 no/m^3 and multiplied by 2, 5, and 10 to account for net clogging, resulting in drift density scenarios of 1.4 no/m^3, 3.4 no/m^3, 6.8 no/m^3.

Compared to other studies, drift densities measured during August of 2016 and 2017 at ARC and BMH appear to be low but within a plausible range. Studies measuring drift within the Logan River, Utah (Allan, 1982), Colombia River Basin (Wall et al., 2015), and the Green River, Utah (Filbert and Hawkins, 1995) have measured drift densities (aquatic, terrestrial, and emergent) ranging from 0.6 no/m^3 to 22 no/m^3. Although their methods of collection were different, this provides evidence that drift densities in the Diamond Fork River and Sixth Water Creek could potentially be low. However, the issues related to net clogging as a result of the extended sample period may provide a better explanation to the low drift density measurements. Muehlbauer et al. (2017) showed that filtration efficiency for a 500-micron mesh net on the Colorado River decreased to 29 percent (100 percent being optimal) after a 2-hour sampling period, and that filtration efficiency decreased beyond that for nets with finer mesh sizes. It is likely

that the actual drift is two or more times higher than the measured samples, hence the use of multiple drift density scenarios.

2.4.2 Hydraulic Modeling

Two-dimensional flow simulations were assessed for accuracy by comparing the modeled WSE to the field surveyed WSE. The 2D hydraulic models for both ARC and BMH produced stable solutions which resulted in mean WSE error (Modeled WSE –

Table 2.4.1. Scenarios of discharge, drift density, temperature, and fish length used for net rate of energy intake models for each site.

Below Monks Hollow (brown trout)

Discharge ft^3/s	Discharge m^3/s	Drift Density no./m^3	Temperature C°, (Percentile)	Fish Length mm
15	0.42	0.7 (August 2016)	12.9, (25^{th})	100
20	0.57	1.4 (2x Aug 2016)	13.9, (50^{th})	150
30	0.85	3.4 (5x Aug 2016)	15.6, (75^{th})	300
40	1.13	6.8 (10x Aug 2016)		
50	1.42			
60	1.70			
70	1.98			
80	2.27			
90	2.55			
100	2.83			

Above Rays Crossing (Bonneville cutthroat trout)

Discharge ft^3/s	Discharge m^3/s	Drift Density no./m^3	Temperature C°, (Percentile)	Fish Length mm
15	0.42	1.1 (August 2017)	11.1, (25^{th})	63
20	0.57	1.8 (August 2016)	12.8, (50^{th})	150
25	0.71	3.6 (2x Aug 2016)	15.1, (75^{th})	300
30	0.85	8.9 (5x Aug 2016)		
32	0.91			
35	0.99			
40	1.13			
45	1.27			
50	1.42			
60	1.70			

Observed WSE) of less than 1 cm for most cases (Table 2.4.2). Only in the cases where discharge was approaching "flood stages" (see Figures 2.2.2 and 2.2.3) did the mean WSE error increase. The likely cause of WSE error increase at high flows is that frictional losses (represented using a constant Manning's n value) decrease as discharge increases to flood stages within a reach. Overall, the hydraulic models for ARC and BMH are sufficiently accurate given that mean WSE error for all discharges are close to 0.0 m (with the exception of 98 cfs at ARC), and that the standard deviation of error is, for most cases, less than the error commonly associated with RTK GPS surveys (≤ 5 cm, Bangen et al., 2014).

Each model was used to simulate 10 discharges ranging from 15 cfs to 100 cfs for BMH and 15 cfs to 60 cfs for ARC (Table 2.4.1). All discharges are less than bankfull flow, and within the range of potential baseflows that could be mandated for the system. Discharge was not considered below 15 cfs for ARC because water quality samples show

Table 2.4.2. Calibration and validation of 2D HEC-RAS Models for each site. Models were calibrated to the surveyed water surface elevation (WSE) for the flow nearest in magnitude to the mandated summer flows of 80 cfs for Diamond Fork and 32 cfs for Sixth Water Creek. Other surveyed flows were used to validate the model.

				Modeled WSE – Surveyed WSE		
Site	Discharge ft^3/s	Discharge m^3/s	Manning's n	Mean WSE Error m	SD WSE Error m	Calibration/ Validation
BMH	57.7	1.63	0.05	0.004	0.034	Validation
BMH	81.8	2.32	0.05	0.000	0.067	Calibration
BMH	97.9	2.77	0.05	-0.023	0.033	Validation
BMH	168	4.76	0.05	-0.009	0.041	Validation
ARC	20.1	0.57	0.1	0.000	0.032	Validation
ARC	29.7	0.84	0.1	-0.001	0.047	Calibration
ARC	50.9	1.44	0.1	-0.015	0.052	Validation
ARC	98	2.78	0.1	0.047	0.051	Validation

that chronic concentrations of Selenium (produced from Strawberry Tunnel) are reached when flow drops below 20 cfs (Wilcock et al., 2019). For BMH, discharge was only modeled as low as 15 cfs because that is approximately the natural baseflow for the lower Diamond Fork. Hydraulic outputs are summarized for each site in Figures 2.4.1, 2.4.2, 2.4.3, and 2.4.4.

Above Rays Crossing

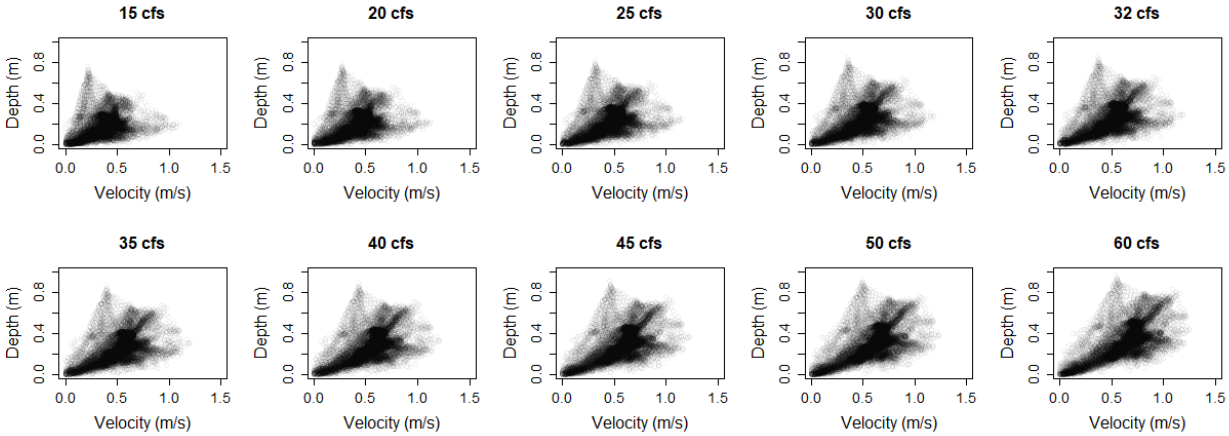

Figure 2.4.1. Depth and velocity plots for Above Rays Crossing on Sixth Water Creek for each modeled discharge.

Below Monks Hollow

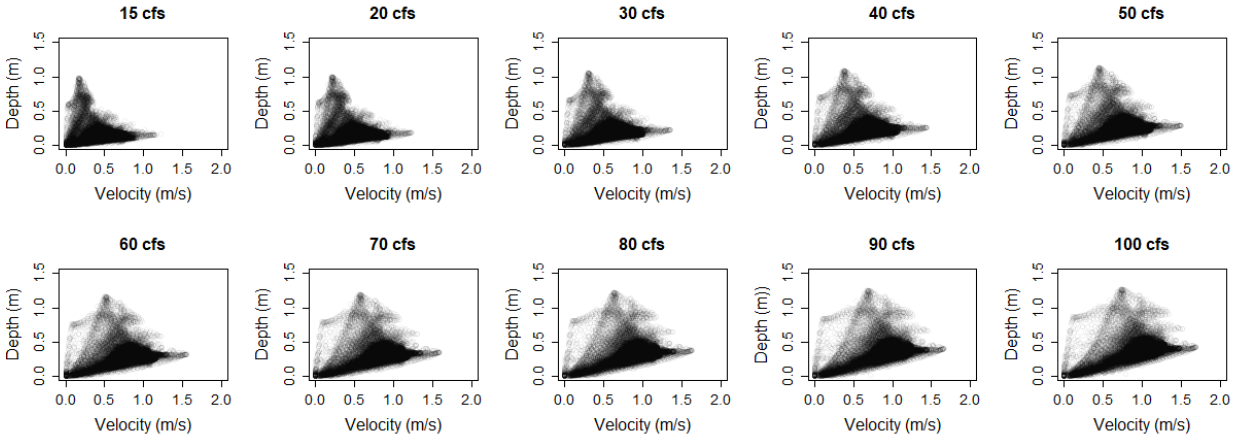

Figure 2.4.2. Depth and velocity plots for Below Monks Hollow on lower Diamond Fork for each modeled discharge.

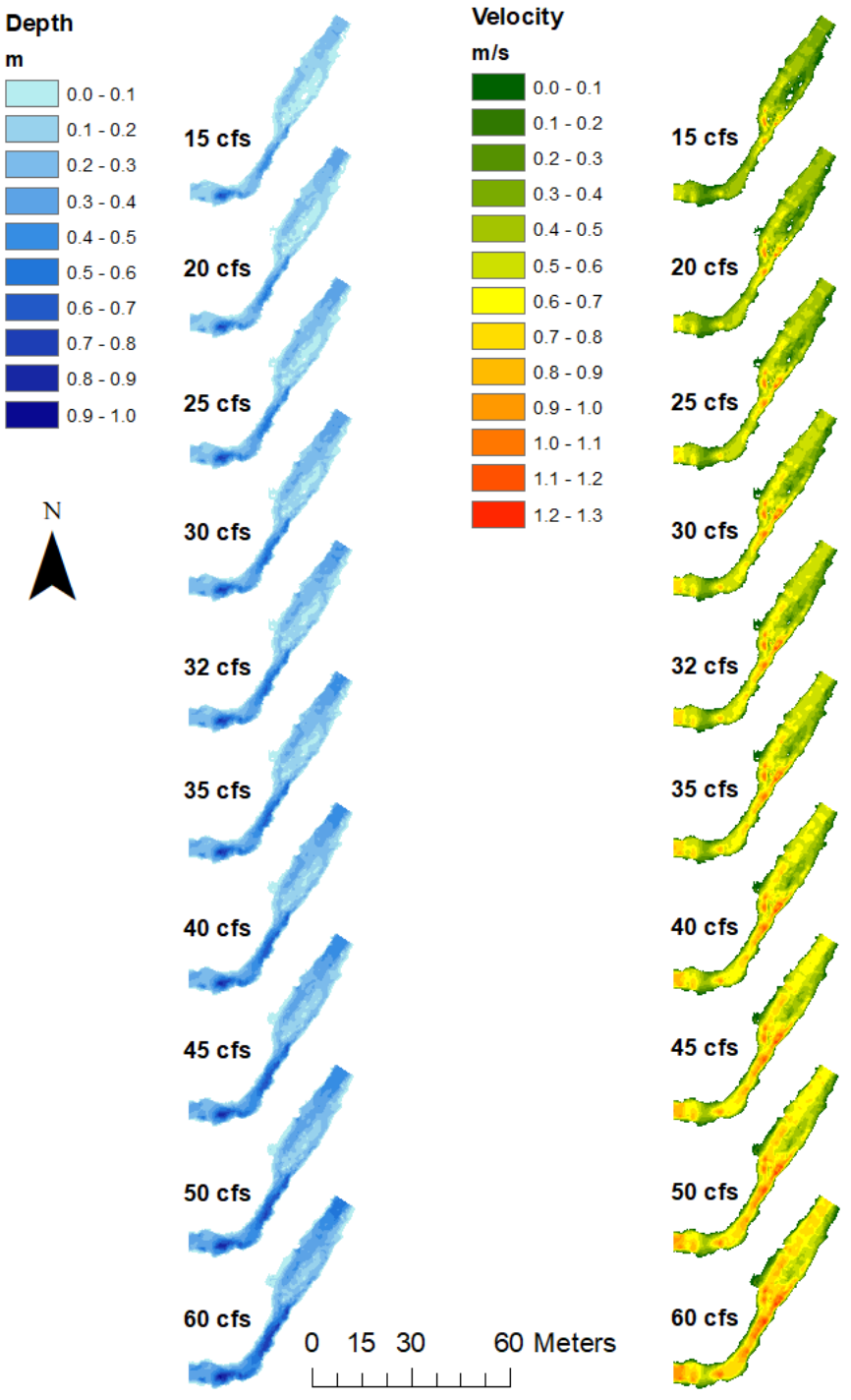

Figure 2.4.3. Depth and velocity raster outputs from HEC-RAS for each of the modeled discharge for the site at Above Rays Crossing on Sixth Water Creek.

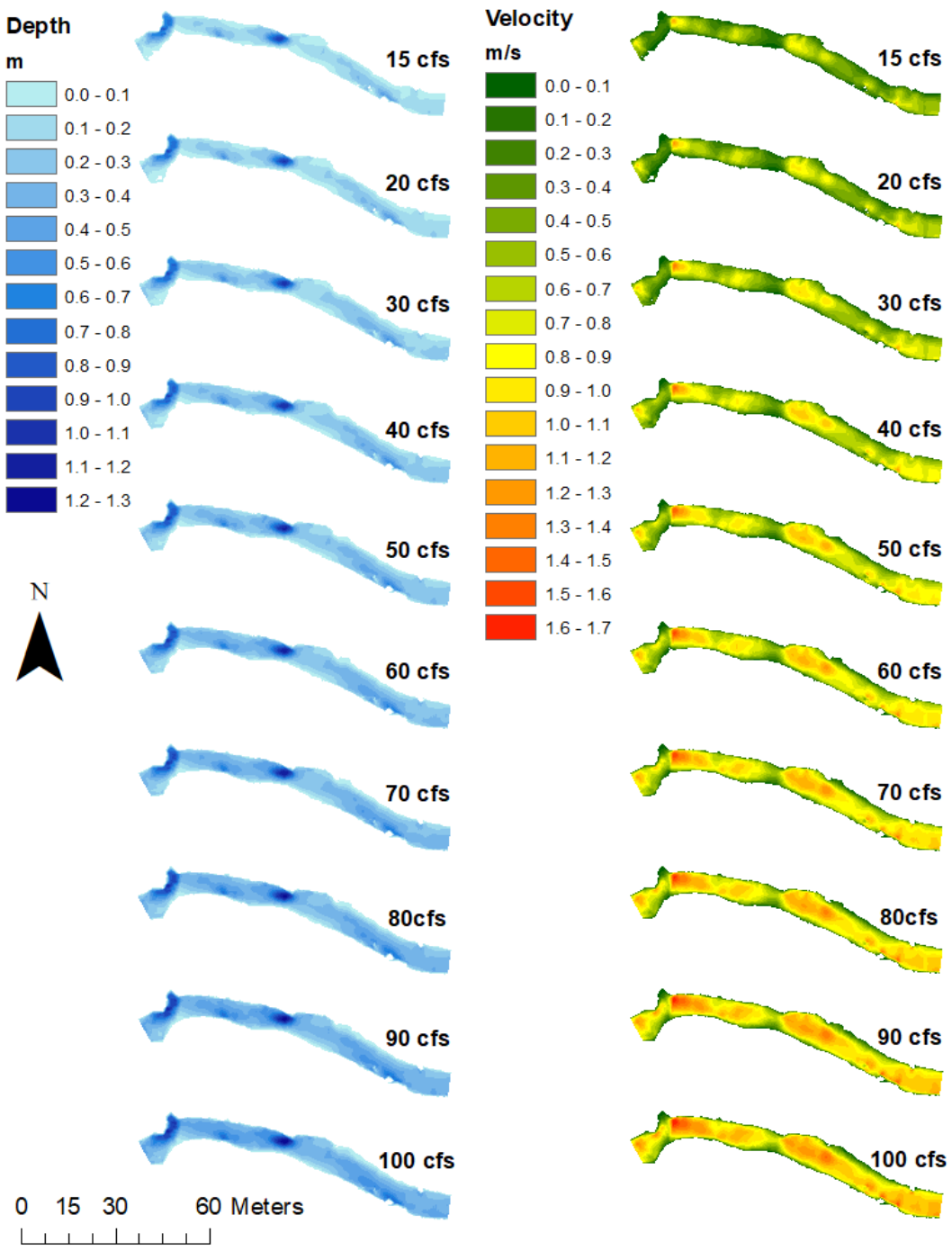

Figure 2.4.4. Depth and velocity raster outputs from HEC-RAS for each of the modeled discharge for the site at Below Monks Hollow on the lower Diamond Fork River.

2.4.3 NREI Predictions

2.4.3.1 Temperature and Drift Density

General responses of carrying capacity curves, observed for all trout sizes, are described with regards to the different scenarios of drift densities and temperatures. For low drift densities (i.e. the measured drift densities), carrying capacity curves are relatively flat with no significant discharge emerging as an optimum. As drift density increases (i.e., 2 times the estimated drift density), an optimum emerges at the lower end of the range of discharges. As drift increases to much higher drift densities (5 to 10 times the estimated drift density), the optimum flow shifts towards larger flows, a finding consistent with Hayes et al. (2016).

When considering temperature, lower temperatures resulted in higher carrying capacities while higher temperatures resulted in lower carrying capacities (Figure 2.4.5). For low drift densities, the difference between high and low temperatures is not as pronounced. As drift density increases, the range of carrying capacity between high and low temperature scenarios increases drastically. At the high drift densities, the range in carrying capacity between high and low temperatures is reduced, indicating that trout are able to compensate for changes in temperature by consuming more food.

2.4.3.2 Sensitivity Analysis

The sensitivity analysis showed that carrying capacity is most sensitive to changes in temperature and drift in comparison to changes in discharge and feeding period. A 20 percent change in discharge or feeding period resulted in less than a 20 percent change in carrying capacity while a 10 percent and 20 percent change in temperature and drift resulted in a 20 to >40 percent change in carrying capacity (Figure 2.4.6). Carrying

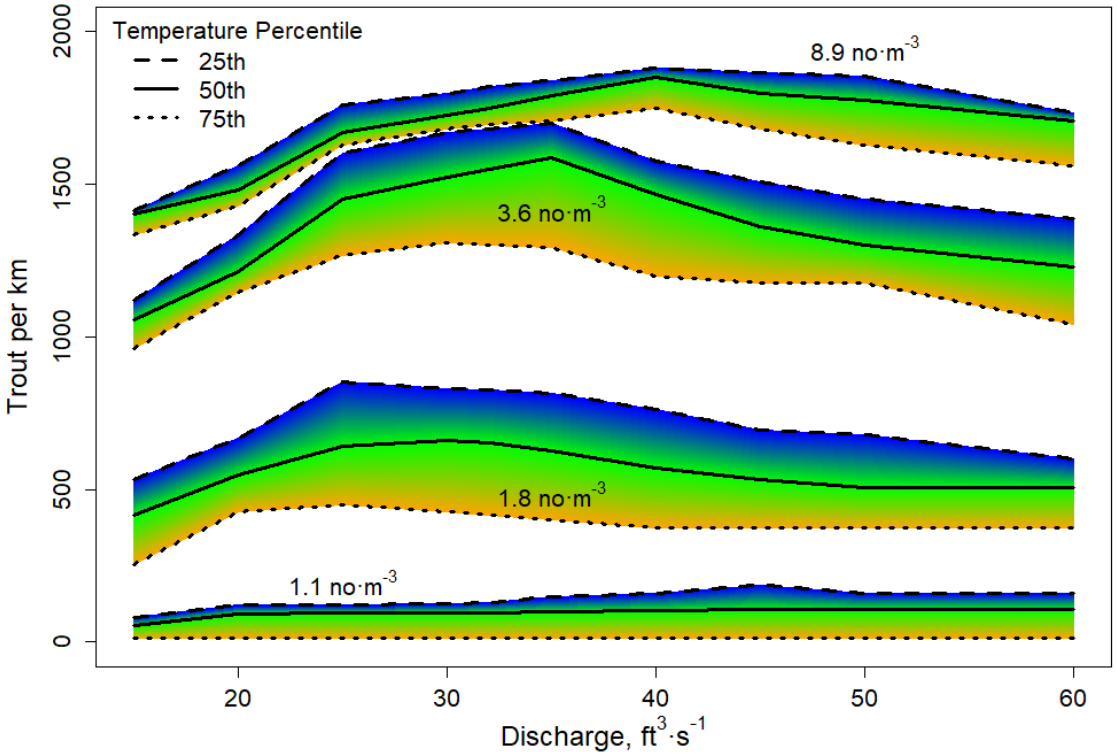

Figure 2.4.5. General carrying capacity responses (expressed as trout per km) to temperature and drift density. These carrying capacity curves are generalized net rate of energy intake results for three temperature scenarios (25th, 50th, and 27th percentiles) and four drift density scenarios (1.1 no/m^3, 1.8 no/m^3, 3.6 no/m^3, and 8.9 no/m^3) for a 150 mm cutthroat trout at Above Rays Crossing and have been adjusted to show overall responses. The color gradient represents the temperature change from warm (orange) to cold (blue) and is a linear interpolation between the three temperature scenarios.

capacity response to these variables in non-linear, particularly for drift. Depending on the magnitude of drift, small changes can have disproportionally large, or small returns.

2.4.3.3 Optimum Range of Discharge: Above Rays Crossing

For ARC, the NREI carrying capacity model results in curves with a maximum within the modeled range (Figure 2.4.7). The NREI model predicts fish within the reach for each scenario of drift and temperature except for low drift density scenarios for large

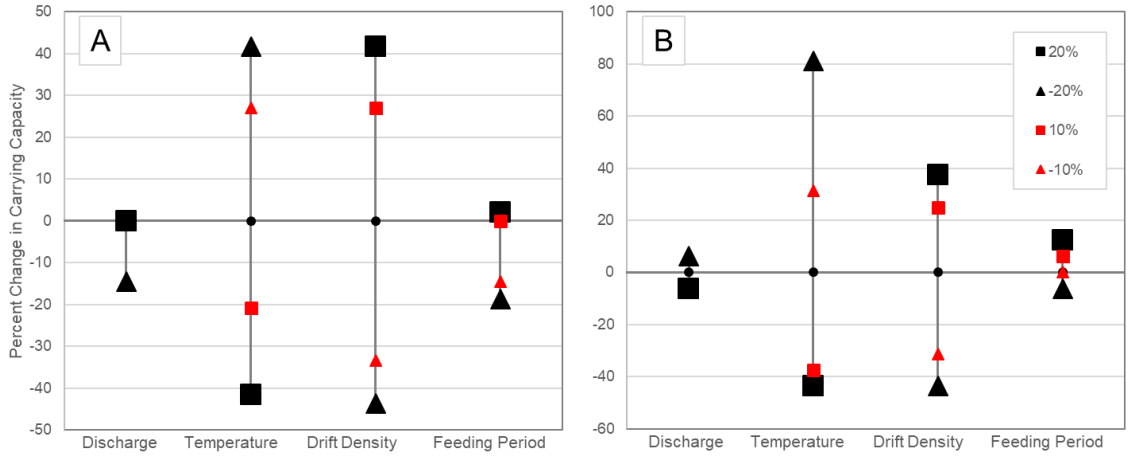

Figure 2.4.6. Sensitivity analysis for a 150 mm sized trout using variables of discharge, temperature, drift density, and feeding period for A) Above Rays Crossing and B) Below Monks Hollow. The analysis was performed by varying each variable by +/- 20 percent and each variable, except discharge, by +/- 10 percent.

adult trout. The carrying capacity is sensitive to changes in drift and temperature for juvenile (63 mm) and young adult (150 mm) sizes and is largest for flows around 25 cfs to 40 cfs. In the presence of lower drift, carrying capacity for ARC is largest between 25 cfs to 32 cfs whereas the maximum is between 35 and 40 cfs with local maximum occurring at 25 cfs for the larger drift densities. The model indicates that drift may be insufficient for large adult fish (300 mm) because it only predicts fish at the highest drift density, resulting in a maximum at 35 cfs. However, the model does not account for selective feeding habits (i.e., preying on larger individuals) or piscivory, which can have added energetic benefits for each gram of prey consumed.

We compared the observed fish densities of August 2016 and August 2017, as estimated from drift-feeding salmonids sampled within the reach, to the 150 mm size class because the mean length of sampled fish was 162 mm for ARC, and observed that the two lowest drift densities underestimated carrying capacity by a few hundred fish/km.

This is likely attributed to underestimated drift estimations due to net clogging. The highest two drift density scenarios appear to be more plausible because they predict carrying capacity in excess of the number of fish observed, a result consistent with the findings of others (Wall et al., 2015; Jensen, 2017), by a few hundred fish/km.

Overall, the carrying capacity for ARC is most likely maximized between 25 cfs to 32 cfs due to the maximums predicted by lower drift densities, and the presence of local maximums at higher drift densities. It is notable that for all scenarios of fish size, temperature, and drift density, 15 cfs was never predicted as the optimal discharge and often predicted significantly less trout. The 25th and 75th (Figures A.1.1, A.1.2, A.1.3) percentile temperature scenarios produce similar results and can be found in Appendix 1.

2.4.3.3 Optimum Discharges: Below Monks Hollow

For BMH, the NREI model estimates maximum carrying capacity within the modeled range of flows (Figure 2.4.8). The NREI model predicts fish within the reach for each scenario of drift and temperature except for low drift density scenarios for large adult trout. The carrying capacity is sensitive to changes in drift and temperature for juvenile (100 mm) and young adult (150 mm) sizes and is largest for flows around 20 cfs to 40 cfs. Like the results for ARC, the model indicates that drift may be insufficient for large adult fish (300 mm) because it only predicts fish at the highest drift density, resulting in a maximum at 30 cfs.

We compared the observed fish densities of August, as estimated from drift-feeding salmonids sampled within the reach, to the 150 mm size class because the mean length of sampled fish was 162 mm for ARC, and observed that the two lowest drift densities underestimated carrying capacity by a several hundred fish/km. The second

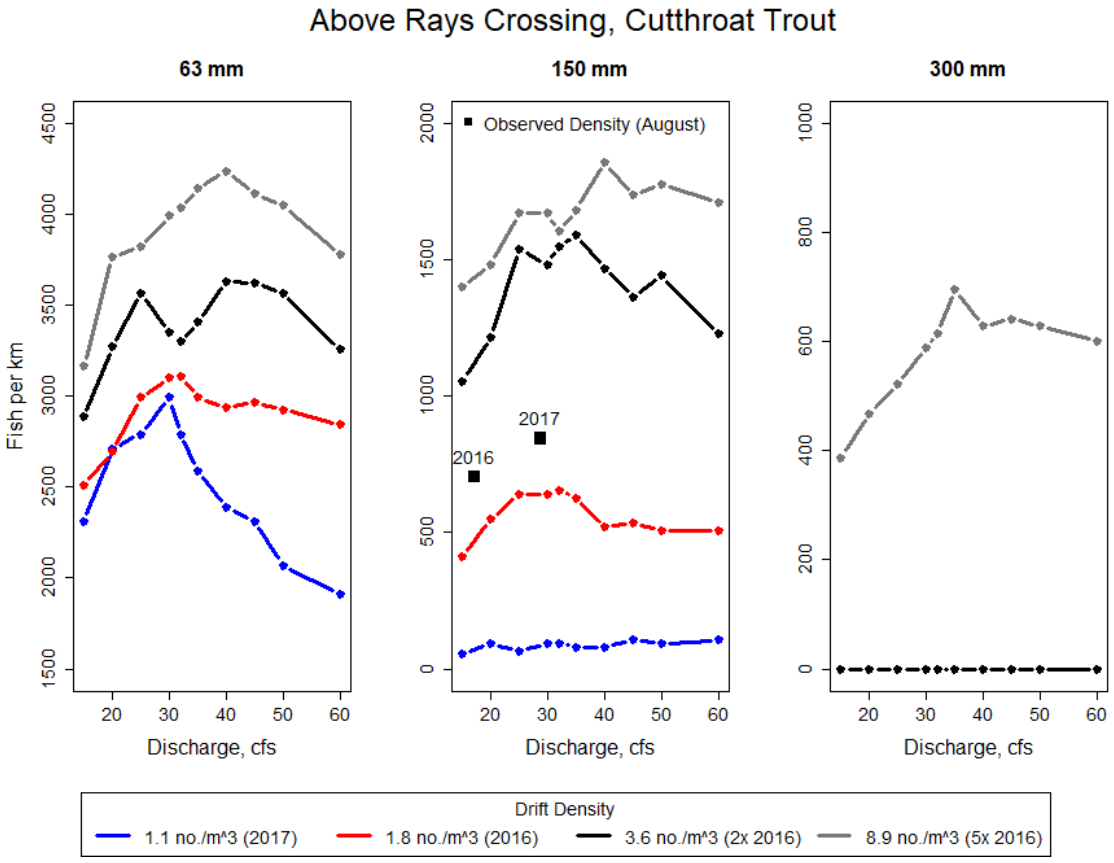

Figure 2.4.7. Net rate of energy intake (NREI) model results of Bonneville cutthroat trout capacity in Sixth Water Creek given August 2016 (1.8 no/m3, red line), August 2017 (1.1 no/m3, blue line), 2x August 2016 (3.6 no/m3, black line), and 5x August 2016 (8.9 no/m3, grey line), given median temperatures from August and September 2016. Observed fish densities consist of all drift-feeding salmonids (population estimate for Bonneville cutthroat trout, rainbow trout, and brown trout) from August 2016 (n = 703 fish/km) and 2017 (n = 845 fish/km) fish sampling events in order to best approximate an "observed carrying capacity" for comparison with NREI model results. The mean fish length from those samples is 162 mm; the mean Bonneville cutthroat trout length is 164 mm.

highest drift density scenario only under predicts the observed fish density while the highest drift density over predicts by a few hundred. Like ARC, it is likely that the two highest drift density scenarios produce more realistic results.

Overall, carrying capacity for BMH is maximized for flows below 40 cfs. The mandated summer flow of 80 cfs was not predicted as the optimal discharge for the reach

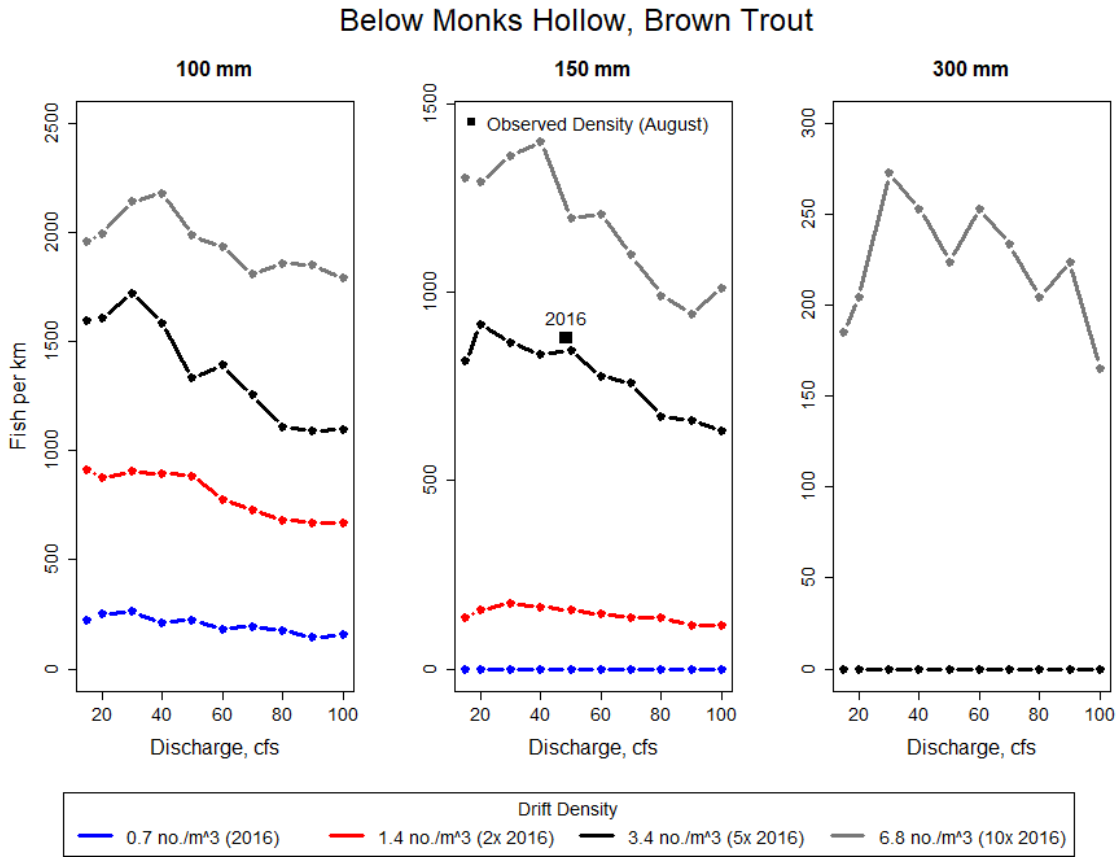

Figure 2.4.8. Net rate of energy intake model results of brown trout capacity in Diamond Fork Creek given August 2016 (0.7 no/m3, blue line), 2x August 2016 (1.4 no/m3, red line), 5x August 2016 (3.4 no/m3, black line), and 10x August 2016 (6.8 no/m3, grey line), given median temperatures from August and September 2016 and 2017. Observed fish densities consist of all drift-feeding salmonids (population estimate for Bonneville cutthroat trout and brown trout) from the August 2016 (n = 878 fish/km) fish sampling event in order to best approximate an "observed carrying capacity" for comparison with NREI model results. The mean fish length from the sample is 167 mm; the mean brown trout length is 167 mm.

and supported significantly fewer trout in the majority of scenarios (Figure 2.4.9).

Additionally, 15 cfs was never predicted as an optimal discharge. Scenarios from the 25th and 75th percentile temperatures produced similar results (Figures A.1.4, A.1.5, A.1.6).

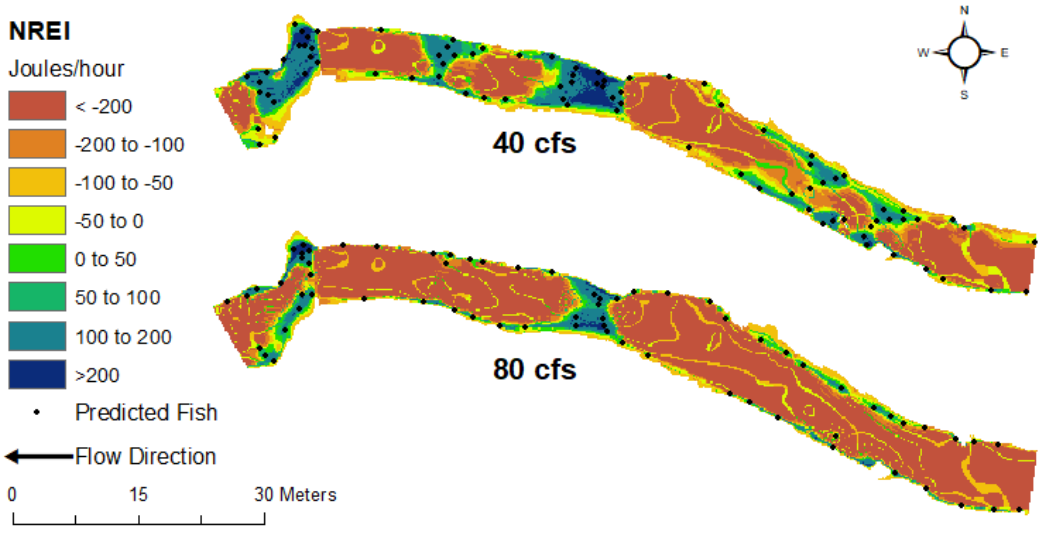

Figure 2.4.9. Net rate of energy (NREI) model results of 40 cfs (top) and 80 cfs (bottom) at the Below Monks Hollow site given the 50th percentile temperature (13.9° C) and a drift density of 3.4 no/m^3. Predicted fish locations are shown as black points.

2.4.4 Stream Width as a Function of Discharge

Width measurements from sites within the lower Diamond Fork indicate that a decrease in flow does result in a decrease in wetted width. The data was fitted with a power function resulting in Equation 2.5, which has a r-squared value of 0.7:

$$W = 3.6 * Q^{0.7} \text{ (lower Diamond Fork)} \quad (2.5)$$

where W is the wetted width (m) and Q is the discharge (cfs) (Figure 2.4.10). A decrease from 80 cfs to 40 cfs results in a width decrease of about 1.1 meters (8.5 m to 7.4 m).

2.4.5 Diamond Fork System Compared to Blue Ribbon Fisheries and Reference Streams

Our hydrologic analysis comparing Blue Ribbon and reference streams to the Diamond Fork system indicates that baseflows for Diamond Fork River and Sixth Water

Creek are on average 3-4 times larger and exceed the 90th percentile streamflow of Blue Ribbon and reference streams (Figure 2.4.11). The augmented flow regime of the Diamond Fork system generates stable flows that exhibit little variability; maximum flows are small relative to the annual discharge. These characteristics are not seen in the majority Blue Ribbon or reference stream hydrographs.

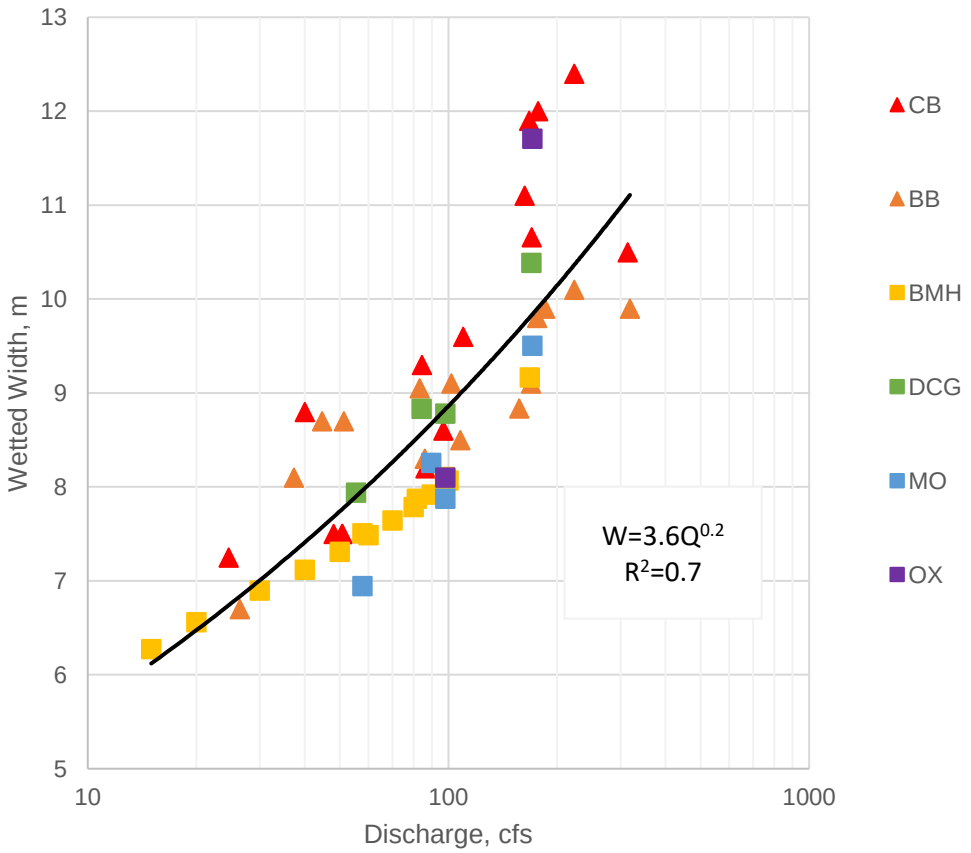

Figure 2.4.10. Wetted width as a function of discharge from sites in the lower Diamond Fork. Width from discharge measurements taken at CB and BB are indicated as triangles, reach averaged widths (wetted area / reach length) from BMH (from HEC-RAS modeling), DCG, MO, and OX (from surveyed water extents) are indicated as squares.

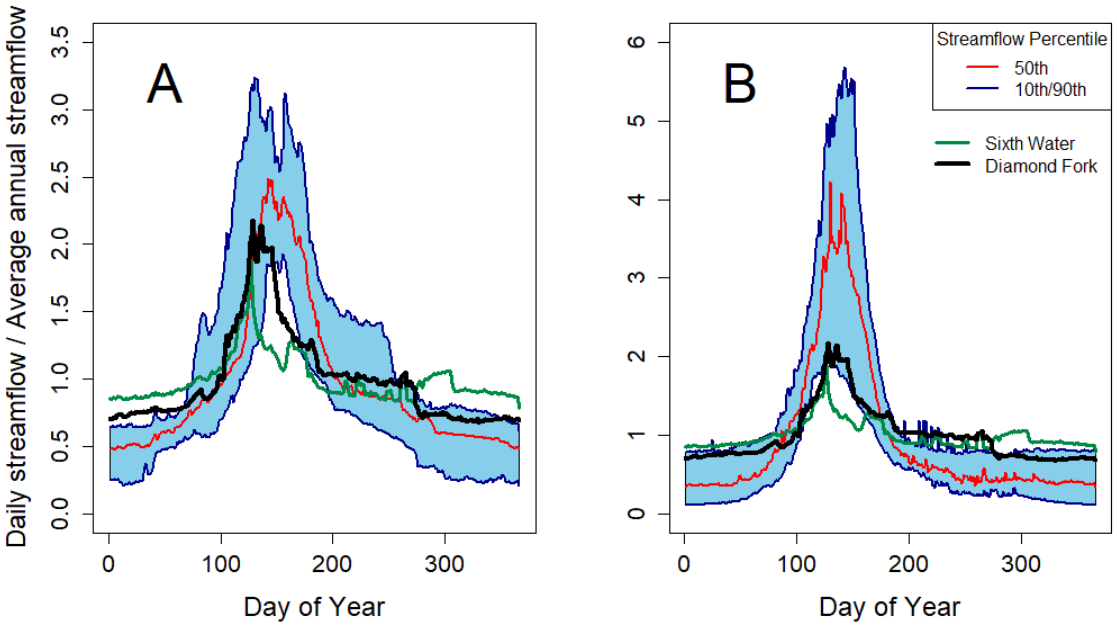

Figure 2.4.11. Dimensionless hydrographs comparing the Diamond Fork River (black line) and Sixth Water Creek (dark green line) to A) Blue Ribbon streams in Utah and B) reference streams within 400 km of the Diamond Fork USGS gage (station ID: 10149400) that have similar basin characteristics as the Diamond Fork watershed.

2.5 Discussion

Our study was designed to evaluate the instream flow requirements for trout in a geomorphically altered river with an augmented flow regime using drift-foraging, or net rate of energy intake, models. Compared to other approaches, the drift-forage modeling approach has been shown to provide more biologically realistic information for flow requirements of drift-feeding salmonids (Rosenfeld et al., 2014, Hayes et al., 2016) by evaluating how the amount of available habitat shifts in response to prey availability and temperature, in addition to depth and velocity. By evaluating the shape and relative changes in carrying capacity in response to discharge, drift density, and temperature, and comparing the results to observed fish densities, we can identify a reasonable range of

flows providing favorable carrying capacity for both BMH and ARC. We examined a range of drift densities to evaluate the uncertainty associated with the small number of drift samples, the effects of net clogging during sampling, and the assumptions of spatially-uniform and flow-constant drift densities. We found, confirming other studies (Hayes et al., 2016; Rosenfeld et al., 2014) that the model is highly sensitive to drift density as well as temperature. The results of our modeling effort compliment the fisheries and aquatic macroinvertebrate studies for the Diamond Fork system by identifying similar trends and flows where fish and macroinvertebrate densities are maximized (Epperly, 2018; Wilcock et al., 2019).

2.5.1 The drift-forage model and instream flow evaluation

Drift-forage models have been recognized for their potential in evaluating instream flow regimes (Hayes et al., 2016; Rosenfeld et al, 2014). These models are generally applied to a single flow, which would be representative of steady flow conditions over a long period of time (Hayes et al., 2016), such as baseflow. The intense procedure to continuously model the fluctuations of NREI and carrying capacity using a drift-forage model in order to capture all aspects of a flow regime (floods, droughts, rapid changes in flow) would require an immense amount of time and effort, especially to incorporate the appropriate seasonal dynamics of drift and temperature. Therefore, we argue that drift-foraging models are currently best suited to evaluate a range of steady state flow regimes, such as the augmented or depleted baseflow regimes produced by water diversions or dam releases.

For the Sixth Water Creek site, ARC, the range of optimal flows for cutthroat trout shifts towards higher flows as drift density increases – a finding similar to Hayes et

al. (2016), who observed that larger drift densities shifted the largest potential carrying capacity towards larger flows as trout were able to occupy more energetically expensive locations by consuming more food (Railsback and Harvey, 2011). Carrying capacity for ARC was maximized between flows of 25 cfs to 32 cfs for lower drift densities while maximized at flows between 35 cfs to 40 cfs for higher drift densities (while maintaining a local maximum at 25 cfs). Epperly (2018) found using a Random Forest statistical model that benthic density (and indirectly drift density) for Sixth Water Creek increased as the maximum flow within a 90-day period prior to sampling decreased. The LME models showed no significant relation between flow and the benthic density of macroinvertebrates (Epperly, 2018). While these results provide insight regarding the sensitivity of the benthic community to the flood regime of Sixth Water Creek, it provides little information on the baseflow requirements for macroinvertebrates and how they might compare to NREI model results.

We compared the NREI model results for the 63 mm cutthroat trout at ARC to a stock-recruitment model for Sixth Water Creek (Wilcock et al., 2019) that was developed to identify flows at which recruitment was maximized. The stock-recruitment model, which is a mixed effects statistical model (entirely independent from the methods and results for the NREI models), uses mean summer flow (June – September) as a predictor of recruitment *a priori*. It indicates that 1) recruitment is maximized for flows below 18.5 cfs, 2) little recruitment is predicted for flows above 30 cfs, and 3) no recruitment is predicted for flows above 40 cfs. These results differ from the NREI model results, for which carrying capacity is predicted as significantly lower for flows below 20 cfs and maximized for flows above 30 cfs in scenarios of higher drift density. This difference

may be because the stock-recruitment model implicitly incorporates all habitat features that juvenile sized fish take advantage of throughout the of the reach (i.e., boulders, woody debris, undercut banks), but does not actually incorporate them as actual model inputs. Potential weaknesses from the stock recruitment model (i.e., small number of individuals) or the NREI model (i.e., drift uncertainty, model assumptions, model resolution) could also be the cause of such differences.

The common ground between the two models is that carrying capacity in the NREI models have local and absolute maximums at flows below 30 cfs. Considering results of both approaches, along with the fact that chronic concentrations of selenium for trout are reached for flows below 20 cfs (Wilcock et al., 2019), it is likely that the beneficial range of flows for trout in Sixth Water Creek is between 20 cfs to 30 cfs given the current channel configuration; the current mandated summer flow regime of 32 cfs is on the margin of this range.

For the lower Diamond Fork site, BMH, we observed that the mandated summer baseflow regime of 80 cfs is an energetically expensive environment for brown trout and much too large when compared to Blue Ribbon streams in Utah and other reference streams (Figure 2.4.11). Flows below 40 cfs provide more suitable brown trout habitat within the current channel. Epperly (2018) found using a linear mixed effects (LME) model that the benthic density of aquatic macroinvertebrates (organisms/m^2) within the lower Diamond Fork exponentially decreased as flows increased. His model, which modeled flows from 40 cfs to over 160 cfs, showed that benthic density was greatest at approximately 40 cfs and decreased by almost half at 80 cfs. He also showed that there was a positive correlation between drift density (organisms/m^2) and benthic density. For

the lower Diamond Fork, it is likely that drift decreases as flow increases, with the highest drift densities occurring at flows around 40 cfs, which in turn would result in a higher carrying capacity. The flow-varying nature of the benthic community and subsequently the drift community as described by Epperly (2018), combined with our results provide substantial evidence as to the beneficial nature of a lower baseflow regime for the lower Diamond Fork, given its current channel geometry.

2.5.2 Key factors and limitations of drift-forage models

Drift-forage models provide process-based results that are easily interpreted and used in understanding the physical-ecological interactions of drift feeding individuals and populations. However, reliable use of these models depends on accurate estimates of model parameters and inputs. Rosenfeld et al. (2014) discusses in detail factors that limit the successful application of drift forage models. Key factors include estimates for swimming cost and capture success (Hill and Grossman, 1993; Grossman et al., 2002; Piccolo et al., 2008; Rosenfeld and Taylor, 2009). Variables such as velocity, turbulence, fish size, distance of prey from the focal point, and temperature all affect the capture success and swimming costs of drift-feeding salmonids (Hill and Grossman, 1993; Van Winkle et al., 1998; Nislow et al., 1999; Grossman et al., 2002; Piccolo et al., 2008; Watz and Piccolo, 2011; Boisclari and Tang, 1993; Hughes and Kelly, 1996; Enders et al., 2003). Failure to account for these variables and how they affect the swimming cost and capture success functions may limit model reliability.

Other major challenges lay within the collection of data, model parameterization and model validation. Drift-forage applications that are linked to hydraulic models require accurate stream topography for reliable predictions (Rosenfeld et al. 2014).

Methods for collecting high resolution topography have been greatly improved (Heritage et al., 2009; Bouwes et al., 2011; Milan et al., 2011; Marcus, 2012), allowing for the development of high resolution hydraulic models which can be used for drift-forage modeling purposes (Hayes et al., 2007; Wall et al., 2015; Nahorniak et al., 2018).

For shallow, rough streams, such as the Diamond Fork River and Sixth Water Creek, converting the 2D hydraulic models to 2.5D hydraulic models using a logarithmic velocity profile could produce bias by misrepresenting the vertical flow field. In low submergence situations such as baseflow, where the depth of the water is less than 10 times the roughness height, turbulent wakes of large roughness elements (boulders, woody debris, gravel bars) cause the form drag to become relatively large (Ferguson, 2007). This can cause considerable disagreement between observed velocities and calculated velocities (Rickenman et al., 2011) which could potentially eliminate foraging positions for fish as predicted by the NREI models.

The accurate characterization of energy flux (drift) is one of the most important variables in producing credible drift-forage models (Hayes et al., 2016; Rosenfeld et al., 2014). Factors such as net clogging can greatly reduce drift density (Slack et al. 1991; Muehlbauer et al. 2017; Mureithi et al. 2018) and bias NREI predictions low. Piscivory, is another avenue by which the NREI predictions may be biased low, particularly for larger drift-feeding salmonids who tend to have a more diverse diet. For example, a fish diet analysis (Wilcock et al. 2019) indicated that for the lower Diamond Fork, 19.6 percent of the diet for brown trout, >200 mm in length, consisted of fish. This could result in as much as a 13 percent energetic advantage, or more, compared to only consuming drift (based on a 2725 J/g energy density of a mayfly, James et al., 2011; and

4500 J/g energy density for juvenile brown trout, Johnson et al., 2017).

Most studies using drift-forage models assume spatially uniform drift concentrations (Hughes et al., 2003; Railsback et al., 2009; Jenkins and Keely, 2010; Urabe et al., 2010; Rosenfeld and Ptolemy, 2012; Wall et al., 2015; Jensen, 2017; McHugh et al., 2018). Hayes et al. (2007; 2016) uses a more complex drift dispersion model to predict the spatial distribution of drift, however, the correct parameterization of this model (invertebrate entry rates, settling velocities, drift depletion, model validation) can be a time consuming and challenging task (Rosenfeld et al., 2014). Hayes et al., (2016) showed that flow-varying drift produces more pronounced peaks in carrying capacity than flow-constant drift, but it requires more data to create the drift-discharge relations. The assumption of spatially uniform, flow-invariant drift density requires significantly less time and data to model, but it smooths out important details that could be crucial for understanding the energetic dynamics of a reach. Modeling several magnitudes of drift may help address some of the uncertainty produced by using a flow-invariant, spatially uniform drift approach; however, it does not outcompete the dynamic, more realistic nature of a flow-varying drift dispersion model. Correct understanding and parameterization of a drift dispersion model is paramount in achieving realistic predictions (Rosenfeld et al., 2014).

2.5.3 Instream Flows and Channel Change

The drift-forage models used in this study, and other models for the macroinvertebrates and fish of the Diamond Fork system (Epperly, 2018; Wilcock et al. 2019), provide useful insight regarding ecosystem health of the Diamond Fork system and how that might change under a different flow regime. However, these relations

between flow and ecology are highly dependent on the current channel configuration. The current flow regime was determined using habitat-hydraulic simulation models (PHABSIM) for the wider, potentially topographically more variable, channel of the late 1990s and early 2000s. For Sixth Water Creek, minimal channel adjustment has been observed since then (Jones, 2018). We assume the stability of the channel is the major reason for the similarities between our results for an optimal range of flow at ARC and the current flow regime of Sixth Water Creek. In the lower Diamond Fork, the channel has considerably narrowed since the late 1990s and early 2000s. The relevance of the mandated flow regime has decreased as a result of channel narrowing and its effect on the flow field.

Jones (2018) suggests that if the current summer baseflows were to be lowered, the lower Diamond Fork channel would likely narrow even further. He proposed that the augmented baseflows may limit channel narrowing by inundating the margins of the channel that would otherwise establish vegetation and collect sediment, build banks, and narrow the channel. Hydraulic geometry for the lower Diamond Fork indicates that a decrease in summer baseflow from 80 cfs to 40 cfs would decrease the wetted width of the stream by 1.1 meters – which could potentially narrow the channel by an equivalent amount.

The evolution of the Diamond Fork would suggest that a reduction in channel width would cause channel simplification and associated habitat degradation. We argue the contrary. Sediment transport within the lower Diamond Fork River is modest and the bed is only partially mobile during regularly occurring floods (Jones, 2018; Wilcock et al., 2019). Sediment transport competence is near it's threshold as indicated by field

observations and gravel tracer experiments (Jones, 2018; Wilcock et al., 2019). A narrower flow width during flood events would cause flows to deepen, velocities to increase (Leopold and Maddock, 1953), and bed shear stress to increase. With an increase of shear stress, and given that sediment mobility is near it's threshold, it is likely that sediment transport could substantially increase (Wilcock et al., 2019). The increased transport would ideally produce a more dynamic and varied topography as pools are scoured and bars are amplified. We observe this phenomenon in sections of the lower Diamond Fork (i.e., MO, above CB) where the channel width is narrower than average and large bars force deep pools: providing prime habitat for trout.

The NREI models indicated that NREI values were greatest in pools and that more fish were placed into them compared to riffles and run. Trout tend to hold in locations where there is an intermediate velocity or a sharp gradient in velocity (i.e., shear zones) (Hill and Grossman, 1993; Fausch, 1984) in order to optimize energy spent swimming, and the amount of food encountered (Grossman et al., 2002). The energetic and predatory refuge provided by pools is a good example of this (Rosenfeld and Boss (2001). Wall (2014) showed that overall NREI and carrying capacity increased by manipulating the instream habitat through the use of woody debris in order to scour pools and diversify hydraulic habitat. An increase in pool habitat within the lower Diamond Fork as a result of narrowing would be beneficial to trout.

The complicated nature of channel change in relation to instream flows highlights the importance for adaptive management. Understanding pool dynamics within the river and how they may change under different flow, sediment, and channel configuration constraints is important. Continued monitoring of streams after flow alterations is key in

determining the success of a prescribed flow regime (Poff et al., 2010).

2.5.4 Management Implications and Future Research Needs

Management of riverine ecosystem health through instream flow requirements has developed over the years into a broad and diverse area of research. For individual, drift-feeding salmonid species, drift-forage models are an avenue to connect flow, habitat, and ecological functions in a comprehensive way. The variety of key factors considered by these models allow managers to investigate processes and conditions influencing the success of fish populations (Hayes et al. 2016). The ability of the drift-forage model to predict a carrying capacity, and its correlation with observed fish biomass and abundance (Urabe et al. 2010; Jenkins and Keeley, 2010; Wall et al. 2015) is a more useful, reliable, and interpretable metric than standard WUA methods. These allow managers to evaluate if reaches are being utilized to their fullest extent or if alterations in flow (and geomorphic units such as pools) can help optimize biological conditions. Drift-forage models provide insight regarding a range of flows that are most beneficial for trout in a reach. However, comprehensive instream flow evaluations should incorporate multiple reaches throughout a stream so that the wider range of instream habitat variability is represented.

It is widely accepted that a naturally variable flow regime is better than minimum instream flow requirements in order to create healthy riverine ecosystems (Poff et al., 1997; Bunn and Arthington, 2002; Postel and Richter, 2003; Annear et al., 2004; Biggs et al., 2005; Poff et al., 2010). Year-to-year flow variability is important in supporting native species, whose life histories are adapted to such changes (Lytle and Poff, 2004). The identified range of flows for the Diamond Fork system gives managers flexibility in

managing flows to optimize ecosystem health while incorporating hydrologic variability, while considering confounding factors such as climate change, water withdrawal restraints, and water rights.

As the science of instream flows progresses, drift-forage models should be used to better understand the flow needs for drift-feeding salmonids (Hayes et al. 2016). Further research and development of drift modeling is necessary so that realistic drift dynamics can be modeled reliably. Finding affordable, time effective ways to collect and process drift, geomorphic, and hydraulic data is crucial for this modeling approach to be accepted by a larger group of managers and scientists. This should include research into the parameterization of drift dynamics and better support for estimating spatial, temporal, and longitudinal changes in drift density (Rosenfeld et al., 2014). Nahorniack et al. (2018) showed that rapid processing of geomorphic data and hydraulic modeling is possible. Using their approach to assess multiple reaches can help cut processing time and costs associated with modeling. The incorporation of channel change in response to changes in flow is imperative so that instream flow requirements remain relevant over longer periods of time.

For the Diamond Fork River and Sixth Water Creek, our study showcases the application of a drift-forage model and its usefulness in evaluating an augmented baseflow regime for a geomorphically altered river. Our results inform managers of potential flow requirements that will benefit trout populations in both streams. Adaptive management techniques are required to ensure the longevity and effectiveness of instream flow prescriptions as the channel adjusts to future alterations in flow and sediment.

References

Allan, J. D. (1982). The effects of reduction in trout density on the invertebrate community of a mountain stream. *Ecology*, *63*(5), 1444-1455.

Anderson, K. E., Paul, A. J., McCauley, E., Jackson, L. J., Post, J. R., & Nisbet, R. M. (2006). Instream flow needs in streams and rivers: the importance of understanding ecological dynamics. *Frontiers in Ecology and the Environment*, *4*(6), 309-318.

Annear, T., Chisholm, I., Beecher, H., Locke, A., Aarrestad, P., Burkhart, N., Coomer, C., Estes, C., Hunt, J., Jacobson, R. and Jobsis, G., 2004. *Instream flows for riverine resource stewardship*. Revised edition. Instream Flow Council, Cheyenne, Wyoming.

Armitage, P. D., Pardo, I., & Brown, A. (1995). Temporal constancy of faunal assemblages in'mesohabitats'—application to management?. *Archiv für Hydrobiologie*, *133*(3), 367-387.

Arthington, A. H., Bunn, S. E., Poff, N. L., & Naiman, R. J. (2006). The challenge of providing environmental flow rules to sustain river ecosystems. *Ecological applications*, *16*(4), 1311-1318.

Bangen, S. G., Wheaton, J. M., Bouwes, N., Bouwes, B., & Jordan, C. (2014). A methodological intercomparison of topographic survey techniques for characterizing wadeable streams and rivers. *Geomorphology*, *206*, 343-361.

Barnes, H. H. (1967). *Roughness characteristics of natural channels* (No. 1849). US Govt. Print. Off.,.

Beauchamp, D. A., Lariviere, M. G., & Thomas, G. L. (1995). Evaluation of competition and predation as limits to juvenile kokanee and sockeye salmon production in Lake Ozette, Washington. *North American Journal of Fisheries Management*, *15*(1), 193-207.

Biggs, B. J., Nikora, V. I., & Snelder, T. H. (2005). Linking scales of flow variability to lotic ecosystem structure and function. *River Research and Applications*, *21*(2-3), 283-298.

BIO-WEST, Inc. (2007). Sixth Water and Diamond Fork Creeks Final 2006 Monitoring Report.

Boisclair, D., & Tang, M. (1993). Empirical analysis of the influence of swimming pattern on the net energetic cost of swimming in fishes. *Journal of Fish Biology*, *42*(2), 169-183.

Blue Ribbon Fisheries. (n.d.). Retrieved from https://wildlife.utah.gov/blue-ribbon-fisheries.html

Bouwes, N., Moberg, J., Weber, N., Bouwes, B., Bennett, S., Beasley, C., ... & Semmens, B. (2011). Scientific protocol for salmonid habitat surveys within the Columbia Habitat Monitoring Program. *Integrated Status and Effectiveness Monitoring Program, Wauconda, WA*, 118.

Brierley, G.J. and Fryirs, K.A, (2005). *Geomorphology and River Management: Applications of the River Styles Framework*. Blackwell Publications.

Brunner W. Gary. (2016). HEC-RAS, River Analysis System, 2D Modeling User's Manual version 5.0. Printed and Distributed by US Army Corps of Engineers Hydrologic Engineering Center (HEC).

Bunn, S. E., & Arthington, A. H. (2002). Basic principles and ecological consequences of altered flow regimes for aquatic biodiversity. *Environmental management*, *30*(4), 492-507.

Carle, F. L., & Strub, M. R. (1978). A new method for estimating population size from removal data. *Biometrics*, 621-630.

Casulli, V. (2009). A high-resolution wetting and drying algorithm for free-surface hydrodynamics. *International Journal for Numerical Methods in Fluids*, *60*(4), 391-408.

Cattanéo, F., Lamouroux, N., Breil, P., & Capra, H. (2002). The influence of hydrological and biotic processes on brown trout (Salmo trutta) population dynamics. *Canadian journal of fisheries and aquatic sciences*, *59*(1), 12-22.

Davies, B. R., Hall, A., & Jackson, P. B. N. (1975). Some ecological aspects of the Cabora Bassa dam. *Biological Conservation*, *8*(3), 189-201.

Dieterman, D. J., Thorn, W. C., & Anderson, C. S. (2004). *Application of a bioenergetics model for brown trout to evaluate growth in southeast Minnesota streams*. Minnesota Department of Natural Resources, Policy Section, Fisheries and Wildlife Division.

Dunbar, M., Gustard, A., Acreman, M. C., & Elliott, C. R. (1998). *Overseas approaches to setting river flow objectives*. Environment Agency.

Dyson, M., Bergkamp, G., & Scanlon, J. (2003). Flow: the essentials of environmental flows. *IUCN, Gland, Switzerland and Cambridge, UK*, 20-87.

Enders, E. C., Boisclair, D., & Roy, A. G. (2003). The effect of turbulence on the cost of swimming for juvenile Atlantic salmon (Salmo salar). *Canadian Journal of Fisheries and Aquatic Sciences*, *60*(9), 1149-1160.

Epperly, Joshua A., "The Effects of Enhanced Flows on Community Structure and Ecosystem Functioning in a Montane Utah River System" (2018). *All Graduate Theses and Dissertations*. 7223. https://digitalcommons.usu.edu/etd/7223

Fausch, K. D. (1984). Profitable stream positions for salmonids: relating specific growth rate to net energy gain. *Canadian journal of zoology*, *62*(3), 441-451.

Ferguson, R. (2007). Flow resistance equations for gravel-and boulder-bed streams. *Water resources research*, *43*(5).

Filbert, R. B., & Hawkins, C. P. (1995). Variation in condition of rainbow trout in relation to food, temperature, and individual length in the Green River, Utah. *Transactions of the American Fisheries Society*, *124*(6), 824-835.

Fraser, J. C. (1972). Regulated discharge and the stream environment. In *River ecology and man* (pp. 263-285).

Gill, D. (1971, January). Damming the Mackenzie: A theoretical assessment of the long-term influence of river impoundment on the ecology of the Mackenzie River Delta. In *Proc. Peace Athabasca Delta Symposium* (pp. 204-222).

Gordon, N. D., McMahon, T. A., Finlayson, B. L. (2002). *Stream hydrology: an introduction for ecologists*. John Wiley and Sons, New York, 526 pp.

Grossman, G. D., Rincon, P. A., Farr, M. D., & Ratajczak Jr, R. E. (2002). A new optimal foraging model predicts habitat use by drift-feeding stream minnows. *Ecology of Freshwater Fish*, *11*(1), 2-10.

Hayes, J. W., Stark, J. D., & Shearer, K. A. (2000). Development and test of a whole-lifetime foraging and bioenergetics growth model for drift-feeding brown trout. *Transactions of the American Fisheries Society*, *129*(2), 315-332.

Hayes, J. W., Hughes, N. F., & Kelly, L. H. (2007). Process-based modelling of invertebrate drift transport, net energy intake and reach carrying capacity for drift-feeding salmonids. *Ecological Modelling*, *207*(2-4), 171-188.

Hayes, J. W., Goodwin, E., Shearer, K. A., Hay, J., & Kelly, L. (2016). Can weighted useable area predict flow requirements of drift-feeding salmonids? Comparison with a net rate of energy intake model incorporating drift–flow processes. *Transactions of the American Fisheries Society*, *145*(3), 589-609.

Heritage, G. L., Milan, D. J., Large, A. R., & Fuller, I. C. (2009). Influence of survey strategy and interpolation model on DEM quality. *Geomorphology*, *112*(3-4), 334-344.

Hill, J., & Grossman, G. D. (1993). An energetic model of microhabitat use for rainbow trout and rosyside dace. *Ecology*, *74*(3), 685-698.

Hughes, N. F., & Dill, L. M. (1990). Position choice by drift-feeding salmonids: model and test for Arctic grayling (Thymallus arcticus) in subarctic mountain streams, interior Alaska. *Canadian Journal of Fisheries and Aquatic Sciences*, *47*(10), 2039-2048.

Hughes, N. F., Hayes, J. W., Shearer, K. A., & Young, R. G. (2003). Testing a model of drift-feeding using three-dimensional videography of wild brown trout, Salmo trutta, in a New Zealand river. *Canadian Journal of Fisheries and Aquatic Sciences*, *60*(12), 1462-1476.

Hughes, N. F., & Kelly, L. H. (1996). A hydrodynamic model for estimating the energetic cost of swimming maneuvers from a description of their geometry and dynamics. *Canadian Journal of Fisheries and Aquatic Sciences*, *53*(11), 2484-2493.

Hynes, H. B. N., & Hynes, H. B. N. (1970). *The ecology of running waters* (Vol. 555). Liverpool: Liverpool University Press.

Imre, I., Grant, J. W. A., & Keeley, E. R. (2004). The effect of food abundance on territory size and population density of juvenile steelhead trout (Oncorhynchus mykiss). *Oecologia*, *138*(3), 371-378.

James, D. A., Csargo, I. J., Von Eschen, A., Thul, M. D., Baker, J. M., Hayer, C. A., ... & Chipps, S. R. (2011). A generalized model for estimating the energy density of invertebrates. Freshwater Science, 31(1), 69-77.

Jenkins, A. R., & Keeley, E. R. (2010). Bioenergetic assessment of habitat quality for stream-dwelling cutthroat trout (Oncorhynchus clarkii bouvieri) with implications for climate change and nutrient supplementation. *Canadian Journal of Fisheries and Aquatic Sciences*, *67*(2), 371-385.

Jensen, Martha L., "The Performance of a Bioenergetics Model in a System with an Abundant Population of Salmonids: A Case Study of Cutthroat Trout in the Logan River, Utah" (2017). *All Graduate Theses and Dissertations*. 5882. https://digitalcommons.usu.edu/etd/5882

Jobling, M. (1995). Simple indices for the assessment of the influences of social environment on growth performance, exemplified by studies on Arctic charr. *Aquaculture International*, *3*(1), 60-65.

Johnson, B. M., Pate, W. M., & Hansen, A. G. (2017). Energy Density and Dry Matter Content in Fish: New Observations and an Evaluation of Some Empirical Models. *Transactions of the American Fisheries Society*, *146*(6), 1262-1278.

Jones, Jabari C., "Historical Channel Change Caused by a Century of Flow Alteration on Sixth Water Creek and Diamond Fork River, UT" (2018). *All Graduate Theses and Dissertations*. 7353. https://digitalcommons.usu.edu/etd/7353

Kelly, L.H., Hay, J., Hughes, N.F., Goodwin, E., and Hayes, J.W. (2012). Flow related models for simulating river hydraulics, invertebrate drift transport, and foraging energetics of drift-feeding salmonids: user guide (version 1.1). *Cawthron Report 922*.

Kenney, T. A., Wilkowske, C. D., & Wright, S. J. (2007). Methods for estimating magnitude and frequency of peak flows for natural streams in Utah.

Legleiter, C. J., Roberts, D. A., & Lawrence, R. L. (2009). Spectrally based remote sensing of river bathymetry. *Earth Surface Processes and Landforms*, *34*(8), 1039-1059.

Lloyd, N., Quinn, G., Thoms, M., Arthington, A., Gawne, B., Humphries, P., & Walker, K. (2004). Does flow modification cause geomorphological and ecological response in rivers. *A literature review from an Australian perspective. CRC for Freshwater Ecology*, *57*.

Leopold, L. B., & Maddock, T. (1953). *The hydraulic geometry of stream channels and some physiographic implications* (Vol. 252). US Government Printing Office.

Lytle, D. A., & Poff, N. L. (2004). Adaptation to natural flow regimes. *Trends in ecology & evolution*, *19*(2), 94-100.

Marcus, W. A. (2012). Remote sensing of the hydraulic environment in gravel-bed rivers. *Gravel-bed rivers: Processes, tools, environments*, 259-285.

Mathur, D., Bason, W. H., Purdy Jr, E. J., & Silver, C. A. (1985). A critique of the in stream flow incremental methodology. *Canadian journal of fisheries and aquatic sciences*, *42*(4), 825-831.

McHugh, P. A., Saunders, W. C., Bouwes, N., Wall, C. E., Bangen, S., Wheaton, J. M., ... & Jordan, C. E. (2017). Linking models across scales to assess the viability and restoration potential of a threatened population of steelhead (Oncorhynchus mykiss) in the Middle Fork John Day River, Oregon, USA. *Ecological modelling*, *355*, 24-38.

Milan, D. J., Heritage, G. L., Large, A. R., & Fuller, I. C. (2011). Filtering spatial error from DEMs: Implications for morphological change estimation. *Geomorphology*, *125*(1), 160-171.

Milewski, C. L., & Brown, M. L. (1994). Proposed standard weight (Ws) equation and length-categorization standards for stream-dwelling brown trout (Salmo trutta). *Journal of Freshwater Ecology*, *9*(2), 111-116.

Muehlbauer, J. D., Kennedy, T. A., Copp, A. J., & Sabol, T. A. (2016). Deleterious effects of net clogging on the quantification of stream drift. *Canadian Journal of Fisheries and Aquatic Sciences*, *74*(7), 1041-1048.

Mureithi, P. W., Mbaka, J. G., M'Erimba, C. M., & Mathooko, J. M. (2018). Effect of drift sampler exposure time and net mesh size on invertebrate drift density in the Njoro River, Kenya. *African Journal of Aquatic Science*, *43*(2), 163-168.

Nahorniak, M., Wheaton, J., Volk, C., Bailey, P., Reimer, M., Wall, E., ... & Jordan, C. (2018). How do we efficiently generate high-resolution hydraulic models at large numbers of riverine reaches?. *Computers & geosciences*, *119*, 80-91.

Naiman, R. J., Bunn, S. E., Nilsson, C., Petts, G. E., Pinay, G., & Thompson, L. C. (2002). Legitimizing fluvial ecosystems as users of water: an overview. *Environmental management*, *30*(4), 455-467.

Nislow, K. H., Folt, C. L., & Parrish, D. L. (1999). Favorable foraging locations for young Atlantic salmon: application to habitat and population restoration. *Ecological Applications*, *9*(3), 1085-1099.

Orsborn, J.F. and C.H. Allman, (1976). Editors. Instream Flow Needs, Proceedings of the Boise Symposium, Idaho, May 1976. American Fisheries Society, Bethesda, Maryland.

Orth, D. J. (1987). Ecological considerations in the development and application of instream flow-habitat models. *Regulated rivers: research & management*, *1*(2), 171-181.

Penaz, M., Kubicek, F., Marvan, P., & Zelinka, M. (1968). Influence of the Vir River Valley Reservoir on the hydrobiological and ichthyological conditions in the River Svratka. *Acta sci. nat. Brno*, *2*(1), 1-60.

Petts, G. E. (2009). Instream Flow Science For Sustainable River Management 1. *JAWRA Journal of the American Water Resources Association*, *45*(5), 1071-1086.

Piccolo, J. J., Hughes, N. F., & Bryant, M. D. (2008). Water velocity influences prey detection and capture by drift-feeding juvenile coho salmon (Oncorhynchus

kisutch) and steelhead (Oncorhynchus mykiss irideus). *Canadian Journal of Fisheries and Aquatic Sciences*, *65*(2), 266-275.

Poff, N. L., Allan, J. D., Bain, M. B., Karr, J. R., Prestegaard, K. L., Richter, B. D., ... & Stromberg, J. C. (1997). The natural flow regime. *BioScience*, *47*(11), 769-784.

Poff, N. L., Richter, B. D., Arthington, A. H., Bunn, S. E., Naiman, R. J., Kendy, E., ... & Henriksen, J. (2010). The ecological limits of hydrologic alteration (ELOHA): a new framework for developing regional environmental flow standards. *Freshwater Biology*, *55*(1), 147-170.

Poff, N. L., & Zimmerman, J. K. (2010). Ecological responses to altered flow regimes: a literature review to inform the science and management of environmental flows. *Freshwater Biology*, *55*(1), 194-205.

Postel, S., & Richter, B. (2012). *Rivers for life: managing water for people and nature*. Island Press.

PRISM Climate Group. (2004). Oregon State University. *PRISM Climate Data*.

Railsback, S. F., Harvey, B. C., Jackson, S. K., & Lamberson, R. H. (2009). InSTREAM: the individual-based stream trout research and environmental assessment model. *Gen. Tech. Rep. PSW-GTR-218. Albany, CA: US Department of Agriculture, Forest Service, Pacific Southwest Research Station. 254 p*, *218*.

Railsback, S. F., & Harvey, B. C. (2011). Importance of fish behaviour in modelling conservation problems: food limitation as an example. *Journal of Fish Biology*, *79*(6), 1648-1662.

Railsback, S. F., & Rose, K. A. (1999). Bioenergetics modeling of stream trout growth: temperature and food consumption effects. *Transactions of the American Fisheries Society*, *128*(2), 241-256.

Raleigh, R. F., Zuckerman, L. D., & Nelson, P. C. (1984). *Habitat suitability index models and instream flow suitability curves: brown trout* (No. 82/10.124). US Fish and Wildlife Service.

Richter, B. D., Baumgartner, J. V., Powell, J., & Braun, D. P. (1996). A method for assessing hydrologic alteration within ecosystems. *Conservation biology*, *10*(4), 1163-1174.

Rickenmann, D., & Recking, A. (2011). Evaluation of flow resistance in gravel-bed rivers through a large field data set. *Water Resources Research*, *47*(7).

Rosenberg, D. M., McCully, P., & Pringle, C. M. (2000). Global-scale environmental effects of hydrological alterations: introduction. *AIBS Bulletin*, *50*(9), 746-751.

Rosenfeld, J. S., & Boss, S. (2001). Fitness consequences of habitat use for juvenile cutthroat trout: energetic costs and benefits in pools and riffles. *Canadian Journal of Fisheries and Aquatic Sciences*, *58*(3), 585-593.

Rosenfeld, J. S., Bouwes, N., Wall, C. E., & Naman, S. M. (2014). Successes, failures, and opportunities in the practical application of drift-foraging models. *Environmental biology of fishes*, *97*(5), 551-574.

Rosenfeld, J. S., & Ptolemy, R. (2012). Modelling available habitat versus available energy flux: do PHABSIM applications that neglect prey abundance underestimate optimal flows for juvenile salmonids?. *Canadian journal of fisheries and aquatic sciences*, *69*(12), 1920-1934.

Rosenfeld, J. S., & Taylor, J. (2009). Prey abundance, channel structure and the allometry of growth rate potential for juvenile trout. *Fisheries Management and Ecology*, *16*(3), 202-218.

Scott, D., & Shirvell, C. S. (1987). A critique of the instream flow incremental methodology and observations on flow determination in New Zealand. In *Regulated streams* (pp. 27-43). Springer, Boston, MA.

Shirvell, C. S. (1986). Pitfalls of physical habitat simulation in the instream flow incremental methodology. *Canadian Technical Report of Fisheries and Aquatic Sciences* 1460.

Slack, K. V., Tilley, L. J., & Kennelly, S. S. (1991). Mesh-size effects on drift sample composition as determined with a triple net sampler. *Hydrobiologia*, *209*(3), 215-226.

Smock, L. A. (1980). Relationships between body size and biomass of aquatic insects. *Freshwater biology*, *10*(4), 375-383.

Stalnaker, C.B., (1994). Evolution of Instream Flow Habitat Modelling. In: The Rivers Handbook, 2, P. Calow and G.E. Petts (Editors). Blackwell Scientific Publications, Oxford, United Kingdom, pp. 276-288.

Stalnaker, C., Lamb, B. L., Henriksen, J., Bovee, K., & Bartholow, J. (1995). The instream flow incremental methodology: a primer for IFIM. *NATIONAL BIOLOGICAL SERVICE FORT COLLINS CO MIDCONTINENT ECOLOGICAL SCIENCE C ENTER*.

Stout, J. (2017). Hydrologic Regime Classification of the Diamond Fork River, HydroShare, http://www.hydroshare.org/resource/d04841d1d5a247389fd48961e7c3e3d8

Tharme, R. E. (1996). Review of international methodologies for the quantification of the instream flow requirements of rivers. *Water Law Review: final report for policy development, South African Department of Water Affairs and Forestry. Freshwater Research Unit: University of Cape Town: Pretoria*.

Tharme, R. E. (2003). A global perspective on environmental flow assessment: emerging trends in the development and application of environmental flow methodologies for rivers. *River research and applications*, *19*(5-6), 397-441.

United States Congress. (1992). Public Law 102-575 – Reclamation Projects Authorization and Adjustment Act of 1992, 61 pp.

Urabe, H., Nakajima, M., Torao, M., & Aoyama, T. (2010). Evaluation of habitat quality for stream salmonids based on a bioenergetics model. *Transactions of the American Fisheries Society*, *139*(6), 1665-1676.

Vâelez de Escalante, S., & Warner, T. J. (1995). *The Domâinguez-Escalante Journal : Their Expedition Through Colorado, Utah, Arizona, and New Mexico in 1776*. Salt Lake City: University of Utah Press. Retrieved from http://dist.lib.usu.edu/login?url=http://search.ebscohost.com/login.aspx?direct=true&db=nlebk&AN=10415&site=ehost-live

Vannote, R. L., & Sweeney, B. W. (1980). Geographic analysis of thermal equilibria: a conceptual model for evaluating the effect of natural and modified thermal regimes on aquatic insect communities. *The American Naturalist*, *115*(5), 667-695.

Van Winkle, W., Jager, H. I., Railsback, S. F., Holcomb, B. D., Studley, T. K., & Baldrige, J. E. (1998). Individual-based model of sympatric populations of brown and rainbow trout for instream flow assessment: model description and calibration. *Ecological Modelling*, *110*(2), 175-207.

Wall, C. Eric, "Use of a Net Rate of Energy Intake Model to Examine Differences in Juvenile Steelhead (Oncorhynchus mykiss) Densities and the Energetic Implications of Restoration" (2014). *All Graduate Theses and Dissertations*. 3880. https://digitalcommons.usu.edu/etd/3880

Wall, C. E., Bouwes, N., Wheaton, J. M., Saunders, W. C., & Bennett, S. N. (2015). Net rate of energy intake predicts reach-level steelhead (Oncorhynchus mykiss) densities in diverse basins from a large monitoring program. *Canadian journal of fisheries and aquatic sciences*, *73*(7), 1081-1091.

Ward, J. F. (1976). Comparative limnology of differentially regulated sections of a Colorado mountain river. *Archiv fur Hydrobiologie*, *78*(3), 319-342.

Watz, J., & Piccolo, J. J. (2011). The role of temperature in the prey capture probability of drift-feeding juvenile brown trout (Salmo trutta). *Ecology of freshwater fish*, *20*(3), 393-399.

Wilcock P., Atwood T., Belmont P., Epperly J., Gaeta J., Hammill E., Jones J. & Stout J. (2019). *Comprehensive study and recommendations for instream flow and requirements on Sixth Water Creek and Diamond Fork River: second interim report.* Department of Watershed Sciences, Utah State University.

Wolman, M. G. (1954). A method of sampling coarse river-bed material. *EOS, Transactions American Geophysical Union*, *35*(6), 951-956.

CHAPTER 3

POOL HABITAT FOR TROUT IN AN ALTERED GRAVEL-BED RIVER

3.1 Introduction

Instream habitat both directly and indirectly affects the ecology of aquatic species and influences the behavior and physiological traits of individuals and populations. Because of this, habitat is often used as a surrogate for biological integrity (Roper et al. 2002). Multiple studies have quantified physical habitat requirements for trout species by observing and modeling the locations where different life stages hold, forage, and spawn (Hickman and Raleigh, 1982; Raleigh et al., 1984; Rosenfeld and Boss, 2001; Harig and Fausch, 2002, Budy et al., 2012). For trout, depth, velocity, substrate, and cover are considered the most important physical habitat variables (Tonina and Jorde, 2013).

Although fish utilize many parts of the stream, many studies have shown trout preference for deeper channel units (Glova, 1984; Heggenes et al., 1991; Lonzarich and Quinn, 1995; Rosenfeld and Boss, 2001) because of the associated energetic and refuge advantages (i.e., predatory, thermal, oxygen) (Rosenfeld and Boss 2001, Hickman and Raleigh 1982, Elliot, 2000). Harig and Fausch (2002) report that models based on stream habitat attributes indicate that translocated trout can be limited by narrow stream width and a lack of deep pools. Young of year (YoY) trout are often more prevalent in riffles due to their ability to take advantage of marginal areas of low velocity, or the presence of larger, predatory trout in pools (Grant and Krammer, 1990; Moore and Gregory, 1988, Glova, 1986). However, pools are a habitat preference for YoY and a requirement for larger trout (Rosenfeld and Boss, 2001). Common standards for Bonneville cutthroat trout (*Oncorhynchus clarkii utah*) and brown trout (*Salmo trutta*) – the two trout species

associated with this study – are to have an equal number of pools and riffles, a channel area consisting of 40% to 60 % pools for cutthroat trout, and a channel area of 50% to 70% pools for brown trout (Hickman and Raleigh, 1982; Raleigh et al., 1984).

The pool-riffle sequence is a common geomorphic feature in gravel bed streams and provides habitat diversity both in terms of flow and sediment (Emery et al., 2003). Classic fluvial geomorphology indicates that pool-to-pool spacing is generally 5-7 channel widths in free formed pool-riffle reaches (Leopold and Wolman 1957; Leopold et al., 1964; Keller, 1972; Keller and Melhorn, 1978). In steeper, step-pool reaches, pool-to-pool spacing is on average 1-4 channel widths (Whittaker, 1987; Chin, 1989; Grant et al., 1990). Montgomery et al. (1995) showed that in forest channels, pool-to-pool spacing decreased from 13 channels widths to less than 1 channel width as LWD increased. Elements such as channel type, channel slope, substrate, LWD loading, channel width, are often highly correlated in the development and spacing of pools (Montgomery et al. 1995).

Pools can be naturally formed by bars and bends in the river, structurally forced by bedrock, boulders, large woody debris, and riparian vegetation, or built by "ecological engineers" such as beaver (Wheaton et al. 2015). Pools are generated as the local shear stress on the bed and banks increases due to flow convergence and turbulent velocity fluctuations, causing the channel bed to scour (Montgomery et al. 1995). They can also be formed through damming (i.e., log jams, beaver dams, landslides), which causes a backwater to form. Pool maintenance generally occurs when sediment, built up from low flow periods, is evacuated by flows equivalent to the 1- to 2-year flood, or even lower depending on the combinations of flow and the size and amount of sediment (Bayat et al.,

2017).

Changing flow and sediment regimes can alter the state of a river, particularly the instream habitat. The form of a river is the balance between channel slope, flow regime, sediment supply, and grain size (Lane, 1955; Leopold and Wolman, 1957; Schumm, 1977). As changes are made to one of more of these variables, the river will adjust its slope, geometry, or grain size to compensate. If these changes are sustained over sufficiently long periods, the river will eventually achieve equilibrium (Leopold and Maddock, 1953; Langbein and Leopold, 1964). There are many methods to predict and quantify channel change with regards to channel gradient, depth, width, grain texture, sinuosity, and planform (Schumm, 1985; Van Steeter and Pitlick, 1998; Kondolf et al., 2002; Liébault and Piégay, 2002; Dietrich et al., 1989; Lisle et al., 1993; Schmidt and Wilcock, 2008; Leopold and Maddock, 1953; James, 1991; Surian et al., 2009; Call et al., 2017; Lauer et al., 2017), however, these methods are often for reach averaged conditions. Tracking these changes over time can be difficult in many areas as streamflow and channel geometry data is limited. Most channel change studies focus on changes in width as historical aerial images and ground photos provide the only long term dataset that captures one of the variables pertaining to hydraulic geometry (Jones, 2018). This makes it possible to describe planform and geometric channel change over time due to changes in flow and sediment regimes.

It is far more difficult to describe instream habitat change over time due to flow and sediment regime alterations. Quantifying instream channel changes is highly reliant upon previous surveys of the stream channel. If surveys exist, channel change can be characterized by cross sections or topographic surveys. Although useful, section scale

surveys can be misleading because they are controlled by local hydraulics and may not be representative of longer reaches (Dean et al., 2016). Remote sensing techniques such bathymetric lidar and sonar make it possible to collect data at high resolutions over large distances. However, the lack of pre-existing data to complement such datasets complicates efforts to describe instream channel change over long time periods. Instead we are left to make inferences from aerial images and existing surveys about the past condition of a channel.

Multispectral aerial imagery has been used to perform continuous mapping of instream habitat, depths, stream power, wood, and other features for entire watersheds, provided that the quality of the image meets certain requirements (Marcus and Fonstad, 2008; Marcus and Fonstad, 2010; Marcus et al. 2003; Legleiter et al. 2004; Legleiter et al 2009; Tamminga et al. 2015; Winterbottom and Gilvear, 1997). Legleiter (2013) used spectral-based depth retrieval methods to map water depth on the Snake and Laramie Rivers in Wyoming using publically available imagery from The U.S. Department of Agriculture (USDA) National Agriculture Imagery Program (NAIP). Due to the coarseness of the images, water depth could not be estimated reliably for the narrower, Laramie River; whereas for the Snake River, a wider river, it performed reasonably well. Results for the Laramie River did indicate that the location of pools and bars could be determined. Legleiter (2013) suggested that due to the efficiency and non-invasive nature of image retrieval that channel change and stream conditions can be monitored using repeat images. For areas with limited instream habitat data, repeat public imagery could be used to coarsely monitor and examine the change of habitat, specifically the of location, number, and areal extent of pools and bars over time.

The Diamond Fork River and its tributary Sixth Water Creek have been subject to altered flow and sediment regimes. During the 20th century diversion flows, the stream was a wide, braided river (Jones, 2018), generally with a primary channel – as identified in aerial images and ground photographs. Since the completion of off-stream flow diversion infrastructure in 1996 and 2004, the channel has narrowed significantly. The confined valleys have experienced the least amount of channel narrowing whereas the partially confined and unconfined valleys have experienced the most narrowing (Jones, 2018). We suspect that instream channel habitat has simplified in concurrence with channel narrowing, as conversations with stakeholders have suggested that pools are generally lacking throughout the system and observations from BIO-WEST, Inc. (2009) indicate that runs were elongating and shortening riffles and pools. Assessing pool condition, number, and size in response to changes in flow and sediment is of interest as changes to the current flow regime are under consideration. The purpose of this chapter is to 1) document pool condition throughout the Diamond Fork system and how it has changed, 2) evaluate the role of flow, sediment, and channel change in pool condition, and 3) consider the role of future flows for improving pool condition. Because spawning gravel substrate is a potentially important element of pool habitat on Sixth Water Creek, we also describe the availability of spawning gravels suitable for Bonneville cutthroat trout (3-80 mm sized gravels, Budy et al., 2012).

3.2 Study Area

Jones (2018) delineated eight distinct process domains throughout the Diamond Fork River and its tributary Sixth Water Creek (Figure 2.2.5). A brief summary of these process domains is given in Chapter 2, with a full description of each provided by Jones

(2018). This chapter focuses on the six of the eight process domains, which contain most of the trout habitat in the system.

For Sixth Water Creek, our focus is on Upper Sixth Water Canyon, Sixth Water Meadows, Syar, and Lower Sixth Water Canyon (from the confluence with Fifth Water up to the Syar process domain) process domains. For the lower Diamond Fork, we focused on the lower two process domains in the lower Diamond Fork: Diamond Campground and Alluvial Valley, particularly from the Childs Bridge sediment transport sampling site to the Diamond Campground monitoring site (Figure 2.2.1).

3.3 Methods

3.3.1 Field Data Collection

3.3.1.1 Geomorphic Unit Mapping

We used the sampling protocol from the PACFISH/INFISH Biological Opinion Monitoring Program (PIBO) and the Geomorphic Unit Classification to identify, measure, and classify pools and other pool-like features (Archer et al., 2016, Wheaton et al. 2015). To characterize the full range of pool habitat, we collected data for all concave topographic features that had a maximum water depth 1.5 times greater than the tail depth at the crest of the downstream feature controlling water level (usually a riffle or some structural feature). All concave features meeting PIBO criteria are hereafter referred to as pools, while the remaining are referred to as pool-like or concave features.

We used a rapid assessment approach during baseflow conditions of the summer and fall of 2017 to record and assess the attributes of concave geomorphic units throughout the system. We measured and recorded attributes of maximum water depth, tail depth, feature length, bankfull width, percent bankfull channel area occupied by the

pool/concave feature, substrate type, and type of concavity. The depth, width, length, bankfull width, and percent area were directly measured until we were "visually calibrated" and measurements could be estimated visually within approximately 10% of the actual value. Direct measurements were periodically made to maintain consistency of visual estimates. Although the degree of accuracy is somewhat compromised by visually estimating pool characteristics, we consider that the greater spatial extent covered using a more rapid assessment survey offsets the reduction in precision.

Substrate type was categorized by the dominant grain size category: fines (<2 mm), gravel (2 mm to 64 mm), cobble (64 mm to 256 mm), boulder (>256 mm) or bedrock. The type of concavity was determined using the Geomorphic Unit Classification taxonomy (Wheaton et al. 2015). Category types were bar-forced pool, structurally-forced pool, dammed pool, plunge pool, confluence pool, beaver dam, shallow thalweg, ramp, or chute. Residual depth, which is independent of stage height and is a good indicator of how sensitive a pool is to changes in water depth (Lisle, 1987), was determined for each concave feature by subtracting the tail depth from the maximum water depth. The area of the pool was estimated by multiplying bankfull width by streamwise length of the concavity then multiplying by the percent area occupied by the concavity.

The rapid assessment for Sixth Water Creek took place between the confluence of Sixth Water Creek and Fifth Water Creek to the first tributary just a few hundred meters downstream of Strawberry Tunnel Outlet. The stream was segmented into 48 reaches, based on identifiable features from aerial imagery, ranging in lengths from 59 m to 848 m (average reach length: 306 m). Individual reaches generally exhibited similar attributes in

terms of average width, depth, slope, and substrate. The number and size of pools were documented for each reach, but actual locations of pools were not identified at the sub-reach scale. The same rapid assessment protocol was used on the lower Diamond Fork between Childs Bridge and the Diamond Campground with the exception that the approximate locations and sizes of concave features were drawn onto aerial images taken from Google Imagery (2017) and later digitized into shapefiles using ArcGIS.

3.3.1.2 Hillslope and Tributary Sediment Sources

As part of describing pool habitat throughout Sixth Water Creek, we noted the presence or absence of spawning sized gravels in pool tails. To understand the dynamics of spawning habitat, we sampled 41 active and semi-active sediment sources throughout Sixth Water Creek to identify and quantify the potential spawning gravel sources. These samples also provided insight regarding the potential for future channel adjustment through recruitment of coarse sediment into the channel. Samples were taken from the channel beds of small ephemeral tributaries and active, non-vegetated hillslopes. Hillslopes were generally in direct contact with the stream or separated by a small vegetated buffer, usually no more than 1 meter wide. We sieved each sample into grain size categories of >64 mm, 64 mm to 22 mm, 22 mm to 8 mm, 8 mm to 2 mm, <2 mm. Each grain size category was weighed, and recorded. Samples weighed no less than 5 kg and the largest grain size rarely exceeded 5 percent of the sample (Jones 2018). Because samples were taken and sieved in the field, smaller grain size categories were likely heavier due to moisture retention. The effect of moisture retention was not considered significant enough to dramatically alter grain size distributions. Locations of sediment source samples were obtained using a hand held GPS.

3.3.2 Geomorphic Unit Classification

Each concave unit was classified using the geomorphic unit classification taxonomy of Wheaton et al. (2015). We used lidar and aerial imagery to confirm initial unit classifications and made revisions based on field observations where necessary. Pools were classified as bar-forced, confluence, dammed, plunge, or structurally-forced. Bar-forced pools included pools forced by bends in the river, mid channel bars, flow-width constrictions, cement breakup (explained below), or a combination of the bar-forcing with a secondary structural element. Flow-width constriction pools were identified as pools forced by a lateral bar, either directly upstream or adjacent to the pool itself.

Within the lower Diamond Fork, portions of the bed are "cemented" due to potential interactions of water chemistry, biological conditions, and the buildup of fine sediments in the bed. Cement breakup is generally triggered by a flow convergence produced by a bar or structural element. When the cemented layer is broken, bed scour forms a local knickpoint that migrates upstream as the cemented surface layer is undercut. The resistive nature of the cemented layer acts as a secondary element by which the pool form is maintained. Cement breakup pools were identified as areas where either 1) a bar deposited and focused flow over a part of the channel causing the "cemented" bed to breakup and scour a pool or 2) the "cemented" bed scoured for reasons unknown and the scoured sediment produces a transverse, channel spanning bar immediately downstream.

Structurally-forced pools included pools forced by large woody debris (LWD), boulders (individual and clusters), bedrock (ledges and outcrops), and anthropogenic

structures such as concrete wedges or pipes. LWD includes logs (referred to as LWD hereafter) and individual root wads. For Sixth Water Creek, plunge pools caused by boulders or bedrock ledges were also included within the structurally-forced pool category. Beaver ponds were classified as an individual pool class.

Locations providing pool-like habitat were classified as chutes, ramps, and shallow thalwegs. For Sixth Water Creek, we differentiated between pool and non-pool features by using the PIBO criteria. The non-pool features were identified as structurally-forced or bar-forced, but no classification is made as to whether they are chutes, ramps, or shallow thalwegs. For lower Diamond Fork, we classified some concave features that did not explicitly meet the PIBO standards of spanning 50% of the wetted channel width as pools. This was usually done for bar-forced or structurally-forced features that still exhibited pool-like qualities and inclusion of them in our analysis provided more evidence to the mechanisms behind pool formation and maintenance.

3.3.2.1 Geomorphic Unit Analysis Using GIS

Channel attributes of width, radius of curvature, sinuosity, and slope were derived using ArcGIS 10.3.1. For Sixth Water Creek, Jones (2018) delineated the active channel from a 2016 NAIP image and then delineated a channel centerline using the Planform Statistics Tool (Lauer, 2006). The channel centerline includes information of active channel width and a 1st order derivation of the radius of curvature (explained in further detail by Lauer, 2006) at points spaced every 10 meters along the centerline. Elevation at each of these points was extracted from the lidar DEM. The beginning and end of each reach for which we characterized pools was delineated and used to split the channel centerline into individual reaches of varying length. For each reach, the mean width,

coefficient of variation of width, median radius of curvature, sinuosity, and slope were derived from the attributes of the channel centerline. The number of pools/km was derived by dividing the number pools within a reach by the reach length itself. Pools-with-gravel/km were derived by including only those pools with spawning sized gravels covering approximately 25-50 percent or more of the bed. We evaluated the spatial distribution of spawning gravels with regards to sediment sources throughout Sixth Water Creek to better understand the availability of spawning habitat for Bonneville Cutthroat trout.

For the lower Diamond Fork, we delineated the wetted channel from the Google 2017 image when discharge was approximately 80 cfs (the summer mandated flow). The wetted channel width delineated from the Google 2017 image and bankfull channel width, as identified from lidar, are nearly identical for much of the lower Diamond Fork. Using the same procedure as described above, we delineated a channel centerline with attributes of width and radius of curvature spaced every 10 meters. We used a 300-meter moving window at 10 meter increments to calculate the mean width, coefficient of variation of width, median radius of curvature, sinuosity, and slope. A 300-meter window was chosen because it was long enough to incorporate a few bends in the river and calculate planform statistics but short enough to capture spatial heterogeneity in planform and pool density. Pools/km were derived by summing the number of pools included within the moving window. The aerial extent of pools was digitized from field maps and used to calculate the area of each pool. This was used to calculate a percent pool area for each reach within the moving window (sum of pool area / wetted channel area). The calculated area for each pool, along with attributes of depth, substrate, and other metrics

collected in the field were used to evaluate the size and configuration of pools throughout the lower Diamond Fork.

3.3.3 Cross Section Comparisons

In 2017, we re-measured the cross sections measured by BIO-WEST, Inc. in 2005, 2006, and 2007 for sites USW, DCG, MO, and OX (BIO-WEST, Inc., 2009). Each site had a total of 6 to 8 cross sections. For USW, located on Sixth Water Creek, we compared all cross sections from 2005, 2006, 2007 to 2017 to evaluate the geometry and location of the channel. For sites within the lower Diamond Fork (DCG, MO, OX), we examined only the wetted portions of cross sections and compared the distribution of water depths between the years 2006 and 2017. We compared wetted points because mean daily discharge for both surveys were fairly similar, 91 cfs in 2006 and 83 cfs in 2017. In this case, comparing water depths was useful and more direct because bankfull channel identification was ambiguous. Each survey at each reach contained approximately 100 to 200 points within the channel.

3.3.4 Spectral Depth Analysis

To constrain how the channel has changed over the current flow regime starting in 2004, we used an adaptation of spectral depth retrieval methods developed by Legleiter (2013). Legleiter (2013) showed that realistic depictions of instream topography could be achieved using multispectral images. A number of factors limit the accuracy of water depth estimated from multispectral analysis. This includes complicating factors such as geo-referencing error, inadequate spatial resolution for characterizing instream features and mitigating effects of pixel mixing along shadow and channel margins, and

insufficient radiometric resolution to detect the full range of depths in pools. For smaller rivers, these complications are more pronounced as pixels with error represent a great proportion of the river. However, the location of bars and pools are still identifiable (Legleiter, 2013). This indicates that the distribution of depths in terms of shallow and deep water are still preserved despite potential errors and allows for semi-quantitative analysis of water depth throughout a reach.

We used compressed, county mosaic NAIP 1-m imagery from 2016 and 2006 to examine changes in bathymetry in nine different reaches of the lower Diamond Fork. Mean daily discharge averaged for all flight dates for 2006 was 90.8 cfs and 46.5 cfs for 2016. We used the criteria from Legleiter et al. (2009) to select the appropriate NAIP imagery: 1) shallow water depth, 2) clear water, such that light attenuation within the water column is primarily due to absorption by pure water and not scattering by suspended particles, 3) bright, reflective substrate, 4) favorable illumination and geometry that avoids strong reflections of the water surface, and 5) minimal atmospheric effects. Only images from 2006 and 2016 met the criteria.

We delineated the visible wetted channel, excluding all shadows and emergent bars, boulders and woody debris. Nine reaches, each approximately 1 km long (range 0.5 km to 1.4 km), were delineated within the lower two process domains of the Diamond Fork. Reach lengths were based on homogeneity of image quality, and similar riverine features such as sinuosity, valley width, riparian controls, and confinement. Three of the reaches included the OX, MO, and DCG sites and were compared to surveyed cross sections from 2006 and 2017. Other process domains could not be included due to the abundance of shade, vegetation, or high water surface reflectance.

Table 3.3.1. Aerial image datasets used to evaluate instream habitat for the Diamond Fork River

Year	Source	Scale/Resolution	Color	Flight Date	Discharge at Diamond Fork gage (cfs)
1993	USGS DOQQ	1:40000	B&W	17-Aug	205
				23-Aug	423
				24-Aug	440
				28-Aug	397
				9-Sep	197
1997	DOQQ	1:40000	B&W	7-Jul	377
				30-Sep	238
				4-Oct	27
				5-Oct	26
2003	USDA NAIP	2 meter	Color	31-Aug	219
				3-Sep	203
2004	NAIP	1 meter	Color	28-Aug	88
2006	NAIP	1 meter	Color	26-Aug	92
				28-Aug	90
				31-Aug	90
				2-Sep	93
				3-Sep	89
2009	NAIP	1 meter	Color	10-Jul	85
				10-Aug	79
2011	NAIP	1 meter	Color	6-Aug	86
2014	NAIP	1 meter	Color	11-Aug	82
				3-Sep	82
2016	NAIP	1 meter	Color	2-Aug	48
				19-Aug	45
2016	Google	6 inch	Color	Unknown	Approximately 50
2017	NCALM	0.1 meter	Color	3-Oct	58
				4-Oct	48
				6-Oct	46
2017	Google	6 inch	Color	Unknown	Approximately 80

The NAIP images were clipped by the wetted channel polygon and a relative depth, *X*, was computed using the red and green bands from the image as shown in equation (3.1):

$$X = \ln\left(\frac{L_B(\lambda_1)}{L_B(\lambda_2)}\right) \quad (3.1)$$

where L_B is the bottom reflected radiance of the red band, λ_2, or the green band, λ_1, from a true color image (Legleiter et al. 2009). Since red light is absorbed more quickly by water than green light, the green to red light ratio increases with increasing water depth. To account for light attenuation within water, the natural log of the green to red ratio is applied, resulting in a linear relation between relative depth and actual water depth (Legleiter et al., 2009). The calculated relative depths from equation (3.1) ranged from approximately -0.25 to 0.25.

Due to geo-referencing errors and a lack of survey data both temporally and spatially for both 2006 and 2016, no attempt was made to correlate the relative depth with surveyed water depths. Instead, relative depths were scaled to the maximum depth, resulting in values from 0 to 1. We assume that the maximum detectable water depth in each reach is the same for both 2006 and 2016. This assumption is based on the spectral depth retrieval limitation that there is insufficient radiometric resolution to detect the full range of depths in pools. This assumption is made possible because each reach contains at least one pool with a depth near or greater than 1.25 m, the depth at which NAIP-derived depths from the Snake River ceased to match field surveyed depths (Legleiter, 2013). According to our pool survey in 2017, depths of 1.25 meters or greater occur on average in less than five percent of a reach. We also assume that differences in water clarity between the two years is negligible as both images were taken during relatively low flow conditions. Our approach allows for a useful, but only semi-quantitative comparison between years.

The distributions of relative depths (scaled 0 – 1) are plotted as a density function to visually assess changes in instream topography from 2006 to 2016 on a reach-to-reach basis. We evaluated the shape and magnitude of each distribution and compared them between years. We used at-a-station hydraulic geometry, derived from discharge measurements made at two sediment sampling sites (BB and CB) within the lower Diamond Fork during 2016 and 2017, to determine the approximate difference in stage between the discharges measured on the flight dates.

3.3.5 Statistical Analysis

3.3.5.1 Random Forest Statistical Regression Model

We used the regression capability of the Random Forest statistical model to evaluate the influence of reach attributes on the magnitude of pools/km for both the lower Diamond Fork and Sixth Water Creek and the percent pool area for the lower Diamond Fork. Random Forest models are an ensemble tree-based statistical tool based on Classification and Regression Tree (CART) methods. They are a recently developed statistical method and are used extensively to help solve classification and regression problems in ecology and other fields (Liaw and Wiener, 2002; Cutler et al., 2007; Stoble et al., 2007, 2008; Olson and Hawkins, 2012). Random Forest models have several advantages compared to classic statistical methods and have been shown to perform just as well or better than even the best available statistical models used in classification and regression (Cutler et al., 2007; Olson and Hawkins, 2012). Random Forest models can handle complex, non-linear, and threshold based datasets. Random Forest models do not assume independence of predictor variables which make it possible to have variables that are somewhat co-related (Cutler et al., 2007). For multivariate datasets, Random Forest

models are able to evaluate the importance of variables and interpret them through the use of partial dependence plots (Vaughan, 2016). The model allows us to identify variables that provide the greatest explanatory power and examine the influence they have on response variables (Vaughan, 2016). A detailed review of Random Forests is outlined in Cutler et al. (2007) and Olsen and Hawkins (2012). We use previously derived variables of average width, coefficient of variation of width, median radius of curvature, sinuosity, and slope as predictor variables.

3.3.5.2 ANOVA

We tested the distributions of relative depth within each of the 9 reaches, as well as surveyed water depths at OX, MO, and DCG using analysis of variance (ANOVA) with an *a priori* alpha value of 0.05. ANOVA is a statistical method used to test the means of two or more independent groups. In the ANOVA procedure, variance is partitioned into terms that quantify the magnitude of overall variance in the response variables attributable to the different sources of variation (Shaw and Mitchell-Olds, 1993). The null hypothesis for the test is that the means of each group are equal to that of each other. A significant result is when the means are unequal. The relative depth for each reach and water depth for each site was compared between years 2006 and 2016, 2017. All statistical analysis was performed using R 3.4.3.

3.3.6 Instream Channel Change Analysis

Using the results from our pool mapping campaign and the geomorphic unit classification, we identified reaches with very few or no pools in 2017. Using the results from the spectral depth analysis and repeat surveys, we evaluate change in channel

topography between 2006 to 2016. Using aerial images listed in Table 3.3.1 and the results from the random forest regression analysis of pool density, we analyzed these reaches to detect any changes in channel width, variability in width, sinuosity, radius of curvature, slope, exposed surfaces (bars and floodplains), channel migration, and vegetation to determine if any of these variables might be correlated with the absence of pools. We qualitatively identified recurring patterns and changes that occurred within these reaches in order to describe the mechanisms behind channel simplification and the creation, maintenance, and disappearance of pools. We evaluated bedload sediment transport measurements from Jones (2018) for grain sizes greater than 8 mm (bar building material) for sites CB and BB in order to better understand the dynamics of channel form, pool formation, and its relation to sediment transport within the lower Diamond Fork. Complete methods and results of those measurements are found within Jones (2018).

3.4 Results

3.4.1 Sixth Water Creek

Attributes for concave features were collected on 14.7 km of Sixth Water Creek from the confluence of Fifth Water and Sixth Water Creeks to just downstream of Strawberry Tunnel Outlet. A total of 676 concave features were identified, 96 percent of which were forced by a structural element. Of the 676 concave features, 320 of them were classified as pools by PIBO standards, 94 percent being structurally-forced pools (300 structurally forced pools, 20 bar-forced pools). Structural elements observed within Sixth Water Creek were boulders, bedrock ledges, vegetation, large woody debris, and beaver dams. Boulders and bedrock were the dominant structural elements within all four

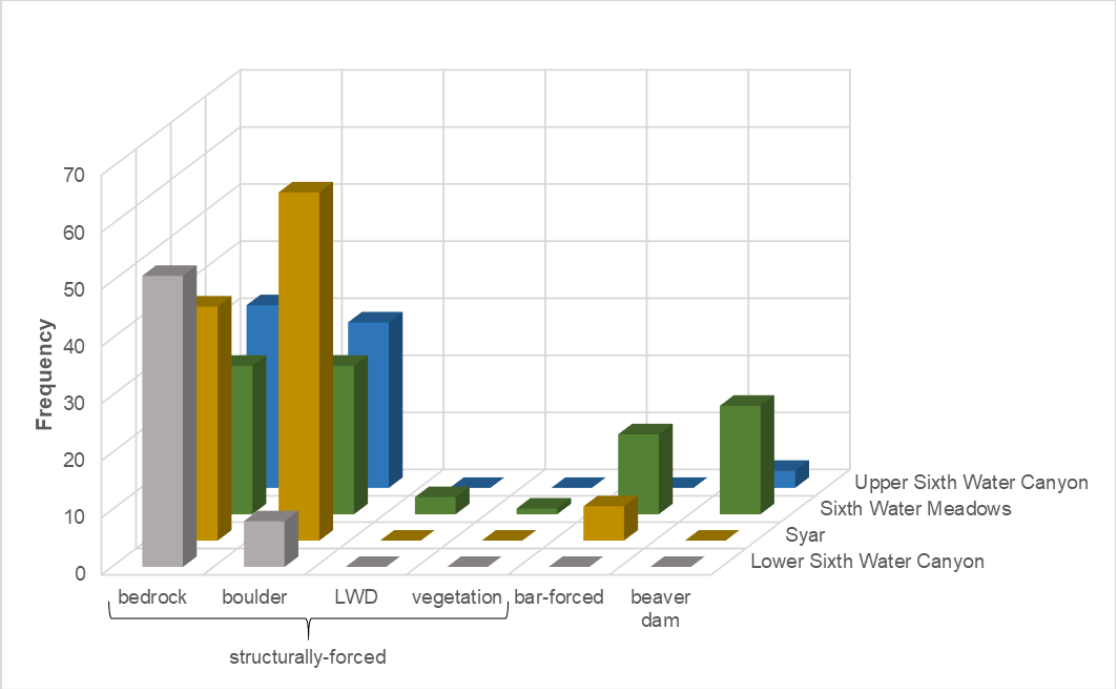

Figure 3.4.1. Frequency of all structurally-force pools, bar-forced pools and beaver dams (320 total) within each of the four process domains (Upper Sixth Water Canyon, Sixth Water Meadows, Syar, and Lower Sixth Water Canyon) for Sixth Water Creek.

distinct process domains on Sixth Water Creek. A total of 22 beaver dams were observed in Sixth Water Creek, but only in the upper two process domains (Sixth Water Meadows and Upper Sixth Water Canyon). Nineteen of the total 22 beaver dams documented were in the Sixth Water Meadows process domain (Figure 3.4.1).

Each process domain exhibited different types of available habitat (Figure 3.4.1, Table 3.4.1). Within Upper Sixth Water Canyon, pools are largely forced by boulders and bedrock. Interbedded limestone and sandstone bedrock ledges form large, deep plunge pools. Boulders, sourced locally from bedrock, form both large and small pools. A single boulder causes scour either downstream or to the side of the boulder, however, due to coarseness of the bed, these pools are generally small and shallow. Clusters of boulders, formed by the interlocking of boulders either parallel or perpendicular to the streamwise

direction, cause plunge pools, scour pools, or dammed pools. The depth and size of these pools depend on the size and orientation of the boulder cluster.

Pool features within Sixth Water Meadows are mostly forced by boulders, and the majority are small in depth and aerial extent. Bedrock ledges and outcrops create plunge pools, but are not as large and defined as they are within the Upper Sixth Water Canyon. Sixth Water Meadows is unique compared to other process domains because of the abundance of beaver activity. Several large beaver dams (average area of 250 m^2, standard deviation of 196 m^2), have been constructed within the last decade or more, resulting in a significant amount of slow water habitat and reconnection with floodplains (Figure 3.4.2). The degree of the connectivity and additional slow water habitat has not been thoroughly quantified.

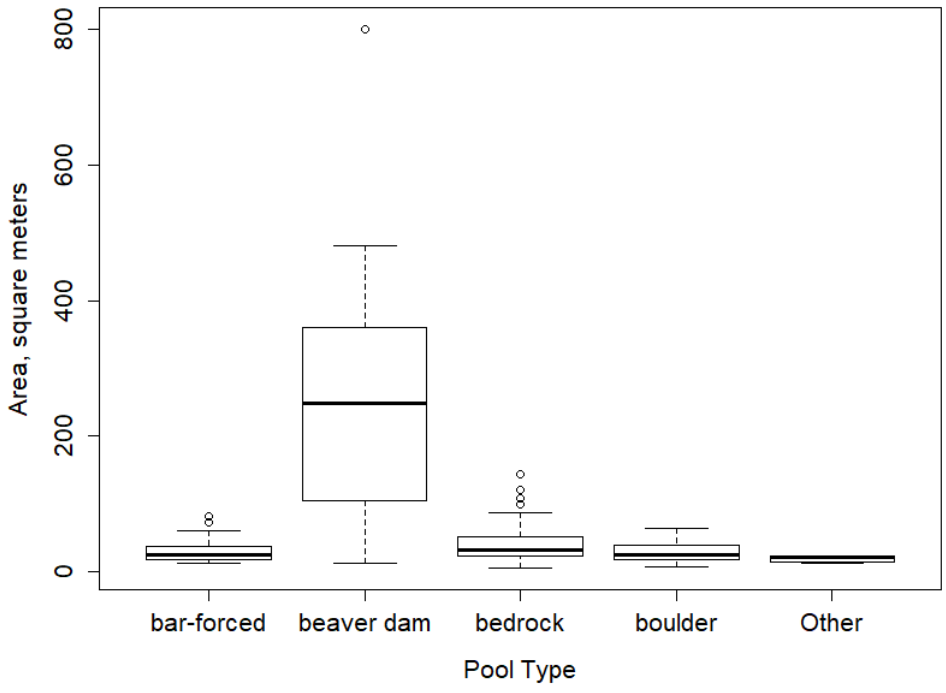

Figure 3.4.2. Distribution in the aerial extent of different types of pools throughout Sixth Water Creek.

The Syar reach is largely influenced by boulders sourced from local bedrock and adjacent alluvial fans. Individually or within a cluster, these boulders form a variety of pools of different shapes and sizes. This process domain features an abundance of spawning sized gravels within the stream channel. Although coarser material still exists within the bed, the finer grain sizes are more susceptible to transport due to scour jets caused by boulders and bedrock ledges, leading to the active formation of gravel bars. The sources and relative abundances of these gravels are discussed below.

Pool features within Lower Sixth Water Canyon are influenced primarily by bedrock. The conglomerate bedrock with interbedded sandstones create resistant outcrops that produce step-pool sequences, as well as large plunge pools. Backwaters and eddies caused by the ledges and boulders result in a significant amount of hydraulic variability within this process domain.

Pool density is high for Lower and Upper Sixth Water Canyon process domains, with an average pool spacing of 2 to 3 channel widths per pool. Sixth Water Meadows and Syar process domains exhibit lower pool density, with a pool spacing of 7 channel widths per pool for each process domain. For Upper Sixth Water Canyon, Sixth Water Meadows, and Syar, the median pool size and depth is 25 to 30 m^2 with a residual depth of 0.3 to 0.4 m. The median pool size and depth for Lower Sixth Water Canyon is 36 m^2 and 0.8 m (Table 3.4.1 and Figure 3.4.3.). Pools within Sixth Water Creek appear to occur in low to moderate density relative to that considered adequate for optimal trout habitat (Hickman and Raleigh, 1982), however, the size and depth of these pools (with the exception of Lower Sixth Water Canyon) may be lacking. Multiple reaches within each process domain contain few small pools or no pools at all, while other reaches

contain many large deep pools (Figures 3.4.4 and 3.4.5). These spatial differences are controlled by a variety of valley and geologic controls. Confined reaches produce bedrock outcrops and large boulder clusters that create both scour and dammed pools, while partially confined reaches are more subject to long riffles and runs due to the absence of instream structure. However, the increased lateral zones that allow an abundance of riparian vegetation to establish encourages the development of beaver dams.

Table 3.4.1. Pool statistics for each of the four process domains located within Sixth Water Creek.

	Lower Sixth Water Canyon	Syar	Sixth Water Meadows	Upper Sixth Water Canyon
Pools/km				
Mean	51	18	16	26
Median	68	16	17	38
Minimum	34	4	0	22
Maximum	72	30	38	70
Pool Spacing (channel widths/pool)				
Mean	2	7	7	3
Median	2	7	8	3
Minimum	1	4	3	1
Maximum	2	28	*No Pools*	5
Residual Depth (m)				
Mean	0.8	0.5	0.6	0.6
Median	0.8	0.4	0.3	0.3
Minimum	0.2	0.2	0.2	0.2
Maximum	1.8	5.6	2.6	2.8
Pool Area (m^2)				
Mean	40	35	78	38
Median	36	30	25	25
Minimum	7	8	6	6
Maximum	100	144	800	304

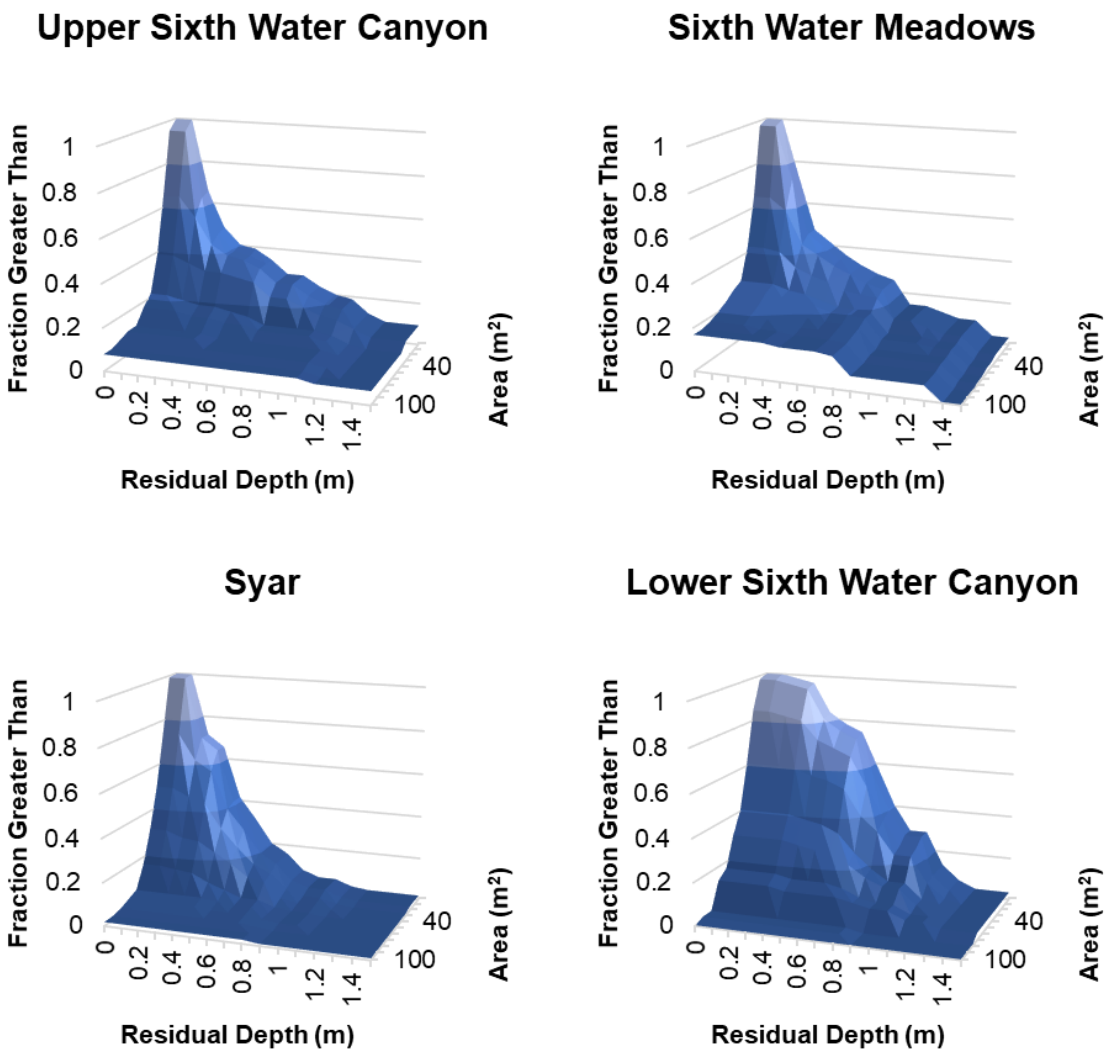

Figure 3.4.3. Two-dimensional cumulative plots of residual depth (m) and area (m^2) for all 320 pools within the four process domains of Sixth Water Creek. These plots show the fraction of pools that are deeper and larger than a pool of a certain size and depth.

3.4.1.1 Sediment Sources from Hillslopes and Tributaries

The majority of sediment sources within Sixth Water Creek occur within the Syar and Lower Sixth Water Canyon process domains (Figure 3.4.4). These two process domains are located within the North Horn formation, consisting primarily of a

conglomerate bedrock with interbedded mudstones and sandstones. The sediment sources on average consist of 25 percent gravel (8 mm to 64 mm), with sources ranging from 1 percent gravel to 49 percent gravel.

The Upper Sixth Water Canyon and Sixth Water Meadows process domains contain fewer active sediment sources, most of which consist largely of fine sediment. These two process domains are located within the Green River formation, which is characterized by shales with interbedded limestone and sandstone. These sediment sources on average consist of 13 percent gravel (range of 1 percent to 51 percent), with the majority being made up of fine silts and clays. Located within Sixth Water Meadows is an active landslide. The landslide consists primarily of fine grained silts and clays with very few larger clasts. The toe of the landslide is in direct contact with Sixth Water Creek for approximately 1 km and is actively eroded throughout the year. Over the course of the study, we observed small failures (less than 1 cubic meter volume) along the river margin that would be removed by the next site visit. The majority and greatest magnitude erosional events were observed to be in the late spring and during rainstorm events.

3.4.1.2 Random Forest Results

We used the regression function of the Random Forest statistical model in R to discern the relation of pools per km with channel attributes of mean width, coefficient of variation for width, median radius of curvature, slope and sinuosity. We also converted pools/km to pool spacing (channel widths/pool) using the mean channel width of Sixth Water Creek in order to compare to standard pool spacing metrics. The model predicted that mean width, slope and sinuosity were the three most important variables, but accounted for only 12 percent of the model variation. These results are consistent with

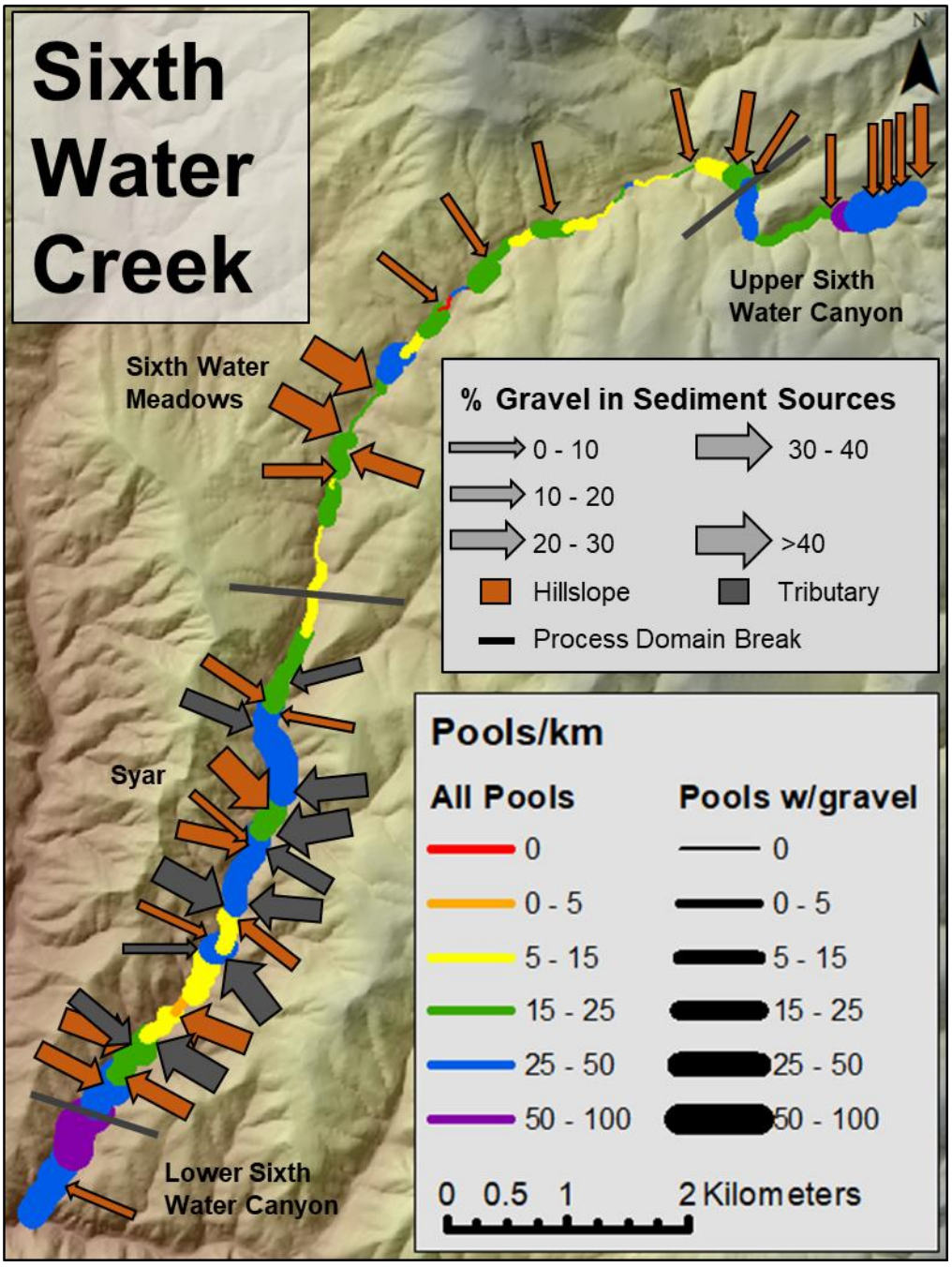

Figure 3.4.4. Spatial distribution of pool density (pool/km) and pool density for pools with gravel (pools with gravel/km) throughout the four process domains of Sixth Water Creek. Major sediment sources, their approximate location and percent composition of gravel (8 mm to 64 mm), and whether they originate from a tributary or a hillslope are shown as well. Dark grey lines represent the breaks between the four different process domains.

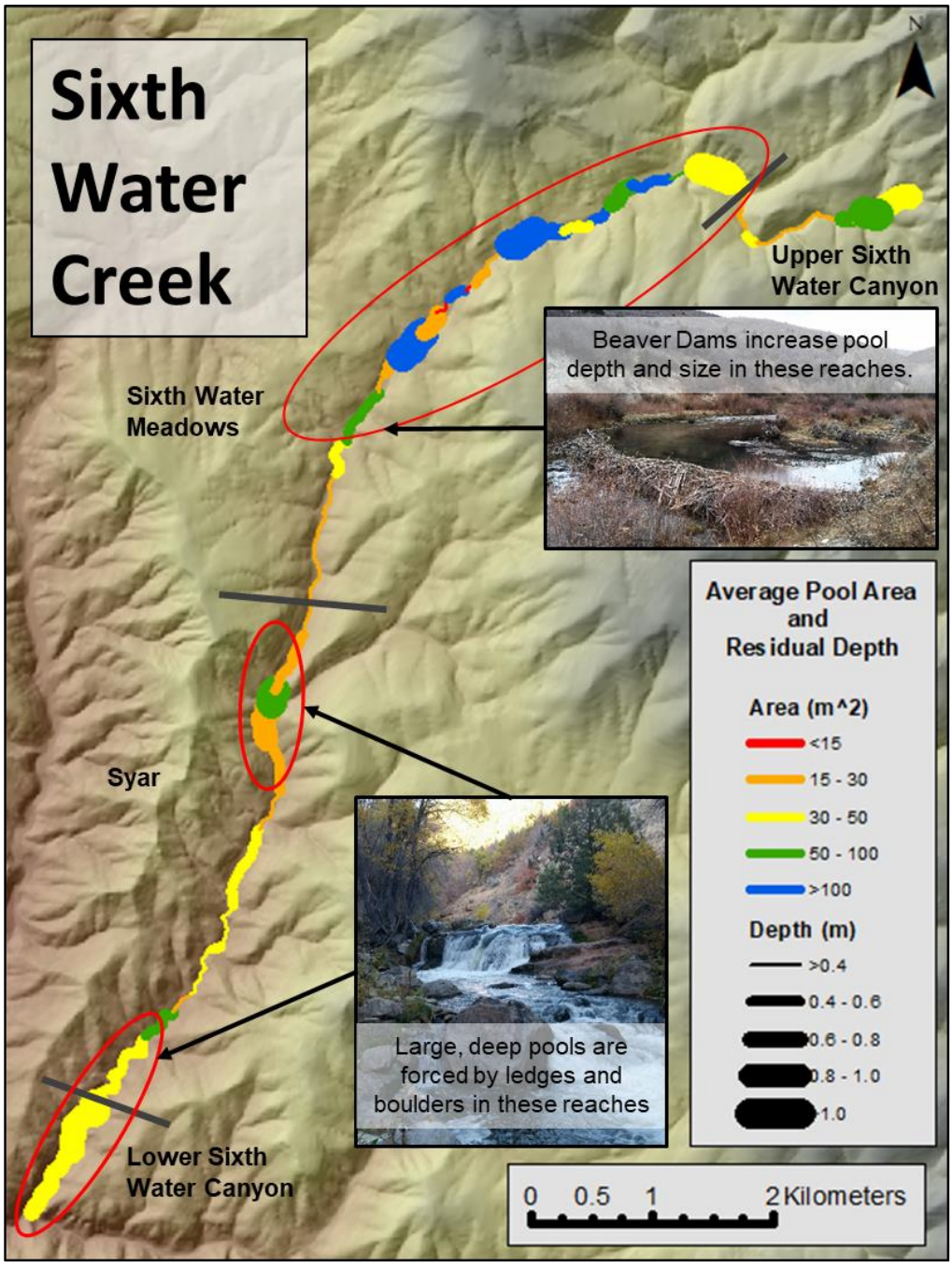

Figure 3.4.5. Spatial distribution of the average pool area (m^2) and average residual pool depth (m) for each reach surveyed throughout Sixth Water Creek. Dark grey lines represent the breaks between the four different process domains.

the strong local controls from bedrock and boulders throughout Sixth Water Creek. Incorporation of a structural-element variable within the model would most likely increase model explanatory power. Steep and wide reaches tend to have more boulders and bedrock ledges that form scour and plunge pools. Model results show that the relations are highly non-linear and that the number of pools per km was greatest for reaches with slopes greater than 0.6, a mean width greater than 10 m, and sinuosity near 1.0 (Figure 3.4.6). Pool spacing is within typical values ranging from 7 channel widths/pool to less than 3 channel widths/pool.

3.4.1.3 Repeat Cross Sections at Upper Sixth Water

We re-surveyed 6 cross sections at the Upper Sixth Water (USW) site, which is located within the Sixth Water Meadows process domain. Inspection of the 2017 cross sections in comparison to cross sections surveyed in 2005, 2006, and 2007 show that the reach has adjusted very little since the completion of Syar Tunnel in 1996 and the

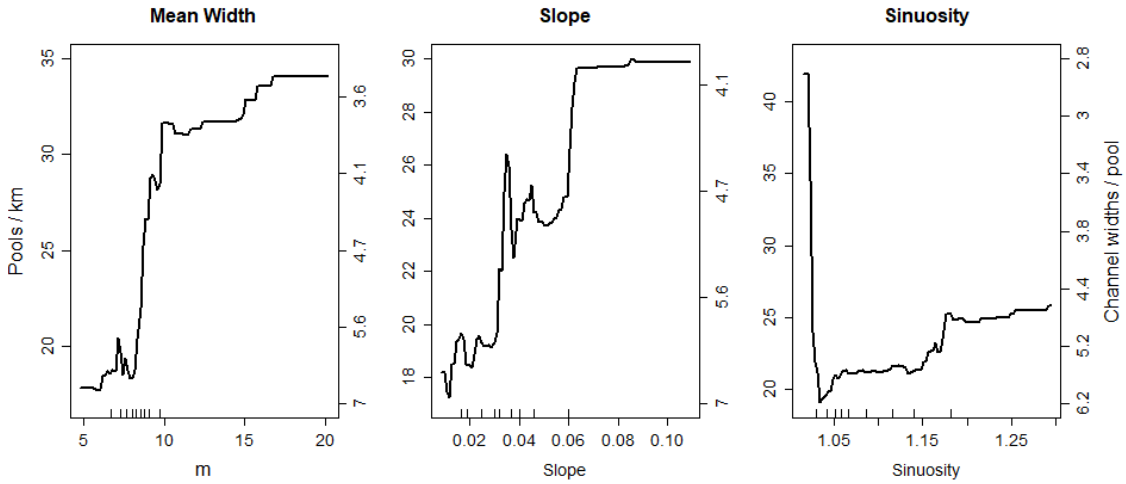

Figure 3.4.6. Partial plots of pool density (pools/km) and pool spacing (channel widths/pool) as a function of mean width, slope, and sinuosity; the top three predictor variables from the Random Forests model. These variables were calculated from the 48 reaches throughout Sixth Water Creek that were evaluated.

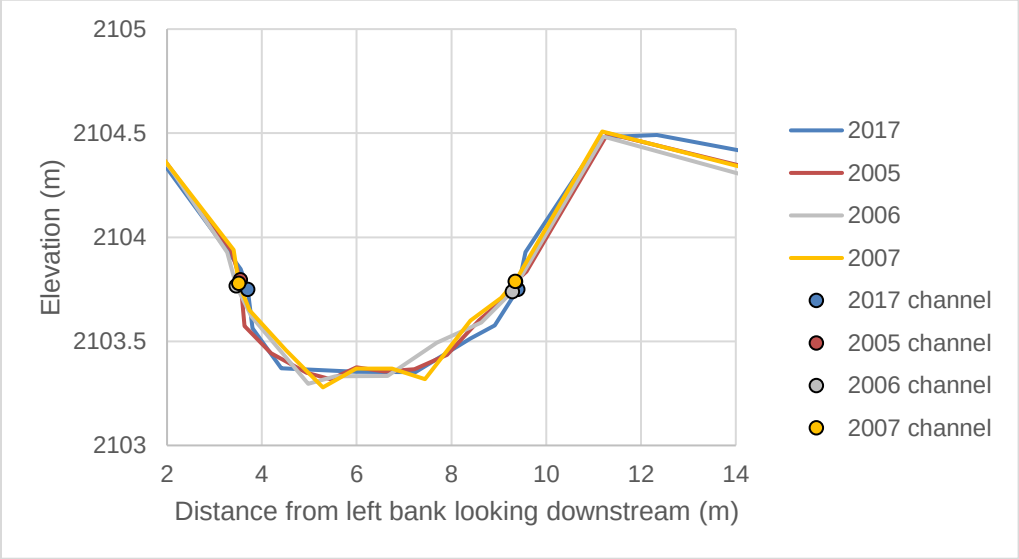

Figure 3.4.7. A repeat cross section (cross-section #5) from Upper Sixth Water site illustrating the stability of the Sixth Water Creek channel over the past decade (Jones, 2018).

Diamond Fork Pipeline in 2004. With the exception of cross sections influenced by beaver dams, each of the cross sections indicate very little adjustment in channel geometry and location (Figure 3.4.7). Because the channel has adjusted so little since 2004, we expect that future adjustment is unlikely, or too slow to observe significant changes over multiple decades.

3.4.2 Diamond Fork River

We mapped and characterized pools for 9.5 km of the lower Diamond Fork, extending from the Childs Bridge site to just upstream of the Diamond Campground monitoring site. This survey encompassed the Alluvial Valley and the Diamond Campground process domains. Because only a fraction of the Diamond Campground process domain was characterized, the analysis was not performed for separate process domains. We mapped a total of 200 concavities, 169 of which classify as pools according

to the PIBO standards. We classified as pools some concave features that did not explicitly meet the PIBO standard of spanning 50% of the wetted channel width because including them in our analysis provides more evidence regarding the conditions and mechanisms for pool formation and maintenance. The majority of pools on Diamond Fork are bar-forced, in contrast to Sixth Water. These bar-forced pools were due to planform shape, mid-channel bars, flow-width constrictions, cement breakup, and a combination of bar-forcing features or a secondary structural element (Figure 3.4.8). Structurally-forced pools were the second most prevalent concave feature. These structurally-forced pools were primarily caused by LWD, then by boulders, either individual or clusters of boulders. Other structural elements observed were individual root wads, concrete wedges, and a channel spanning pipe (an RFID antenna which had scoured a pool over the course of the experiment). No beaver dams were observed in this reach.

Pools area is on average 101 m^2 with an average residual depth of 0.8 m (median is 86 m^2 and 0.7 m). Pools are 1.7 times larger in area and 3.5 times deeper than non-pool concave features. Bar-forced pools are on average 1.7 time larger in area and 1.3 times deeper than structurally-forced pools. Bar-forced pools are on average 107 m^2 with an average residual depth of 0.9 m while structurally forced-pools have an average size of 64.6 m^2 with an average residual depth of 0.6 m. Average pool density is 17 pool/km for a pool spacing of 7 channels widths/pool and a percent pool area of 12 percent. Pool density ranges from 0 pools/km to 50 pools/km, while percent pool area ranges from 0 percent to 37 percent. Of the 9.5 km mapped, 22 reaches of 100 meters or greater have no pools, 9 of which had reach lengths greater than 200 m (Figure 3.4.9).

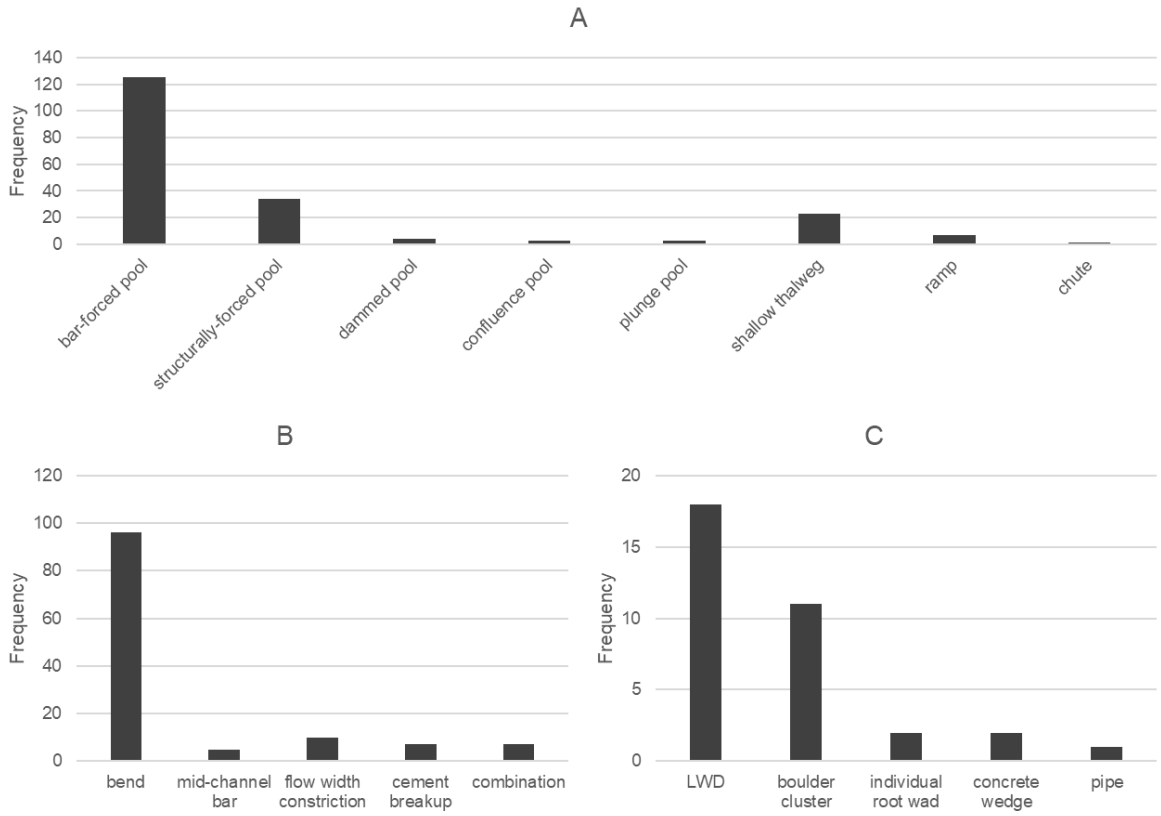

Figure 3.4.8. Frequency and type of A) all concave features, B) bar-forced pools, and C) structurally-forced pools within the lower Diamond Fork.

3.4.2.1 Random Forest Results

We used a Random Forest regression model in R to determine the relation of the number of pools per km and the percent pool area against 5 channel attributes derived over a 300 m reach: mean channel width, coefficient of variation, median radius of curvature, slope, and sinuosity. Of the 5 variables, mean channel width, the median radius of curvature, and the coefficient of variation for width were determined as the 3 most important predictor variables. Slope and sinuosity were not as important but increased model explanatory power. These 5 variables explained 91 percent of the variance within the model for pool density and 90 percent of the variance within the model for percent

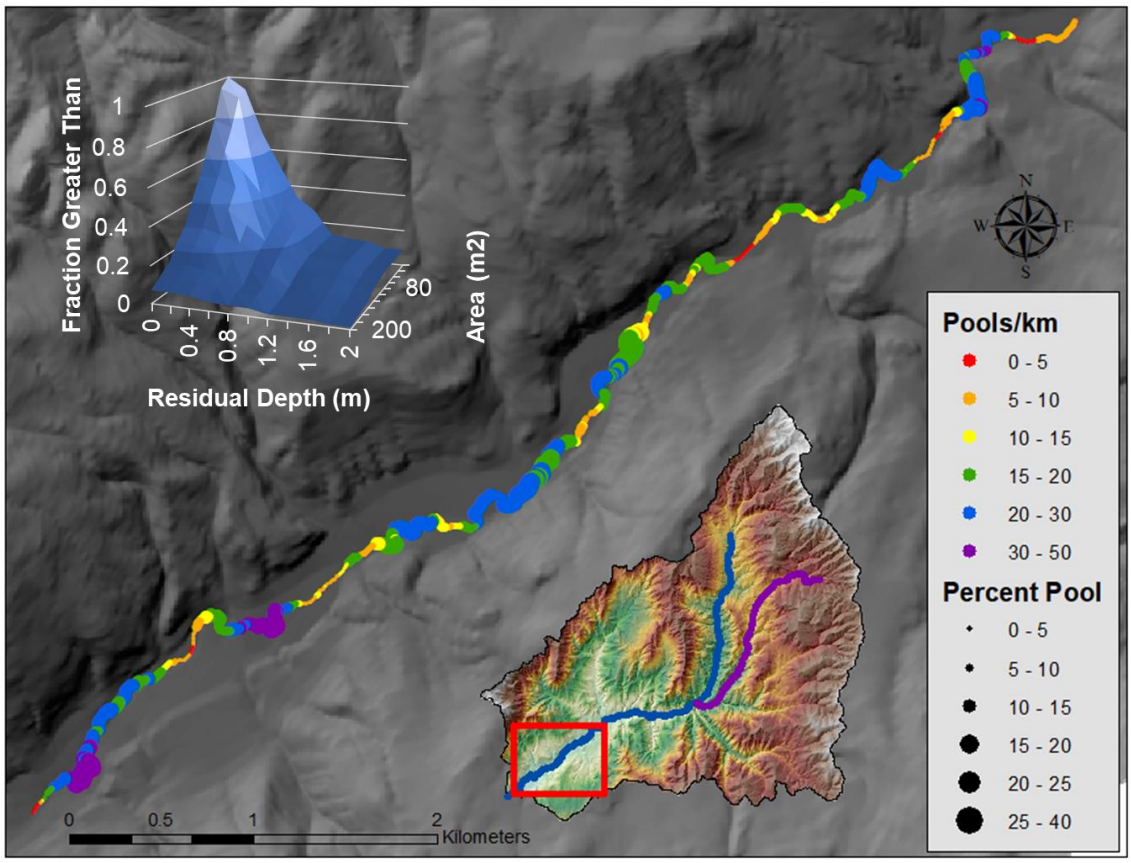

Figure 3.4.9. Spatial distribution of pool density and percent pool area between Childs Bridge and the Diamond Campground. The two-dimensional plot in the upper left-hand corner demonstrates the fraction of pools larger (aerial) and deeper than a pool of given area and depth. The number of mapped pools throughout this reach equal 169.

pool area. These variables are significant for the lower Diamond Fork because they are directly related to river-formed elements that create pools. In contrast, the Random Forest model for Sixth Water Creek had little explanatory power because of pool dependence onlocal (mostly bedrock) structural elements rather than planform variables. Pool density converted to pool spacing, which was calculated using the mean width of the lower Diamond Fork reach surveyed for pools, indicates that pool spacing falls within the ideal values of 5 to 7 channel widths per pool. However, percent pool area is much lower than the 50 to 70 percent considered ideal for trout habitat (Raleigh et al., 1984). Partial

dependence plots for pool density (and pool spacing) and percent pool area (Figures 3.4.10 and 3.4.11) show that the number of pools/km and percent pool area increase as 1) mean channel width becomes narrower than 9 to 10 meters and remains high for widths narrower than 7 m, 2) the median radius of curvature within a reach falls below 100 m, 3) the coefficient of variation increases from 10 to 30 percent, remaining high above 30 percent, 4) slope decreases below 0.01, and 5) sinuosity increases from 1.0 to 1.4, remaining high above 1.4. For pool density, these changes result in an approximate 11 percent to 85 percent increase in pools (approximate average for all variables: 43 percent), whereas for percent pool area the changes result in a 36 percent to 78 percent increase in pool areas (approximate average for all variables: 60 percent). A comparison of these two models suggest that as the channel becomes narrower with greater width variability, more sinuous, and less steep, the area of pools grows disproportionately to the number of pools. We would therefore expect to observe more pools that are larger in aerial extent.

3.4.2.2 Spectral Depth Analysis

The distributions of relative depth from 2006 and 2016 can be used to partition out different geomorphic zones, revealing the nature of habitat variability within the channel. Pasternack & Hopkins (2017) showed that high points (peaks) in the distributions generally indicate the toe of geomorphic features while low points (troughs) are typically the top of a features. Relative water depth in 2006 was multimodal, indicating a mix of pools, runs, and shallow riffles, whereas water depth in 2016 has a stronger unimodal distribution at smaller flow depths (Figure 3.4.12).

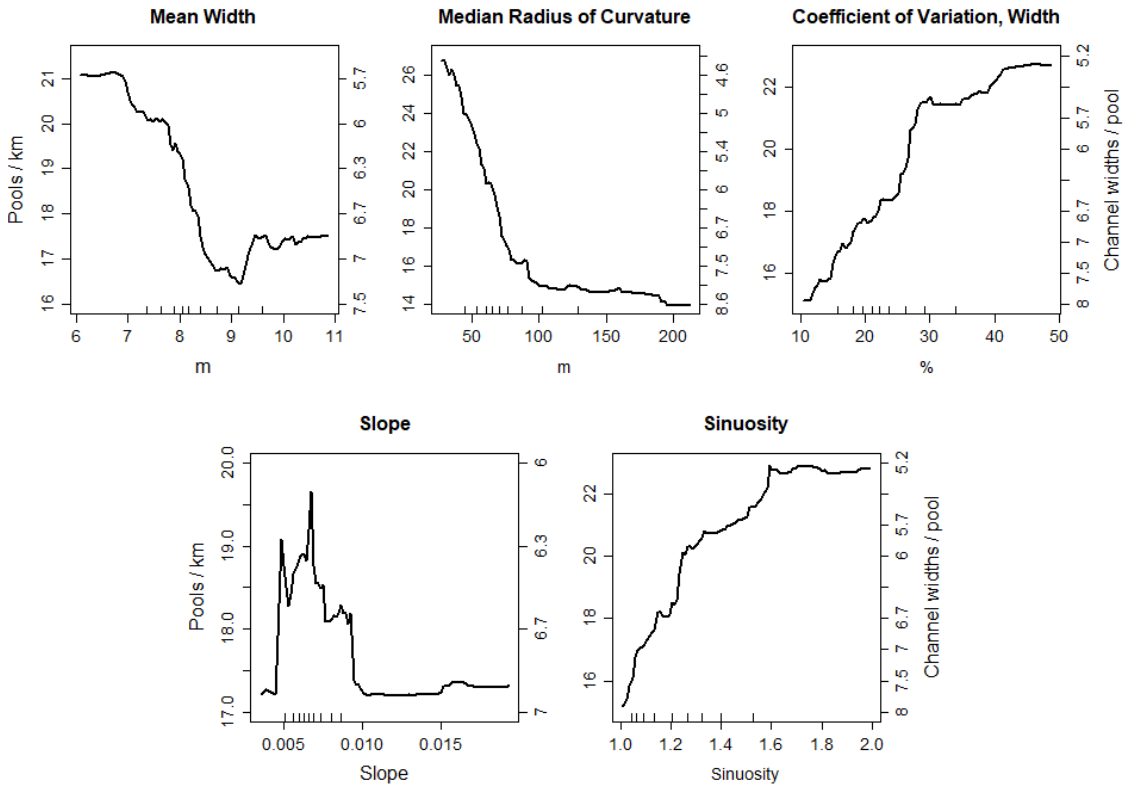

Figure 3.4.10. Partial plots of pool density (pools/km) and pools spacing (channel widths/pool) in response to variables of mean channel width, median radius of curvature, coefficient of variation for width, slope, and sinuosity. These variables were calculated using a 300 meter moving window at 10 meter increments. Each variable is plotted in order of importance (left to right, top to bottom) with mean width as the most important variable in explanatory power and sinuosity as the least important variable.

Discharge was 90.8 cfs for 2006 and 46.5 cfs for 2016. Using at-a-station hydraulic geometry determined from discharge measurements made at the Childs Bridge and Brimhall Bridge sediment transport sites during 2016 and 2017, there is approximately a 7 cm increase in stage from 47 cfs to 91 cfs. The change in width as determined from discharge measurements, HEC-RAS models, and surveyed water extents (Figure 2.4.10) indicates that the change in wetted width is approximately 1.1 meters. The stage height difference would shift the distributions of relative water depths

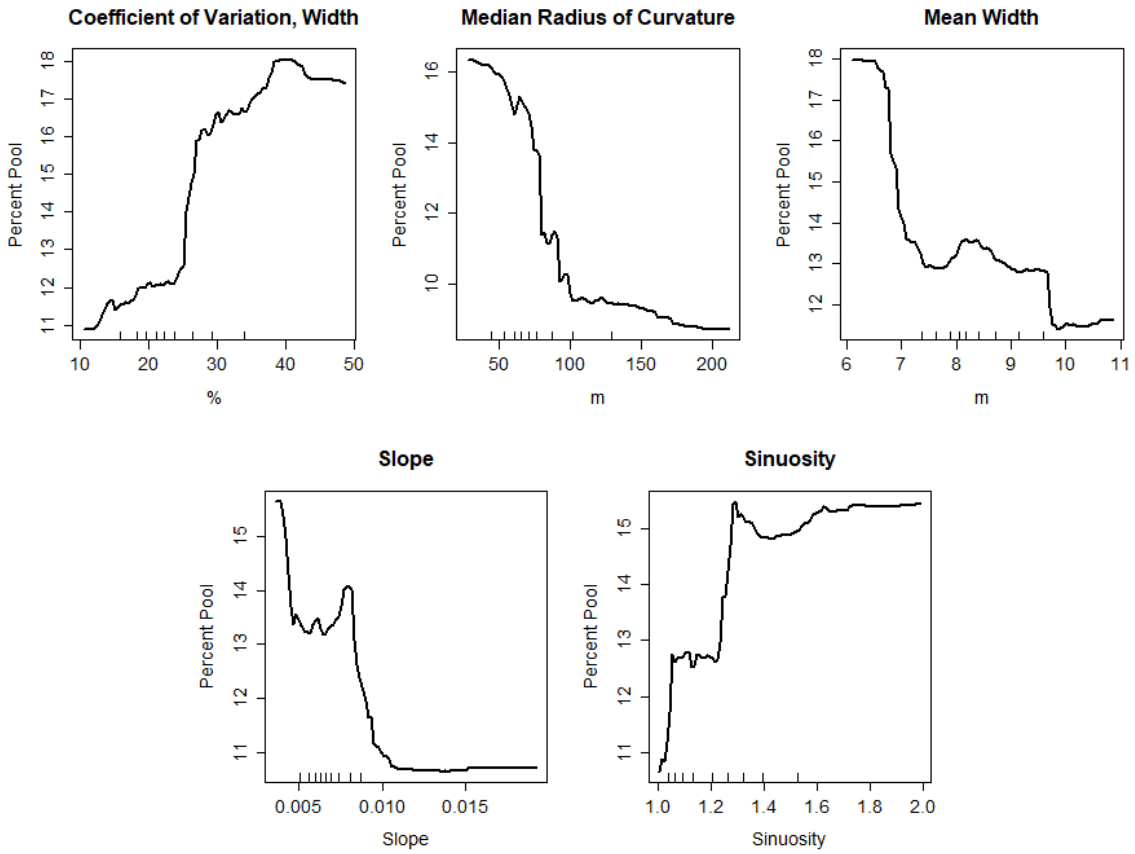

Figure 3.4.11. Partial plots of percent pool area (percent pool) in response to variables of mean channel width, median radius of curvature, coefficient of variation for width, slope, and sinuosity. These variables were calculated using a 300 meter moving window at 10 meter increments. Each variable is plotted in order of importance (left to right, top to bottom) with the coefficient of variation for width as the most important variable in explanatory power and sinuosity as the least important variable.

for 2016 to the right while the change in width could increase the frequency of either shallow or deep water. Given that imagery resolution is 1-meter and 7 cm of water depth is small relative to range of actual depths, we consider that the smaller discharge in 2016 does not significantly alter the results. Of the 9 reaches, reaches 1, 4, 5, 7, and 8 appear to have had more deep water habitat in 2006 than in 2016; reaches 2, 3, 6, and 9, may have more or equal amounts of deep water habitat in 2016 than in 2006. Results for the ANOVA test indicate that all 9 reaches have significantly different mean relative water

depth, with each ANOVA test for each reach displaying a p-value much less than 0.0001. The comparisons of relative depth provide evidence that in-channel topography has simplified from 2006 to 2016 and that the frequency of deep water habitat has decreased over the same time period, during which the channel has narrowed significantly (Jones, 2018).

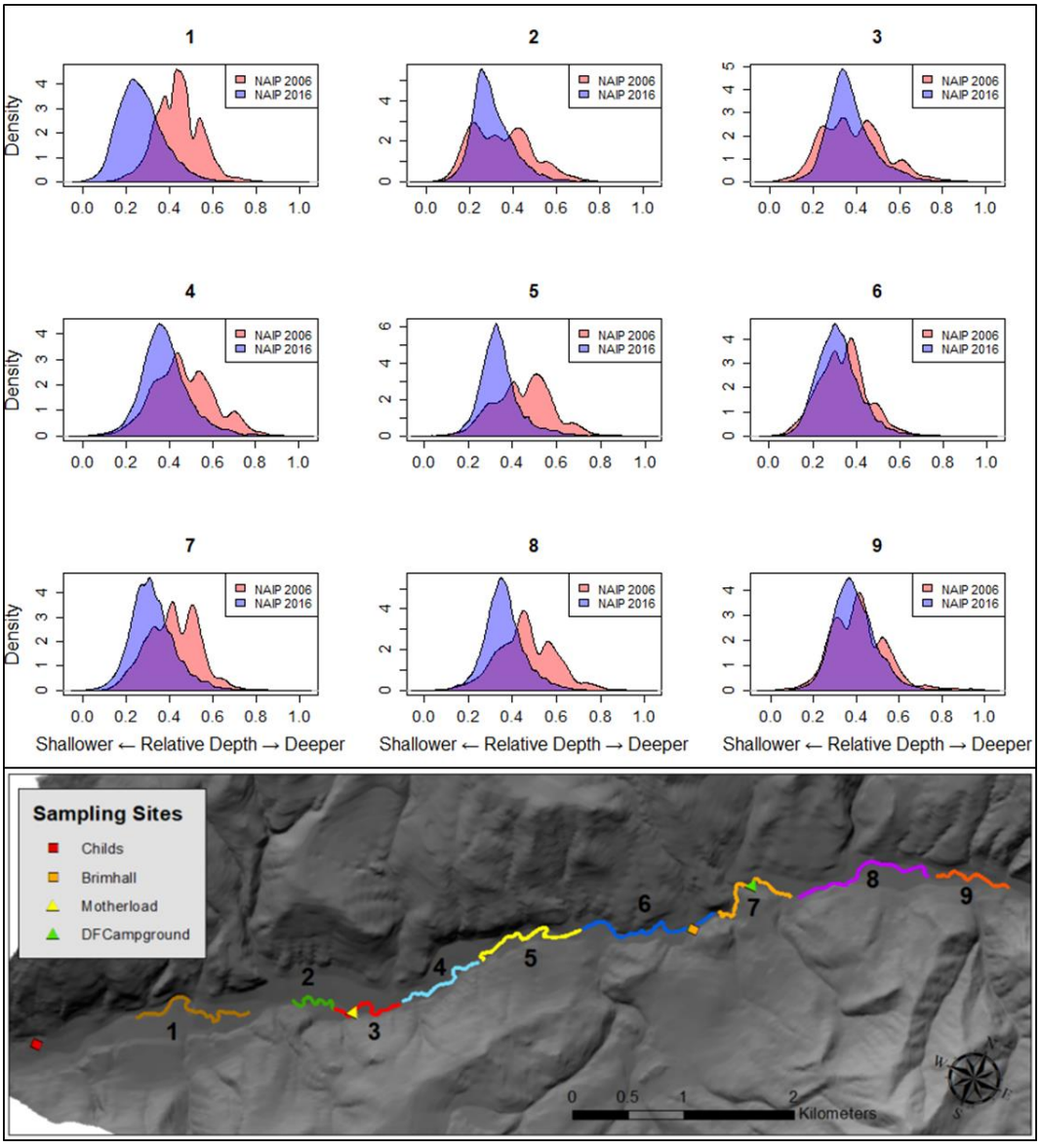

Figure 3.4.12. Distributions of relative depth, as determined from spectral depth analysis, for 2006 (pink) and 2016 (purple) for 9 sub-reaches in the Lower Diamond Fork.

3.4.2.3 Repeat Cross Sections on the lower Diamond Fork

Similar to the Upper Sixth Water Creek sites, we re-surveyed 21 cross sections at 3 sites along the lower Diamond Fork: Diamond Campground (7 cross sections), Motherlode (6 cross sections), and Oxbow (8 cross sections). We compared the water depths from 2006 and 2017 surveys (Figure 3.4.13) and found that mean water depth in 2017 is significantly deeper, as indicated by an ANOVA test, than mean water depth in 2006. Even though discharge during the 2017 surveys (83 cfs) is less than the discharge during the 2006 surveys (91 cfs), OX is on average 0.03 m deeper, MO is 0.07 m deeper, and DCG is 0.1 m deeper. The 2017 depth distributions appear to be more variable, with multi-modal shapes, than the depth distributions from 2006.

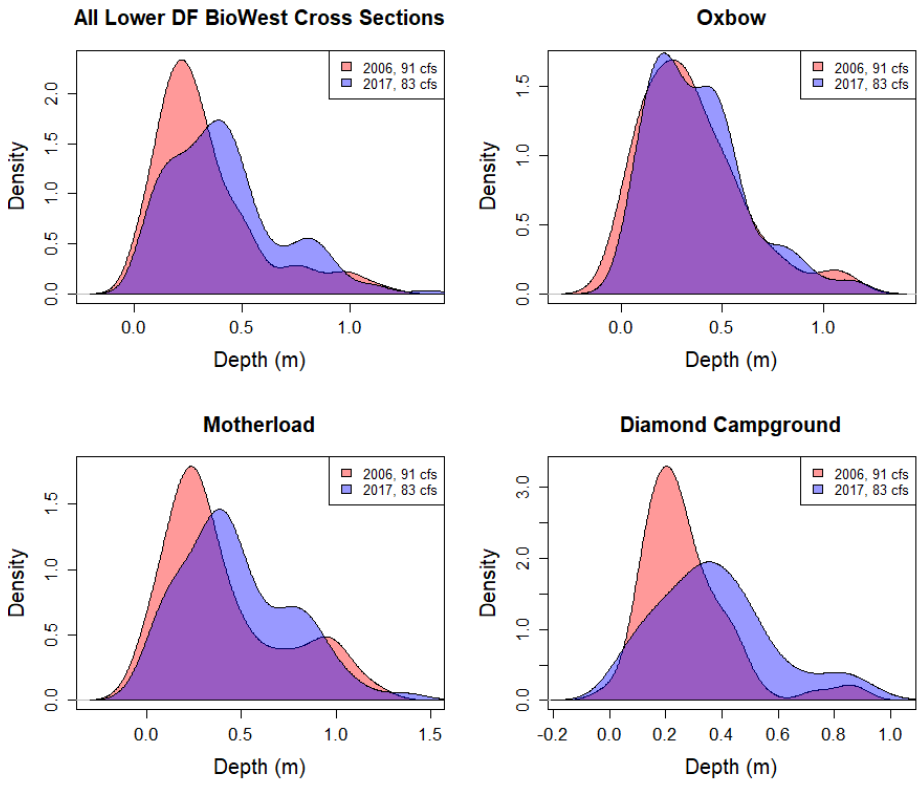

Figure 3.4.13. Water depth distributions from repeat cross sections taken in 2006 and 2017 for sites within the lower Diamond Fork.

3.4.2.4 The Evolution of Instream Habitat

Pools within the unconfined and partially-confined portions of the alluvial valley in the lower Diamond Fork are primarily bar-forced pools. Bars obstruct flow and cause it to converge, producing bed scour that can form a pool. These pools are formed and maintained as long as adequate flow obstructions remain in place. Observations from the 2016 and 2017 field seasons indicate that pools developed in conjunction with the formation of gravel-bars during the 2017 spring runoff. We observed that as gravel bars were built over the course of the spring flood, the adjacent thalweg would deepen by scouring. Sediment to build these gravel bars was observed to come from the bed and banks of upstream reaches.

We observed the formation of new bars and pools at the Motherlode site in 2017 due to such processes (Figure 3.4.14). During the spring flood of 2017, a gravel bar and adjacent pool began to form at the Motherlode site, as well as another gravel bar and pool downstream of the site. By analyzing Google aerial images from 2016 and 2017, we discovered that the banks had eroded a few meters approximately 200 meters upstream. We surmise that local sediment surplus produced from the eroding banks was transported downstream and deposited in the gravel bar. This bar caused flow to converge and velocities to increase to the point that the bed began to scour and a new pool was formed. Scour material from the new pool, as well as other passing particles, were deposited further downstream in another bar which then scoured a new pool. This illustrates two important components of pool formation in the lower Diamond Fork: 1) new pools can be formed as bars are built and 2) bars are built from the locally sourced material of the beds and banks of upstream reaches. To form and maintain pools throughout the lower

Diamond Fork, it is necessary that the supply of gravel is sufficient to maintain and build bars of large enough magnitude to force pools. Buffington et al. (2002) stated that pool volume in alluvial systems could be reduced in scenarios of sediment deficits. As the amplitude of bars is decreased due to sediment starvation, pool volume may be diminished.

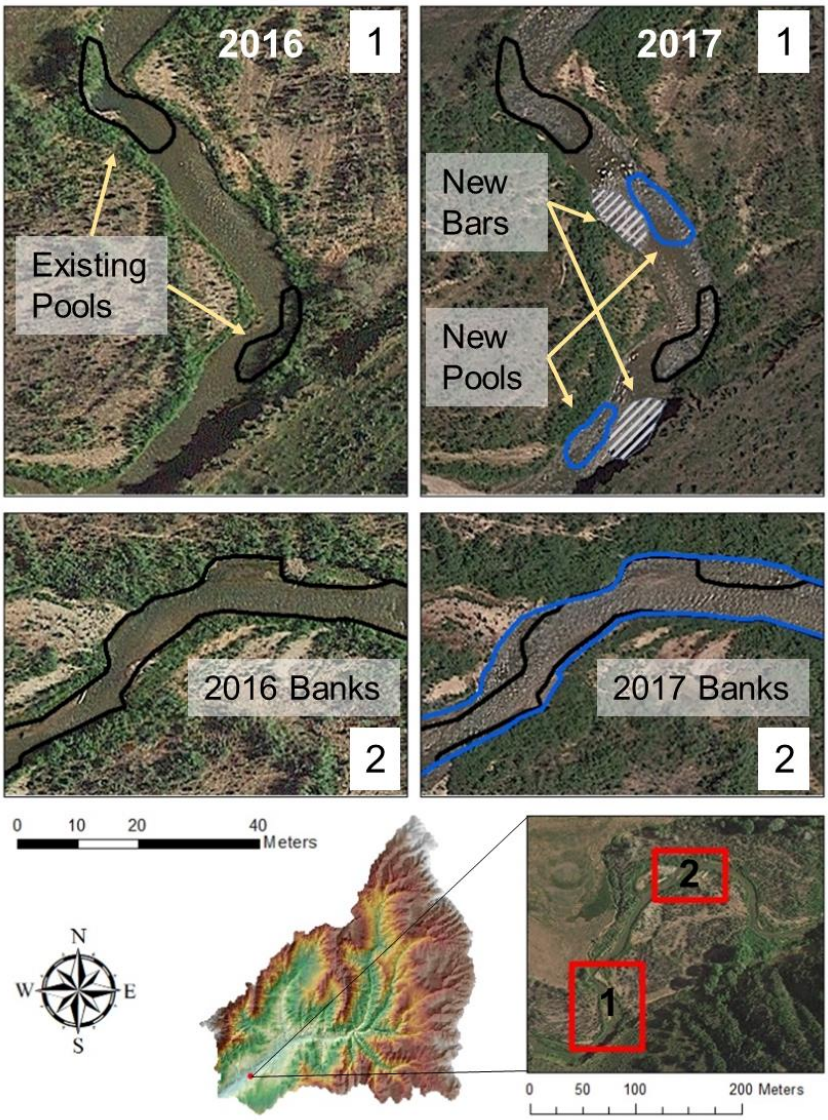

Figure 3.4.14. Map illustrating the formation of pools (at the Motherlode monitoring site) as sediment is sourced upstream for bank erosion and deposited downstream in the form of bars.

From our pool mapping results, we identified 22 reaches 100 m or longer that were entirely devoid of pools. We focused our attention on nine such reaches, each over 200 m long. From these 9 reaches, we identified two common reach types that have undergone channel simplification and loss of pools. The first types of pool devoid reaches are those with legacy channel effects. These are reaches where the 2016 active channel is approximately the same width and in the same location as the active channel from the 20th century era or the 1996-2004 era. These reaches often tend to be wide, maintain a uniform width, and have little sinuosity. Inspection of these reaches using spectral depth retrieval results indicates that the channel was more complex with considerably more identifiable pools in 2006, whereas in 2016, the channel is much simpler. We identified a few pools using the 2016 NAIP image, however overall channel complexity appears to have decreased. Figure 3.4.15 illustrates how the channel in 2016 has remained in the nearly the exact same place, with the exception of two meander bends, since 2003. We observe that in 2006, the channel had more variability in bed topography and that larger areas of deep water are visible. In 2011, a year with a large spring runoff, the channel remains in the same location with little to no erosion or active bar building. By 2016, the variability in bed topography has decreased, and areas of deep water are nearly gone.

Because these reaches are wide and relatively steep, it is likely that the transport capacity of the channel reliably exceeds that of the sediment supply, preventing deposition within the reach. Routine floods are largely contained within the channel and can evacuate readily available sediment from the reach, reduce bar amplitude, and simplify the instream channel topography. The absence of depositional features like bars eliminates focused flow leading to bed and bank erosion. An absence of bank erosion

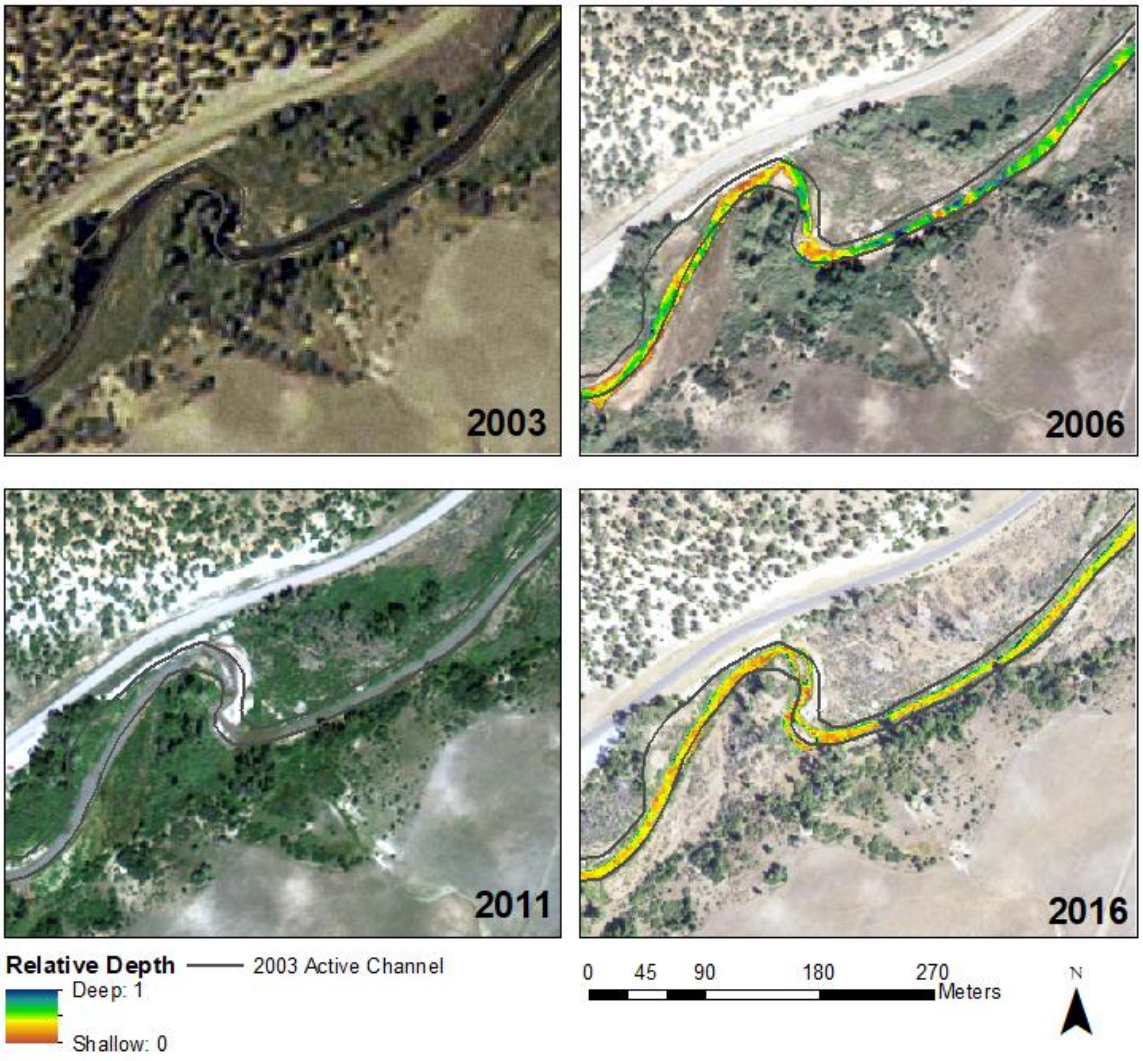

Figure 3.4.15. Map illustrating channel simplification in a reach that has remained in the same location since before the 2004 flow regime change. The grey lines represent the active channel as mapped by Jones (2018) for the year 2004.

allows riparian vegetation to establish and further strengthen the banks.

The second type of pool devoid reaches are those that evolved between 2004 and 2011, but ceased to evolve after 2011. Spectral depth results indicate that these reaches have simplified from 2006 to 2016. Using the aerial imagery from 1993 to 2016, we observe that in these reaches the channel has become less sinuous over time. In 2006, a significant flood produced a great deal of bare ground surfaces, mostly bars, on which

vegetation then became established. In 2011, the second largest flood on record occurred, producing a flood with an approximate 20-year recurrence interval. The 2011 NAIP image (post spring runoff) indicates that banks in pool limited reaches remained vegetated with no visible bars. The 2016 channel remains in its 2011 location and bare surfaces are largely vegetated. Figure 3.4.16 illustrates how a reach above the Motherlode site has decreased in sinuosity and channel complexity. In 2006, large units of deep and shallow water are easily identifiable. By 2016, those units have been reduced to a more uniform bed topography with shallow to medium water depths.

These reaches, much like those that experience legacy channel effects, are likely the product of sediment transport capacity exceeding the sediment supply. The lack of deposition within the reach does not challenge the bed or banks sufficiently to create channel complexity. As floodplains and bars become vegetated, the sediment necessary to build and maintain bars becomes unavailable. During large floods, such as in 2011, established vegetation inhibits the conveyance of overbank flow, causing more flow to be directed into the main channel. With decreased local sediment supply, decreased overbank flow capacity, and increased bank strength, bars and any readily mobile sediment are evacuated from the reach. As bar amplitude is diminished, the presence of pools within the reach is also diminished. Regular occurring floods in subsequent years, such as the small magnitude floods that followed the 2011 flood, do little geomorphic work and the simplified channel persists.

Contrary to the reaches that have simplified and lost pools, some reaches have been able to maintain pools and instream topographic variability. These are reaches are continually adjusting (Figure 3.4.17). One of the patterns observed in reaches with

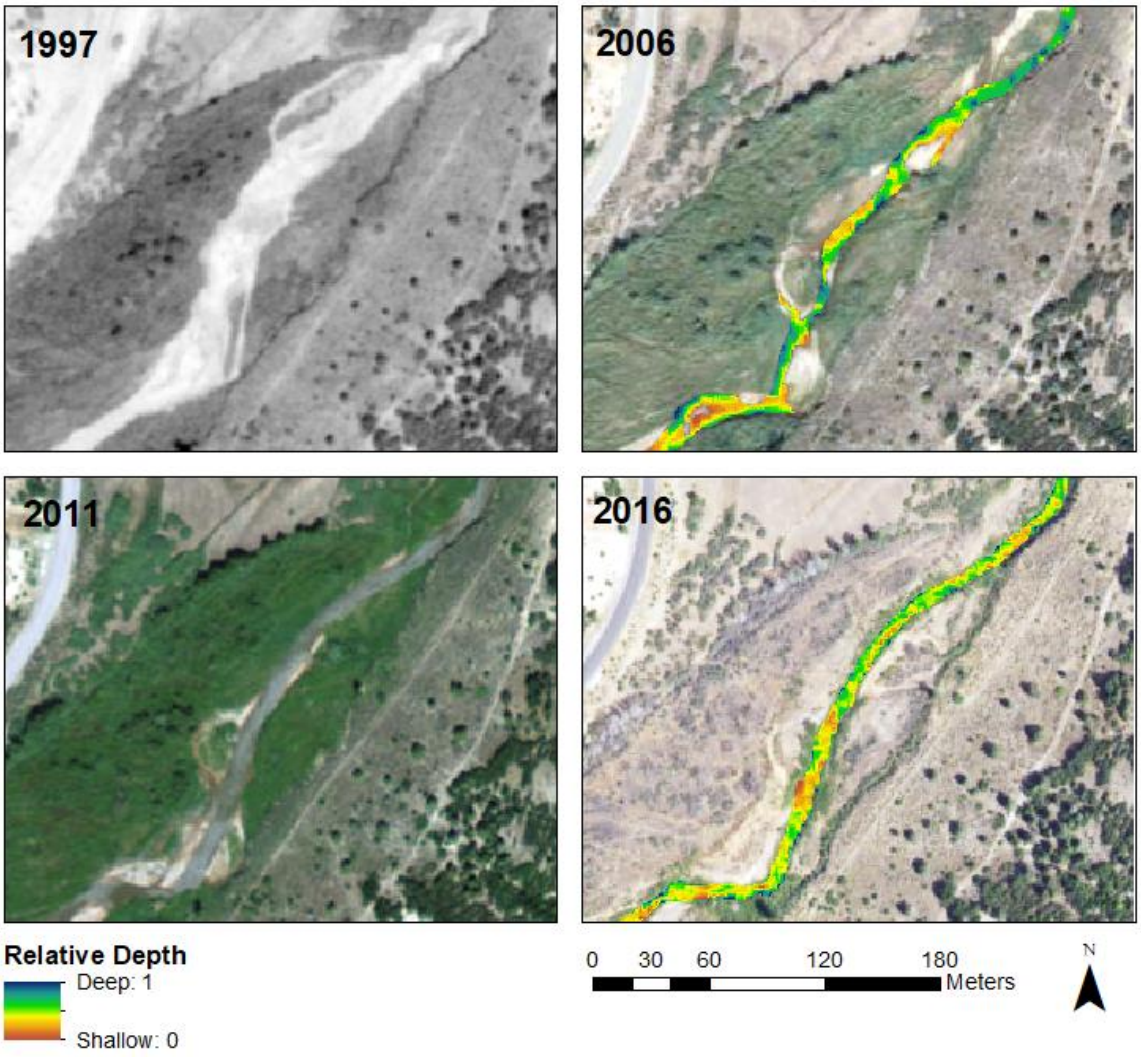

Figure 3.4.16. Map illustrating channel simplification in a reach that has become straighter and more vegetated since the flow regime change in 2004. This reach is located a few hundred meters upstream of the Motherlode monitoring site.

persistent pools is that fresh gravel bars can be observed in the 2011 NAIP image. These reaches have maintained a higher level of sinuosity and have been able to store coarse sediment recruited from upstream reaches so that bars are actively maintained and built.

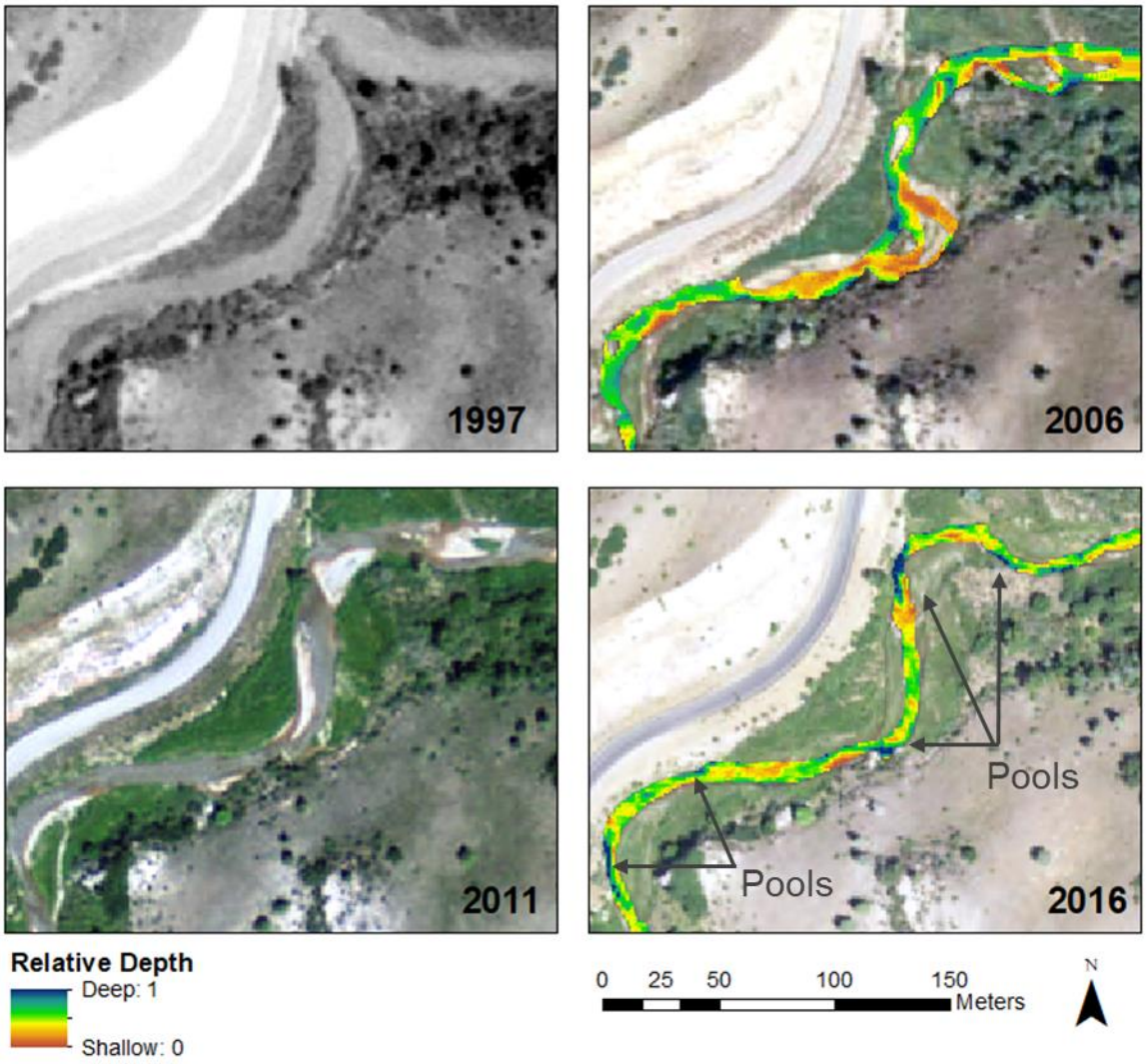

Figure 3.4.17. Map illustrating maintenance of pools in a reach that had active bar formation/maintenance in 2011, and maintained sinuosity over time. This reach is located at the Diamond Campground monitoring site.

3.4.2.5 Sediment Transport

We evaluated the sediment transport measurements at CB and BB sampling sites for grain sizes greater than 8 mm (bar building material) (Figure 3.4.18). The reach directly upstream of CB is narrow and sinuous, with a considerable amount of bar development. It has a desirable number of large and deep pools. The reach directly upstream of BB is wide, straight and steep with few to no pools. Sediment transport was

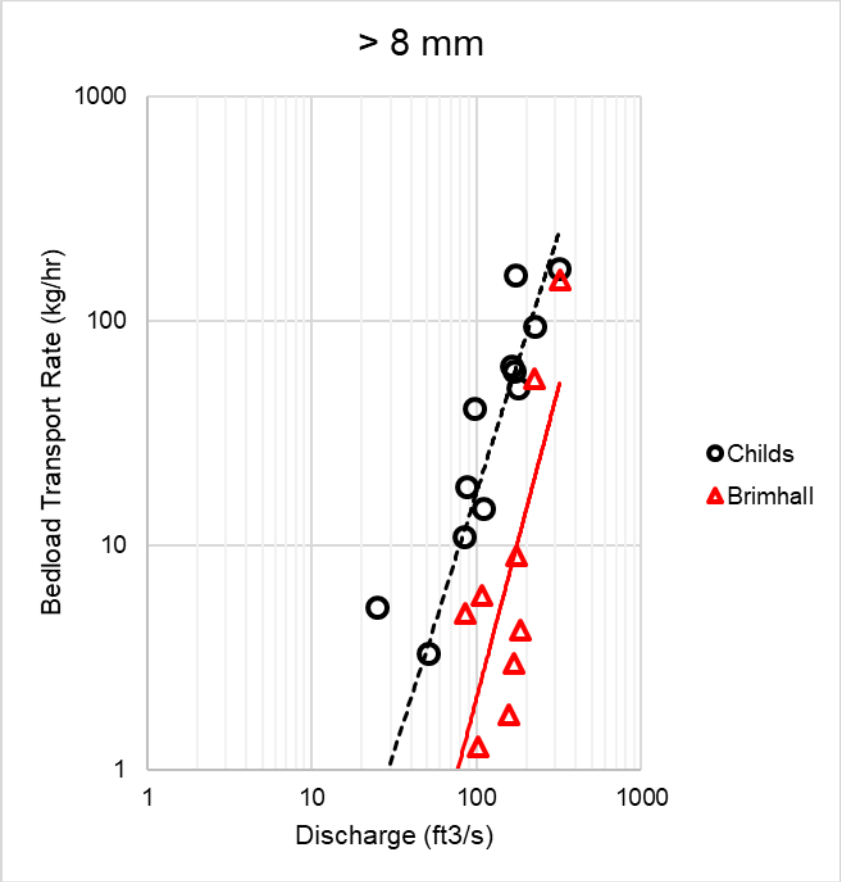

Figure 3.4.18. Bedload sediment transport measurements for Childs Bridge and Brimhall Bridge sites analyzed for grain sizes greater than 8 mm.

moderate at each site, but was approximately 4 to 7 times greater at CB than at BB. We observe that as discharge increases above 200 cfs, sediment transport rates for both sites begins to converge.

3.5 Discussion

3.5.1 Sixth Water Creek

Pools play a major role in the different life history stages of trout. They are a preferred instream unit for all sizes because swimming costs are greatly reduced within a pool. For YoY, pools are preferred, although their small size makes it possible for them

to take advantage of micro-habitat refuge within riffles. For larger trout, pools are absolutely necessary as the energy expenditure in riffles is too great to sustain over long periods of time (Rosenfeld and Boss, 2001).

The number of pools on Sixth Water creek are within or smaller than the range considered suitable for trout habitat (Leopold and Wolman 1957; Leopold et al., 1964; Keller, 1972; Keller and Melhorn, 1978; Raleigh et al., 1984; Hickman and Raleigh 1982; Whittaker, 1987; Chin, 1989; Grant et al., 1990). Pool-to-pool spacing for the confined Lower and Upper Sixth Water Canyon process domains were on average 2 and 3 channel widths per pool, consistent with step-pool reaches which generally exhibit pool-to-pool spacing of 1-4 channel widths. (Whittaker, 1987; Chin, 1989; Grant et al., 1990). For Sixth Water Meadows and Syar process domains, pool-to-pool spacing is approximately 7 channels widths per pool; smaller than we would expect for a headwater stream. Furthermore, most of these pools are small and shallow. This is the case for most of Sixth Water Creek with the exception of the Lower Sixth Water Canyon process domain where large boulders and bedrock ledges create large and deep plunge pools.

During spawning season, pool tails provide the correct hydraulic conditions for spawning (Raleigh et al., 1984; Baxter and Hauer, 2000). An increase in the number of pools with spawning sized substrate (3-80 mm, Budy et al., 2012) provides more area and opportunity for spawning success, while reducing competition and redd disturbance at the same time. In much of Sixth Water Creek, the presence of spawning sized gravels in pool tails is low. We observed that the largest amount of spawning gravel is directly downstream of active sediment sources and declines with distance downstream. As sediment is introduced into the river, finer particles are swept away during high flow and

winnowed out during periods of low flow. The coarser components of the sediment source are left behind and can accumulate to provide sufficient spawning habitat. The Syar and Lower Sixth Water Canyon process domains have significantly more active sediment sources and spawning habitat. We attribute this to the local geologic controls as sediment sources in these process domains have a higher proportion of gravels due to the conglomerate formations from which they are sourced. Furthermore, lateral connectivity with sediment sources is far greater in these process domains.

Although there are reaches with sufficient pools, the overall number and size of pools on Sixth Water Creek is relatively small and may be a potential limiting factor in terms of trout habitat. As pools are an important requirement for large trout, the low degree of available habitat for holding, foraging, and spawning raises concern. A further factor is that 2 to 3 meter tall waterfall is located a few hundred meters downstream of the Sixth Water Flow Control Structure (pictured in Figure 3.4.5). This waterfall likely acts as a fish passage barrier. The majority of prime spawning gravels are located downstream of the waterfall, whereas much of the better rearing and holding habitat may be located upstream of the waterfall (i.e., beaver ponds, colder water temperatures during summer). Although trout populations within the stream are sustainable, they may not be reaching their potential.

Channel change analysis from Jones (2018) shows that Sixth Water Creek stream channel has adjusted very little since the exclusion of trans-basin diversion flows in 1996. Based on the nature of the pools, most of which are forced by boulder or bedrock ledges, and the insignificant channel adjustments observed in repeat cross sections, we suggest that the current state of pool habitat has been largely fixed since the late 1990s, and will

likely remain unchanged for the foreseeable future. Sediment inputs for Upper Sixth Water Canyon and Sixth Water Meadows process domains appear to be exhausted or disconnected insomuch that new pool formation from bar building or additional structural elements such as boulders is unlikely. The only active formation of pools observed throughout Sixth Water Creek is provided by the construction of beaver dams.

We observed multiple beaver dams throughout Sixth Water Creek, with the majority located in the Sixth Water Meadows process domain. These beaver dams provide slow water habitat in reaches that would have otherwise been long runs and riffles. Over the course of our study, we observed the addition of several beaver dams in reaches that otherwise have few pools. Beaver dams were observed to be built in areas with nearby mature populations of willow and other large woody species such as water birch and narrowleaf cottonwood. These beaver dams increased lateral connectivity with floodplains and the riparian corridor and significantly increased the magnitude of slow water habitat. Multiple studies have investigated the hydrologic, geomorphologic and hydraulic impacts of beaver dams (Meentemeyer and Butler, 1999; Nyssen et al., 2011; Pollock et al., 2007; Westbrook et al., 2006). Beavers dams have been shown to be beneficial to fish populations by creating pool habitat (Scholsser, 1995). They increase habitat heterogeneity (Snodgrass and Meffe, 1999), especially in headwater streams which are likely to have little pool formation without them (White and Rahel, 2008). Stout et al. (2017) showed that a relatively low number of beaver dams result in a significant change in channel hydraulics. These changes in channel hydraulics provide water depths and velocities that benefit multiple life stages of trout.

The percentage of pool area will continue to increase if the population of beavers

continues to increase. Key factors for the establishment and success of beaver dams is a healthy riparian corridor. In areas with mature, healthy riparian vegetation, we observe active building of beaver dams. There are many areas along Sixth Water Creek that do not have adequate riparian resources to support beavers. Some of these areas are in confined reaches where cut banks and minimal floodplains do not allow for significant riparian vegetation. Other reaches simply do not have adequate riparian resource notwithstanding the presence of floodplains (i.e., a few kilometers downstream of Above Rays Crossing). It is possible that intense grazing operations in the past may have subdued riparian vegetation along portions of Sixth Water Creek. The potential to increase pool habitat within Sixth Water Creek will most likely come from the increased beaver population, which can be supported by maintaining and increasing riparian vegetation.

3.5.2 Lower Diamond Fork

Pools in the lower Diamond Fork are primarily bar-forced pools and form on the outside of bends in the river. These pools are significantly larger than pools in Sixth Water Creek, but make up a small proportion of the wetted channel area. The pool-to-pool spacing for the entire reach (Childs Bridge to Diamond Campground) is approximately 7 channel widths per pool; within the range of expected pool spacing for alluvial systems (Leopold and Wolman 1957; Leopold et al., 1964; Keller, 1972; Keller and Melhorn, 1978). However, the percent pool area for the entire reach is 12 percent, which is much lower than the suggested 50 to 70 percent pool area required for brown trout (Raleigh et al. 1984). Investigation of sub-reaches show that some reaches have significantly more pools and percent pool area, whereas other reaches are entirely devoid

of pools. The results from the random forests statistical analysis suggest that reaches that are narrower, have higher width variability, higher sinuosity, lower slope, and lower radius of curvature values tend to have more pools and percent pool area. These factors can reduce sediment transport capacity, thereby increasing the deposition of bars and promoting pool development. Reaches may be associated with one or more of these variables in order to exhibit increased pool numbers.

Our understanding of the current channel configuration with regards to pools is increased as we consider channel condition of the past and how it evolved to what it is today. We documented a reach wide simplification of instream channel topography from 2006 to 2016 – a time frame when the lower Diamond Fork was actively narrowing (Jones, 2018). The shift from a multi-modal distribution of water depth in 2006 to a unimodal distribution by 2016 likely took place as bars were trimmed, pools were filled, and sediment sources were locked up by encroaching vegetation. By investigating reaches that currently are devoid of pools, we identified two mechanisms by which channel simplification occurs within the lower Diamond Fork. Both of these mechanisms involve a reach transport capacity that exceeds sediment supply, preventing deposition of bars and their associated pools.

Local reduction in sediment supply is a mechanism by which size and number of pools are reduced. The formation of gravel bars in the lower Diamond Fork is key to the formation and maintenance of pools. These bars are what cause flow to converge and scour the bed. In the presence of a sediment deficiency, pool volume can be decreased as the amplitude of bars is diminished (Buffington et al., 2002) to the point that pools are eliminated from the reach. The lack of bar development reduces the capacity of the

channel to meander and recruit more sediment for downstream reaches by eroding outer banks. Eventually, these reaches lose their sinuosity as bars are trimmed. The current sediment transport dynamics for these pool-poor reaches are not currently known, but the absence of sediment deposition indicates that slope and channel geometry of the reach is sufficient to transport all supplied sediment. Sediment transport measurements taken at CB and BB (Figure 3.4.18) support this notion and demonstrate that the narrower, more sinuous reach with multiple large, deep pools and active bars directly above the CB transport sampling site has more active transport and transports approximately 4 to 7 times more sediment than the wide, straight and steep reach above the BB transport sampling site, which once contained more pools but is largely devoid of them today.

The second mechanism is vegetation encroachment on floodplains, bars, and banks. This is closely related to the first mechanism as it is one of the drivers for sediment supply deficits. As the channel narrowed over time, we observed increased vegetation on the previously exposed floodplains, bars, and banks. We suggest that the vegetation of these surfaces “lock up” local sediment sources. During high flow conditions, exposed surfaces could be readily accessed from which coarse material could be recruited for downstream bar development. As vegetation established on these surfaces, material was not as easily accessed, thus reducing the supply of sediment to downstream reaches. The establishment of vegetation on these surfaces also reduces the overbank conveyance of flow during flood events. If a larger fraction of flood flow is contained with the channel, sediment transport capacity is increased. As illustrated in Figure 3.4.17, reaches where the banks and floodplains remained vegetated during the 2011 spring runoff are places where channel simplification is most noticeable. Contrary

to that, reaches that had exposed surfaces after the 2011 spring runoff still maintain pools today. We would argue that these exposed surfaces are likely where bars were formed that subsequently narrowed the channel sufficiently in order to form and maintain pools that are present today.

For these mechanisms of channel simplification and loss of pools, pools on the lower Diamond Fork are formed where local sediment sources are activated during high flow events and bars are formed with the material. We observed pool formation in several areas of the lower Diamond Fork following the spring runoff of 2017. Spring runoff peaked at 377 cfs, which has a return interval between 5 and 10 years (Figure 2.2.3; Kenney et al., 2007), but maintained flows well above the 2-year flood for nearly two consecutive weeks. During this time, we observed and measured moderate, but significant amounts of sediment transport at multiple sites along the lower Diamond Fork (Jones, 2018). Repeat cross sections surveyed in 2017 suggested that the channel had indeed become deeper and more complex since 2006 (Figure 3.4.13). The flood of 2011 was even larger than that in 2017, yet the air photo analysis between 2006 to 2016 indicates that the river channel generally became simpler. This may indicate that the effect of a larger flood in producing more pools extends only for five years or less. Alternatively, the river channel may have narrowed to the point that increasing portions of the reach are able to produce significant transport and erosion at ever smaller floods.

While the 2017 spring runoff was impressive and formed multiple pools, its return interval was much larger than the 1- to 2- year floods that are required to perform pool formation and maintenance (Keller, 1971; Thompson, 2011; Bayat et al., 2017). It appears that within the lower Diamond Fork, the effectiveness of smaller, regularly

occurring floods have been reduced such that only the larger, rarer floods are capable of doing significant work. We suggest that this phenomenon is largely attributable to channel width, which is perhaps too wide to produce and maintain desirable instream habitat. Jones (2018) suggested that the augmented baseflow regime reduced the amount of narrowing that took place within the lower Diamond Fork since 2004 by completely inundating the bed and inhibiting the establishment of vegetation that would have induced further narrowing. Analysis of channel geometry indicates that lowering the augmented baseflow (80 cfs to 40 cfs) could cause the channel to potentially narrow by approximately 1 meter (discussed in Chapter 1; Wilcock et al., 2019). In theory, the wider channel would take a larger flow to actively transport material in order to create bars and pools. If the channel were narrower, the effectiveness of floods, particularly smaller floods, would be increased. Wilcock et al. (2019) tested this by using 1D hydraulic models for the CB, BB, and MO sites. By narrowing the channel by one meter, bed shear stress increased about 5% to 10%. While this increase is proportionally small, Wilcock et al. (2019) noted that under conditions of small transport that are near incipient motion, the response in transport as a function of increased bed shear stress would likely be much stronger than a linear. Therefore, we would expect that if the channel width were to decrease as a result of lowering the baseflow regime, sediment transport would increase and likely enhance the formation and maintenance of pools within the lower Diamond Fork.

3.5.2.1 Large woody debris in the lower Diamond Fork

In most streams, large woody debris is an important factor in the formation of pools. LWD is an important instream habitat structure as individual logs and log jams

create hydraulic diversity and help scour pools. LWD is lacking within the lower Diamond Fork, particularly the reach we surveyed from Childs Bridge to Diamond Campground. We did not perform a census of LWD with the lower Diamond Fork as there was little wood in or near the channel. Cottonwoods are nearly non-existent throughout much of this reach due to the large 20th century flows that stripped the floodplain of cottonwoods. Willows are now the dominant species along the river banks. In the Below Confluence and Monks Hollow process domains, the presence of cottonwoods is much greater. Although not thoroughly described in this study, we observed that LWD loading from fallen cottonwoods in those process domains played a significant role in increasing pool size and number for these reaches. The introduction of more LWD as a structural element to increase pool habitat within the lower Diamond Fork is needed. If the channel were to narrow, the likelihood of LWD being stored within the channel would increase as the size of the channel would be smaller relative to the length of available LWD. However, given the lack of a healthy cottonwood gallery, passive recruitment of large woody debris could take tens to hundreds of years for cottonwoods to grow, die, and be recruited into the channel.

Habitat enhancement projects can be performed through channel reconstruction and structural element placement (beaver dam analogs, post assisted log structures, boulder and log vanes, j-hooks, etc.). Mechanical introduction of structural elements can easily form pools within the system. We observed that over the course of the study, a pool scoured downstream of a PVC pipe containing an antenna and placed perpendicular to flow to record RFID tagged gravels and leaves as they passed by. Using habitat enhancement techniques is a viable method, but require a great deal of time and money to

perform. For the overall longevity of enhanced habitat, a natural load of LWD is required. This is highly dependent on the establishment and success of a cottonwood gallery.

3.5.3 Management implications and future research

Our study illustrates that for much of the Diamond Fork system, pools are present in size and number relative to conditions thought to favor trout. For Sixth Water Creek, managers should consider the installation of beaver dam analogs (BDAs) to encourage more beaver dam development while managing riparian vegetation in order to sustain the needs of beavers. We observed a low degree of spawning habitat in the Sixth Water Meadows and Upper Sixth Water Canyon process domains. Field observations indicated that little spawning occurs in the Syar and Lower Sixth Water Canyon process domains where more abundant spawning gravel is available. Future research for this stream should be aimed at understanding spawning behavior and where it occurs throughout Sixth Water Creek. Currently, the Syar and Lower Sixth Water Canyon process domains have the best spawning habitat for cutthroat trout. Further observations are needed to confirm if spawning takes place there or not.

Our results for the lower Diamond Fork illustrate that a narrower, variable width, sinuous/lower slope channel tends to have more pools. A narrower channel makes floods more effective which in turn produces more sediment transport (Wilcock et al. 2019), a necessary component for the formation and maintenance of bars and pools. Lowering the baseflow will likely allow for such narrowing. The narrower channel will allow for the activation of local sediment sources as the bed and banks are challenged more frequently by smaller floods. Managers should consider this as they pursue habitat enhancement

projects and channel reconstruction. Sequential years of drought and reduced spring runoff peak magnitudes may be mitigated by prescribed flushing flows in order to maintain pools.

Future monitoring of the system is recommended in order to track and evaluate changes to the system, especially if a new flow regime is prescribed. Ensuring that the system experiences sediment mobilizing flows on a regular basis, and that sediment sources remain active (i.e., vegetation encroachment does not become too great) is crucial for the long term formation and maintenance of pools. Improving and maintaining riparian conditions such that more vegetation is available for beaver dam construction in Sixth Water Creek and more cottonwoods can provide LWD loading to the lower Diamond Fork is recommended for producing sustainable numbers of large pools throughout the Diamond Fork system.

References

Archer, Eric K.; Henderson, Richard; Ojala, Jeffrey V.; Gavin, Amanda and Burke, Karen K. (2016). PacFish InFish Biological Opinion (PIBO) Monitoring Program: Effectiveness Monitoring Sampling Methods for Stream Channel Attributes. Unpublished paper on file with PIBO Monitoring Program.

Baxter, C. V., & Hauer, F. R. (2000). Geomorphology, hyporheic exchange, and selection of spawning habitat by bull trout (Salvelinus confluentus). *Canadian Journal of Fisheries and Aquatic Sciences*, *57*(7), 1470-1481.

Bayat, E., Rodríguez, J. F., Saco, P. M., de Almeida, G. A., Vahidi, E., & García, M. H. (2017). A tale of two riffles: Using multidimensional, multifractional, time-varying sediment transport to assess self-maintenance in pool-riffle sequences. *Water Resources Research, 53*(3), 2095-2113.

BIO-WEST, Inc. (2009). Sixth Water and Diamond Fork Creeks Final 2007 Monitoring Report, 436 p.

Budy, P., Wood, S., & Roper, B. (2012). A study of the spawning ecology and early life history survival of Bonneville cutthroat trout. *North American Journal of Fisheries Management, 32*(3), 436-449.

Buffington, J. M., Lisle, T. E., Woodsmith, R. D., & Hilton, S. (2002). Controls on the size and occurrence of pools in coarse-grained forest rivers. *River Research and Applications*, *18*(6), 507-531.

Call, B. C., Belmont, P., Schmidt, J. C., & Wilcock, P. R. (2017). Changes in floodplain inundation under nonstationary hydrology for an adjustable, alluvial river channel. *Water Resources Research*, *53*(5), 3811-3834.

Chin, A. (1989). Step pools in stream channels. *Progress in physical geography*, *13*(3), 391-407.

Cutler, D. R., Edwards Jr, T. C., Beard, K. H., Cutler, A., Hess, K. T., Gibson, J., & Lawler, J. J. (2007). Random forests for classification in ecology. *Ecology*, *88*(11), 2783-2792.

Dean, D. J., Topping, D. J., Schmidt, J. C., Griffiths, R. E., & Sabol, T. A. (2016). Sediment supply versus local hydraulic controls on sediment transport and storage in a river with large sediment loads. *Journal of Geophysical Research: Earth Surface*, *121*(1), 82-110.

Dietrich, W. E., Kirchner, J. W., Ikeda, H., & Iseya, F. (1989). Sediment supply and the development of the coarse surface layer in gravel-bedded rivers. *Nature*, *340*(6230), 215.

Elliott, J. M. (2000). Pools as refugia for brown trout during two summer droughts: trout responses to thermal and oxygen stress. *Journal of fish biology*, *56*(4), 938-948.

Emmett, W. W., Leopold, L. B., & Myrick, R. M. (1983). Some characteristics of fluvial processes in rivers: Second International Symposium on River Sedimentation. *Nanjing, China, 1983, Proceedings*.

Glova, G. J. (1984). Management implications of the distribution and diet of sympatric populations of juvenile coho salmon and coastal cutthroat trout in small streams in British Columbia, Canada. *The Progressive Fish-Culturist*, *46*(4), 269-277.

Glova, G. J. (1986). Interaction for food and space between experimental populations of juvenile coho salmon (Oncorhynchus kisutch) and coastal cutthroat trout (Salmo clarki) in a laboratory stream. *Hydrobiologia*, *131*(2), 155-168.

Grant, G. E., Swanson, F. J., & Wolman, M. G. (1990). Pattern and origin of stepped-bed morphology in high-gradient streams, Western Cascades, Oregon. *Geological Society of America Bulletin*, *102*(3), 340-352.

Grant, J. W., & Kramer, D. L. (1990). Territory size as a predictor of the upper limit to population density of juvenile salmonids in streams. *Canadian Journal of Fisheries and Aquatic Sciences*, *47*(9), 1724-1737.

Harig, A. L., & Fausch, K. D. (2002). Minimum habitat requirements for establishing translocated cutthroat trout populations. *Ecological Applications*, *12*(2), 535-551.

Heggenes, J., Northcote, T. G., & Peter, A. (1991). Seasonal habitat selection and preferences by cutthroat trout (Oncorhynchus clarki) in a small coastal stream. *Canadian Journal of Fisheries and Aquatic Sciences*, *48*(8), 1364-1370.

Hickman, T. J., & Raleigh, R. F. (1982). *Habitat suitability index models: cutthroat trout* (No. 82/10.5). US Fish and Wildlife Service.

James, L. A. (1991). Incision and morphologic evolution of an alluvial channel recovering from hydraulic mining sediment. *Geological Society of America Bulletin*, *103*(6), 723-736.

Jones, Jabari C., "Historical Channel Change Caused by a Century of Flow Alteration on Sixth Water Creek and Diamond Fork River, UT" (2018). *All Graduate Theses and Dissertations*. 7353.
https://digitalcommons.usu.edu/etd/7353

Keller, E. A. (1971). Areal sorting of bed-load material: the hypothesis of velocity reversal. *Geological Society of America Bulletin*, *82*(3), 753-756.

Keller, E. A. (1972). Development of alluvial stream channels: a five-stage model. *Geological Society of America Bulletin*, *83*(5), 1531-1536.

Keller, E. A., & Melhorn, W. N. (1978). Rhythmic spacing and origin of pools and riffles. *Geological Society of America Bulletin*, *89*(5), 723-730.

Kenney, T. A., Wilkowske, C. D., & Wright, S. J. (2007). Methods for estimating magnitude and frequency of peak flows for natural streams in Utah.

Kondolf, G. M., Piégay, H., & Landon, N. (2002). Channel response to increased and decreased bedload supply from land use change: contrasts between two catchments. *Geomorphology*, *45*(1-2), 35-51.

Lane, E. W. (1955). Importance of fluvial morphology in hydraulic engineering. *Proceedings (American Society of Civil Engineers); v. 81, paper no. 745*.

Langbein, W. B., & Leopold, L. B. (1964). Quasi-equilibrium states in channel morphology. *American Journal of Science*, *262*(6), 782-794.

Lauer, J. W. (2006). Channel Planform statistics toolbox. *National Center for Earthsurface Dynamics, Minneapolis, MN, 55414*.

Lauer, J. W., Echterling, C., Lenhart, C., Belmont, P., & Rausch, R. (2017). Air-photo based change in channel width in the Minnesota River basin: Modes of adjustment and implications for sediment budget. *Geomorphology*, *297*, 170-184.

Legleiter, C. J., Roberts, D. A., Marcus, W. A., & Fonstad, M. A. (2004). Passive optical remote sensing of river channel morphology and in-stream habitat: Physical basis and feasibility. *Remote Sensing of Environment*, *93*(4), 493-510.

Legleiter, C. J., Roberts, D. A., & Lawrence, R. L. (2009). Spectrally based remote sensing of river bathymetry. *Earth Surface Processes and Landforms*, *34*(8), 1039-1059.

Legleiter, C. J. (2013). Mapping river depth from publicly available aerial images. *River Research and Applications*, *29*(6), 760-780.

Leopold, L. B., & Maddock, T. (1953). *The hydraulic geometry of stream channels and some physiographic implications* (Vol. 252). US Government Printing Office.

Leopold, L. B., & Wolman, M. G. (1957). *River channel patterns: braided, meandering, and straight*. US Government Printing Office.

Leopold, L. B.,Wolman, M. G., and Miller, J. P. (1964) *Fluvial processes in geomorphology*. San Francisco, California,W. H. Freeman, 522 p.

Liaw, A., & Wiener, M. (2002). Classification and regression by randomForest. *R news*, *2*(3), 18-22.

Liébault, F., & Piégay, H. (2002). Causes of 20th century channel narrowing in mountain and piedmont rivers of southeastern France. *Earth Surface Processes and Landforms: The Journal of the British Geomorphological Research Group*, *27*(4), 425-444.

Lisle, T. E. (1987). Using" residual depths" to monitor pool depths independently of discharge. *Res. Note PSW-RN-394. Berkeley, CA: US Department of Agriculture, Forest Service, Pacific Southwest Forest and Range Experiment Station. 4 p*, *394*.

Lisle, T. E., Iseya, F., & Ikeda, H. (1993). Response of a channel with alternate bars to a decrease in supply of mixed-size bed load: A flume experiment. *Water Resources Research*, *29*(11), 3623-3629.

Lonzarich, D. G., & Quinn, T. P. (1995). Experimental evidence for the effect of depth and structure on the distribution, growth, and survival of stream fishes. *Canadian Journal of Zoology*, *73*(12), 2223-2230.

Marcus, W. A., & Fonstad, M. A. (2008). Optical remote mapping of rivers at sub-meter resolutions and watershed extents. *Earth Surface Processes and Landforms, 33*(1), 4-24.

Marcus, W. A., & Fonstad, M. A. (2010). Remote sensing of rivers: the emergence of a subdiscipline in the river sciences. *Earth Surface Processes and Landforms, 35*(15), 1867-1872.

Marcus, W. A., Legleiter, C. J., Aspinall, R. J., Boardman, J. W., & Crabtree, R. L. (2003). High spatial resolution hyperspectral mapping of in-stream habitats, depths, and woody debris in mountain streams. *Geomorphology*, *55*(1-4), 363-380.

Meentemeyer, R. K., & Butler, D. R. (1999). Hydrogeomorphic effects of beaver dams in Glacier National Park, Montana. *Physical Geography*, *20*(5), 436-446.

Montgomery, D. R., Buffington, J. M., Smith, R. D., Schmidt, K. M., & Pess, G. (1995). Pool spacing in forest channels. *Water Resources Research*, *31*(4), 1097-1105.

Moore, K. M., & Gregory, S. V. (1988). Response of young-of-the-year cutthroat trout to manipulation of habitat structure in a small stream. *Transactions of the American Fisheries Society*, *117*(2), 162-170.

Nyssen, J., Pontzeele, J., & Billi, P. (2011). Effect of beaver dams on the hydrology of small mountain streams: example from the Chevral in the Ourthe Orientale basin, Ardennes, Belgium. *Journal of hydrology*, *402*(1-2), 92-102.

Olson, J. R., & Hawkins, C. P. (2012). Predicting natural base-flow stream water chemistry in the western United States. *Water Resources Research*, *48*(2).

Pasternack, G. B., & Hopkins, C. (2017, December). Near-census Delineation of Laterally Organized Geomorphic Zones and Associated Sub-width Fluvial Landforms. In *AGU Fall Meeting Abstracts*.

Pollock, M. M., Beechie, T. J., & Jordan, C. E. (2007). Geomorphic changes upstream of beaver dams in Bridge Creek, an incised stream channel in the interior Columbia River basin, eastern Oregon. *Earth Surface Processes and Landforms*, *32*(8), 1174-1185.

Raleigh, R. F., Zuckerman, L. D., & Nelson, P. C. (1984). *Habitat suitability index models and instream flow suitability curves: brown trout* (No. 82/10.124). US Fish and Wildlife Service.

Roper, B. B., Kershner, J. L., Archer, E., Henderson, R., & Bouwes, N. (2002). AN EVALUATION OF PHYSICAL STREAM HABITAT ATTRIBUTES USED TO

MONITOR STREAMS 1. *JAWRA Journal of the American Water Resources Association*, *38*(6), 1637-1646.

Rosenfeld, J. S., & Boss, S. (2001). Fitness consequences of habitat use for juvenile cutthroat trout: energetic costs and benefits in pools and riffles. *Canadian Journal of Fisheries and Aquatic Sciences*, *58*(3), 585-593.

Schlosser, I. J. (1995). Critical landscape attributes that influence fish population dynamics in headwater streams. *Hydrobiologia*, *303*(1-3), 71-81.

Schmidt, J. C., & Wilcock, P. R. (2008). Metrics for assessing the downstream effects of dams. *Water Resources Research*, *44*(4).

Schumm, S. A. (1977). *The fluvial system* (Vol. 338). New York: Wiley.

Schumm, S. A. (1985). Patterns of alluvial rivers. *Annual Review of Earth and Planetary Sciences*, *13*(1), 5-27.

Shaw, R. G., & Mitchell-Olds, T. (1993). ANOVA for unbalanced data: an overview. *Ecology*, *74*(6), 1638-1645.

Snodgrass, J. W., & Meffe, G. K. (1999). Habitat use and temporal dynamics of blackwater stream fishes in and adjacent to beaver ponds. *Copeia*, 628-639.

Strobl, C., Boulesteix, A. L., Zeileis, A., & Hothorn, T. (2007). Bias in random forest variable importance measures: Illustrations, sources and a solution. *BMC bioinformatics*, *8*(1), 25.

Stout, T. L., Majerova, M., & Neilson, B. T. (2017). Impacts of beaver dams on channel hydraulics and substrate characteristics in a mountain stream. *Ecohydrology*, *10*(1), e1767.

Surian, N., Rinaldi, M., Pellegrini, L., Audisio, C., Maraga, F., Teruggi, L., ... & Ziliani, L. (2009). Channel adjustments in northern and central Italy over the last 200 years. *Management and restoration of fluvial systems with broad historical changes and human impacts: geological society of America Special Paper*, *451*, 83-95.

Tamminga, A., Hugenholtz, C., Eaton, B., & Lapointe, M. (2015). Hyperspatial remote sensing of channel reach morphology and hydraulic fish habitat using an unmanned aerial vehicle (UAV): a first assessment in the context of river research and management. *River Research and Applications*, *31*(3), 379-391.

Thompson, D. M. (2011). The velocity-reversal hypothesis revisited. *Progress in Physical Geography*, *35*(1), 123-132.

Tonina, D., & Jorde, K. (2013). Hydraulic modelling approaches for ecohydraulic studies: 3D, 2D, 1D and non-numerical models. *Ecohydraulics: An integrated approach*, 31-74.

Van Steeter, M. M., & Pitlick, J. (1998). Geomorphology and endangered fish habitats of the upper Colorado River: 1. Historic changes in streamflow, sediment load, and channel morphology. *Water Resources Research*, *34*(2), 287-302.

Vaughan, Angus A., "Discharge-Suspended Sediment Relations: Near-channel Environment Controls Shape and Steepness, Land Use Controls Median and Low Flow Conditions" (2016). *All Graduate Theses and Dissertations*. 5191. https://digitalcommons.usu.edu/etd/5191

Westbrook, C. J., Cooper, D. J., & Baker, B. W. (2006). Beaver dams and overbank floods influence groundwater–surface water interactions of a Rocky Mountain riparian area. *Water Resources Research*, *42*(6).

Wheaton, J. M., Fryirs, K. A., Brierley, G., Bangen, S. G., Bouwes, N., & O'Brien, G. (2015). Geomorphic mapping and taxonomy of fluvial landforms. *Geomorphology*, *248*, 273-295.

Whittaker, J. G. (1987). Sediment transport in step-pool streams. *Sediment Transport in Gravel-Bed Rivers. John Wiley and Sons New York. 1987. p 545-579, 20 fig, 40 ref.*

Wilcock P., Atwood T., Belmont P., Epperly J., Gaeta J., Hammill E., Jones J. & Stout J. (2019). *Comprehensive study and recommendations for instream flow and requirements on Sixth Water Creek and Diamond Fork River: second interim report.* Department of Watershed Sciences, Utah State University.

Winterbottom, S. J., & Gilvear, D. J. (1997). Quantification of channel bed morphology in gravel-bed rivers using airborne multispectral imagery and aerial photography. *Regulated Rivers: Research & Management: An International Journal Devoted to River Research and Management*, *13*(6), 489-499.

CHAPTER 4

CONCLUSION

The Diamond Fork River and Sixth Water Creek have been highly altered both geomorphically and ecologically due to exceptionally large, trans-basin diversion flows during the 20th Century. These augmented flows exceeded most natural floods and caused extensive channel change in the form of incision in Sixth Water Creek and active channel migration on lower Diamond Fork. In 1996 and 2004, infrastructure was completed to have diversion flows completely bypass the river. In an effort to mitigate the effects of the irrigation flows, minimum instream flows about 3-4 times larger than natural baseflows (which were based on the wider, more dynamic channel left over from the 20th century hydrologic alterations) were prescribed in the hopes of maximizing the amount of available fish habitat. Since removal of the full trans-basin diversion flows and implementation of base flows in 2004, Sixth Water Creek has experienced minimal changes as the channel from the 20th century has largely remained intact due to an exhausted sediment supply (Jones, 2018). The lower Diamond Fork on the other hand has narrowed and increased in sinuosity as alluvial deposits from the trans-basin diversions era have been reworked.

As the channels within the Diamond Fork system have changed, the appropriateness of the mandated instream flows has also changed. Instream flows for Sixth Water Creek, as indicated by NREI models, are on the margin of being too large and smaller values could benefit trout. Pools within Sixth Water Creek are generally small and few in number and are not likely to change due to the static nature of the channel and the exhausted sediment supply. Beavers are the most likely mechanism by

which the channel will actively change and develop more pool habitat.

For the lower Diamond Fork, we documented a reach wide simplification of instream habitat and loss of deep water features throughout the lower Diamond Fork in concurrence with the channel narrowing that occurred following the implementation of minimum instream flows. The extent of narrowing was likely limited by the augmented baseflow regime, which prevents establishment of vegetation and storage of sediment within the permanently wetted channel (Jones, 2018; Wilcock et al., 2019). Our analysis of instream flows showed that a baseflow smaller than the mandated regime would benefit trout by reducing the energetic requirements to forage. A smaller baseflow is likely to induce further channel narrowing, which may produce more sediment transport and increase the effectiveness of smaller floods (Wilcock et al., 2019). We expect that a further narrowing of the channel would create and maintain more pools more frequently over spatial and temporal scales. These changes in instream habitat would be beneficial for the entire riverine ecosystem and would likely not compromise the success of a lower instream flow in the future.

The Diamond Fork system is an example of a case in which potential channel change was not considered in developing recommended environmental flows. While there are many methods to predict and quantify channel change with regards to channel gradient, depth, width, grain texture, sinuosity, and planform (Schumm, 1985; Van Steeter and Pitlick, 1998; Kondolf et al., 2002; Liébault and Piégay, 2002; Dietrich et al., 1989; Lisle et al., 1993; Schmidt and Wilcock, 2008; Leopold and Maddock, 1953; James, 1991; Surian et al., 2009; Call et al., 2017; Lauer et al., 2017), these methods are often for reach averaged conditions and provide little information about the quality and

quantity of instream habitat, such as pools. The development of methods and tools to integrate instream habitat changes with instream flows is crucial for the long term success of instream flow prescriptions.

Our research showcases the utility of NREI models for evaluating environmental flows for fish and demonstrates that one can detect and make predictions about the quality and quantity of instream habitat, how it has changed over time in response to changes in flow and sediment, and how it may change in the future under a new instream flow prescription. Using our observations of the channel from the past and comparing to current conditions, we are able to make predictions as to the direction and relative magnitude of change in instream habitat that we would expect to observe given a new flow regime and make predictions as to the beneficial nature of those changes.

The history of the Diamond Fork system highlights and re-emphasizes the need for adaptive management and continued monitoring of the impacts from instream flows. Despite the major channel degradation as a result of the 20th century trans-basin diversions, the Diamond Fork system has largely recovered since the introduction of minimum instream flows in 2004. To the untrained eye, one might applaud the success of the mandated instream flows and consider the Diamond Fork to be "restored". An evaluation of the stream's evolution over time and its current condition today reveals a different narrative. The channel change that occurred within the Diamond Fork system in the 15 years of mandated flows suggests that greater success can be achieved with flows different from those prescribed.

While many frameworks and methods focus on developing hydrologic and geomorphic classifications and flow alteration-ecology response relations in order to

prescribe instream flows for streams and rivers that have undergone hydrologic alterations (Tharme, 2003; Annear et al., 2004; Arthington et al., 2006; Poff et al., 2010), they lightly address the influence of channel change on the success of instream flows. They stress the need for adaptive management, which recognizes the potential for channel change, but provide little to no guidance for how to incorporate channel change into an instream flow prescription. This is not to say that methods for detecting and predicting channel change do not exist, only that the two sciences have not been fully integrated. Future instream flow research should work towards incorporating elements of channel change and developing methods and tools in order to better predict the direction and magnitude of instream habitat changes and how that will affect the effectiveness of instream flows.

References

Annear, T., Chisholm, I., Beecher, H., Locke, A., Aarrestad, P., Burkhart, N., Coomer, C., Estes, C., Hunt, J., Jacobson, R. and Jobsis, G., 2004. *Instream flows for riverine resource stewardship*. Revised edition. Instream Flow Council, Cheyenne, Wyoming.

Arthington, A. H., Bunn, S. E., Poff, N. L., & Naiman, R. J. (2006). The challenge of providing environmental flow rules to sustain river ecosystems. *Ecological applications*, *16*(4), 1311-1318.

Call, B. C., Belmont, P., Schmidt, J. C., & Wilcock, P. R. (2017). Changes in floodplain inundation under nonstationary hydrology for an adjustable, alluvial river channel. *Water Resources Research*, *53*(5), 3811-3834.

Dietrich, W. E., Kirchner, J. W., Ikeda, H., & Iseya, F. (1989). Sediment supply and the development of the coarse surface layer in gravel-bedded rivers. *Nature*, *340*(6230), 215.

James, L. A. (1991). Incision and morphologic evolution of an alluvial channel recovering from hydraulic mining sediment. *Geological Society of America Bulletin*, *103*(6), 723-736.

Jones, Jabari C., "Historical Channel Change Caused by a Century of Flow Alteration on Sixth Water Creek and Diamond Fork River, UT" (2018). *All Graduate Theses and Dissertations*. 7353. https://digitalcommons.usu.edu/etd/7353

Kondolf, G. M., Piégay, H., & Landon, N. (2002). Channel response to increased and decreased bedload supply from land use change: contrasts between two catchments. *Geomorphology*, *45*(1-2), 35-51.

Lauer, J. W., Echterling, C., Lenhart, C., Belmont, P., & Rausch, R. (2017). Air-photo based change in channel width in the Minnesota River basin: Modes of adjustment and implications for sediment budget. *Geomorphology*, *297*, 170-184.

Leopold, L. B., & Maddock, T. (1953). *The hydraulic geometry of stream channels and some physiographic implications* (Vol. 252). US Government Printing Office.

Liébault, F., & Piégay, H. (2002). Causes of 20th century channel narrowing in mountain and piedmont rivers of southeastern France. *Earth Surface Processes and Landforms: The Journal of the British Geomorphological Research Group*, *27*(4), 425-444.

Lisle, T. E., Iseya, F., & Ikeda, H. (1993). Response of a channel with alternate bars to a decrease in supply of mixed-size bed load: A flume experiment. *Water Resources Research*, *29*(11), 3623-3629.

Poff, N. L., Richter, B. D., Arthington, A. H., Bunn, S. E., Naiman, R. J., Kendy, E., ... & Henriksen, J. (2010). The ecological limits of hydrologic alteration (ELOHA): a new framework for developing regional environmental flow standards. *Freshwater Biology*, *55*(1), 147-170.

Schmidt, J. C., & Wilcock, P. R. (2008). Metrics for assessing the downstream effects of dams. *Water Resources Research*, *44*(4).

Schumm, S. A. (1985). Patterns of alluvial rivers. *Annual Review of Earth and Planetary Sciences*, *13*(1), 5-27.

Surian, N., Rinaldi, M., Pellegrini, L., Audisio, C., Maraga, F., Teruggi, L., ... & Ziliani, L. (2009). Channel adjustments in northern and central Italy over the last 200 years. *Management and restoration of fluvial systems with broad historical changes and human impacts: geological society of America Special Paper*, *451*, 83-95.

Tharme, R. E. (2003). A global perspective on environmental flow assessment: emerging trends in the development and application of environmental flow methodologies for rivers. *River research and applications*, *19*(5-6), 397-441.

Van Steeter, M. M., & Pitlick, J. (1998). Geomorphology and endangered fish habitats of the upper Colorado River: 1. Historic changes in streamflow, sediment load, and channel morphology. *Water Resources Research*, *34*(2), 287-302.

Wilcock P., Atwood T., Belmont P., Epperly J., Gaeta J., Hammill E., Jones J. & Stout J. (2019). *Comprehensive study and recommendations for instream flow and requirements on Sixth Water Creek and Diamond Fork River: second interim report.* Department of Watershed Sciences, Utah State University.

APPENDICES

APPENDIX 1

SUPPORTING FIGURES FOR CHAPTER 2

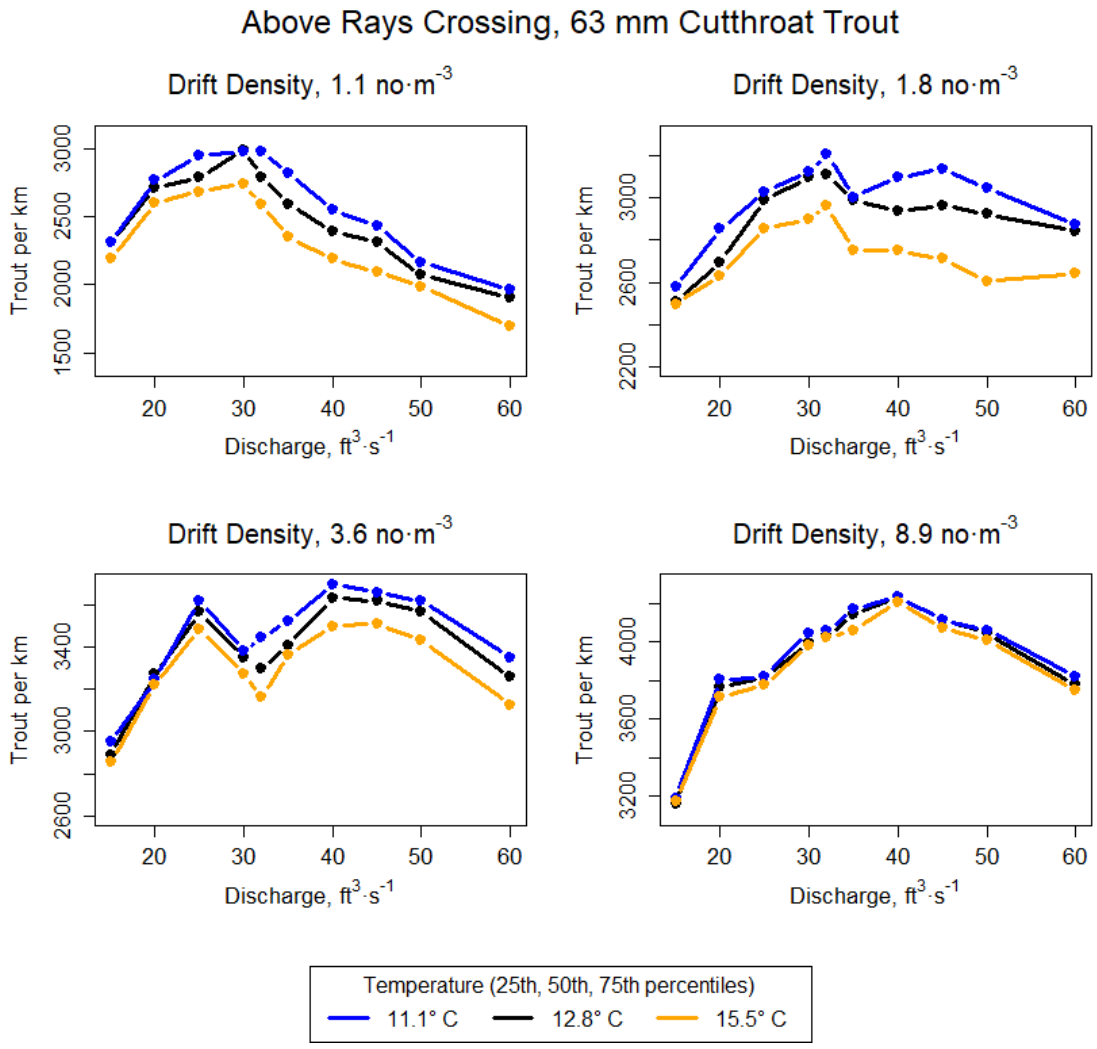

Figure A.1.1. Net rate of energy intake (NREI) model results for 63 mm Bonneville cutthroat trout capacity in Sixth Water Creek given August 2016 (1.8 no/m3), August 2017 (1.1 no/m3), 2x August 2016 (3.6 no/m3), and 5x August 2016 (8.9 no/m3), given the 25th, 50th, and 75th percentile temperatures from August and September 2016.

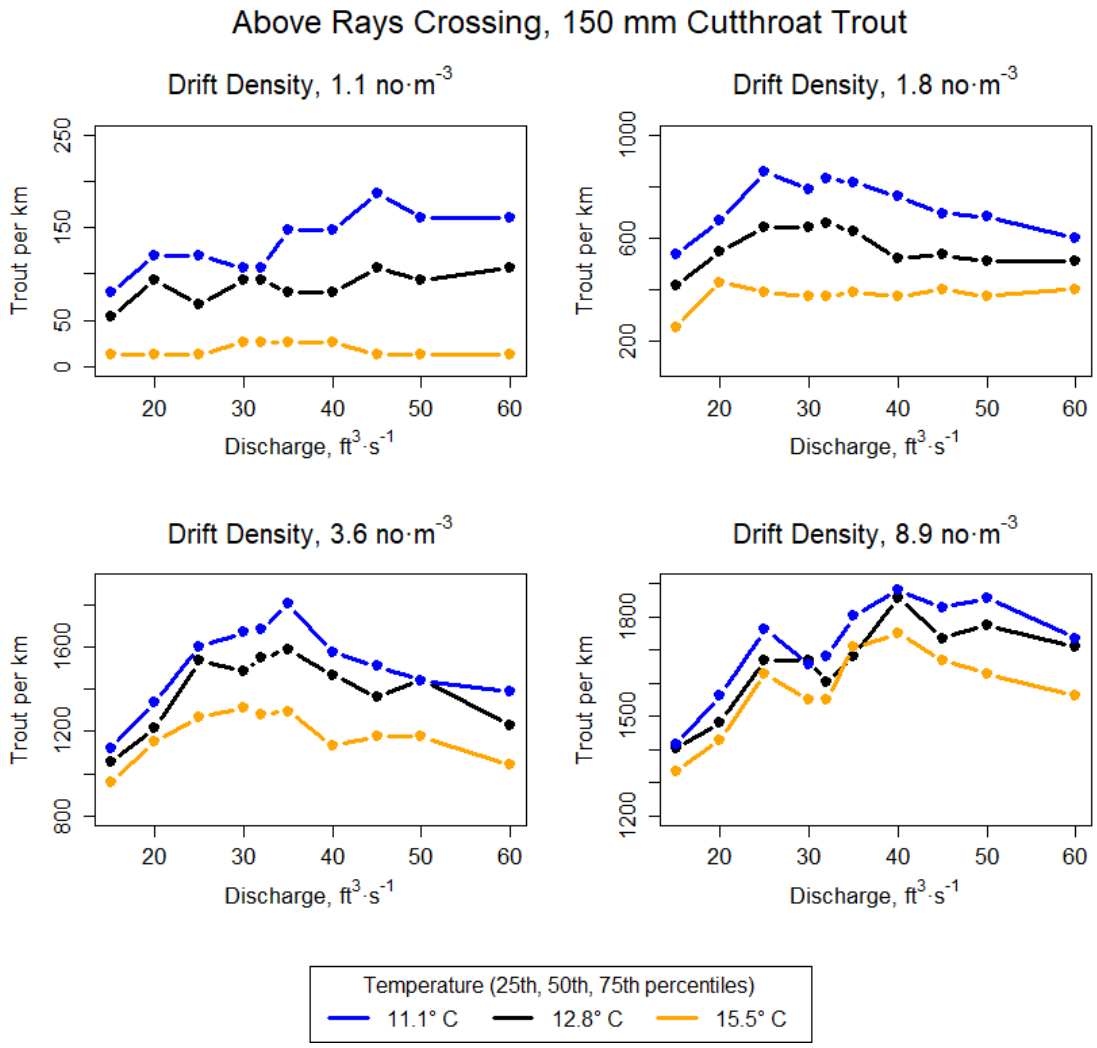

Figure A.1.2. Net rate of energy intake (NREI) model results for 150 mm Bonneville cutthroat trout capacity in Sixth Water Creek given August 2016 (1.8 no/m3), August 2017 (1.1 no/m3), 2x August 2016 (3.6 no/m3), and 5x August 2016 (8.9 no/m3), given the 25th, 50th, and 75th percentile temperatures from August and September 2016.

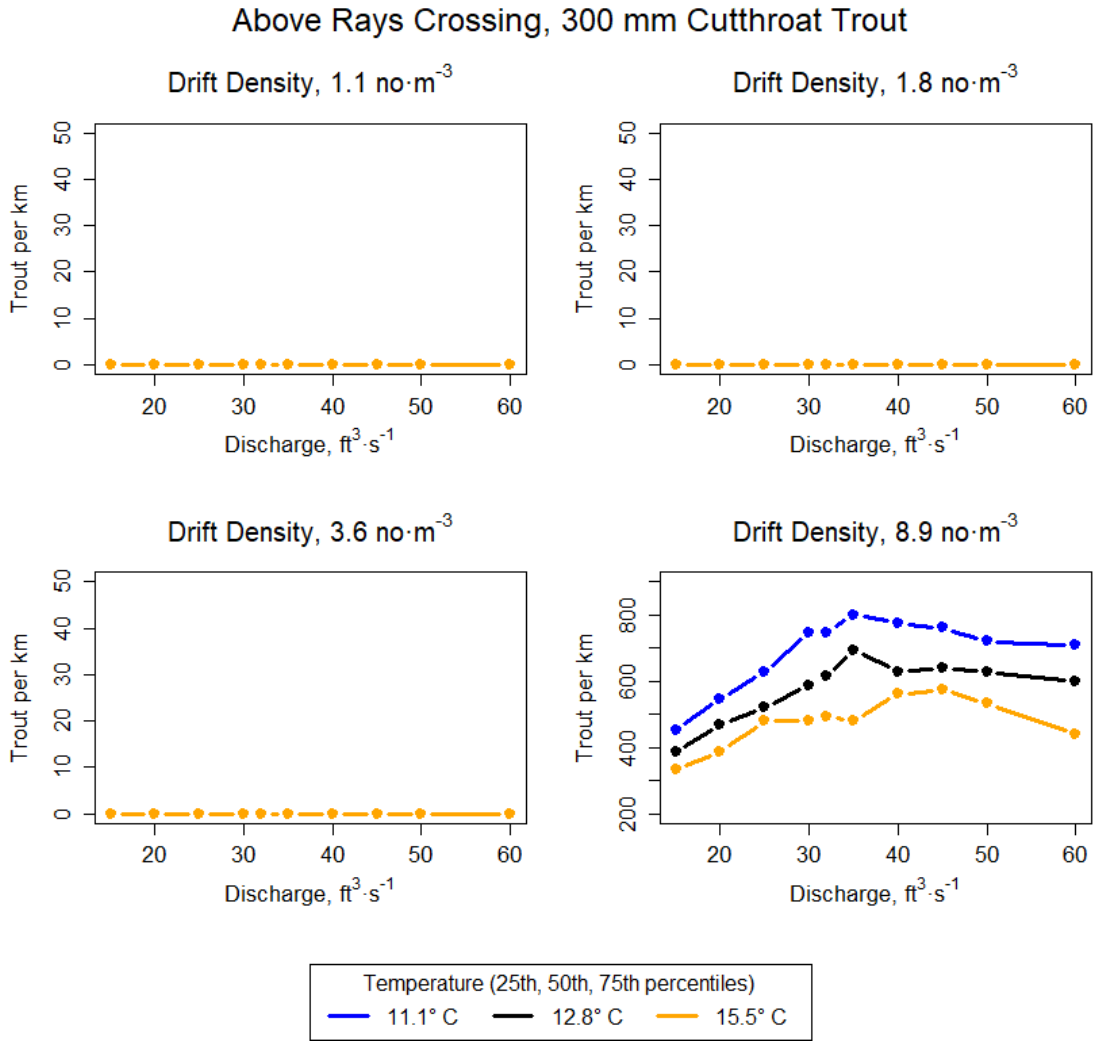

Figure A.1.3. Net rate of energy intake (NREI) model results for 300 mm Bonneville cutthroat trout capacity in Sixth Water Creek given August 2016 (1.8 no/m3), August 2017 (1.1 no/m3), 2x August 2016 (3.6 no/m3), and 5x August 2016 (8.9 no/m3), given the 25th, 50th, and 75th percentile temperatures from August and September 2016.

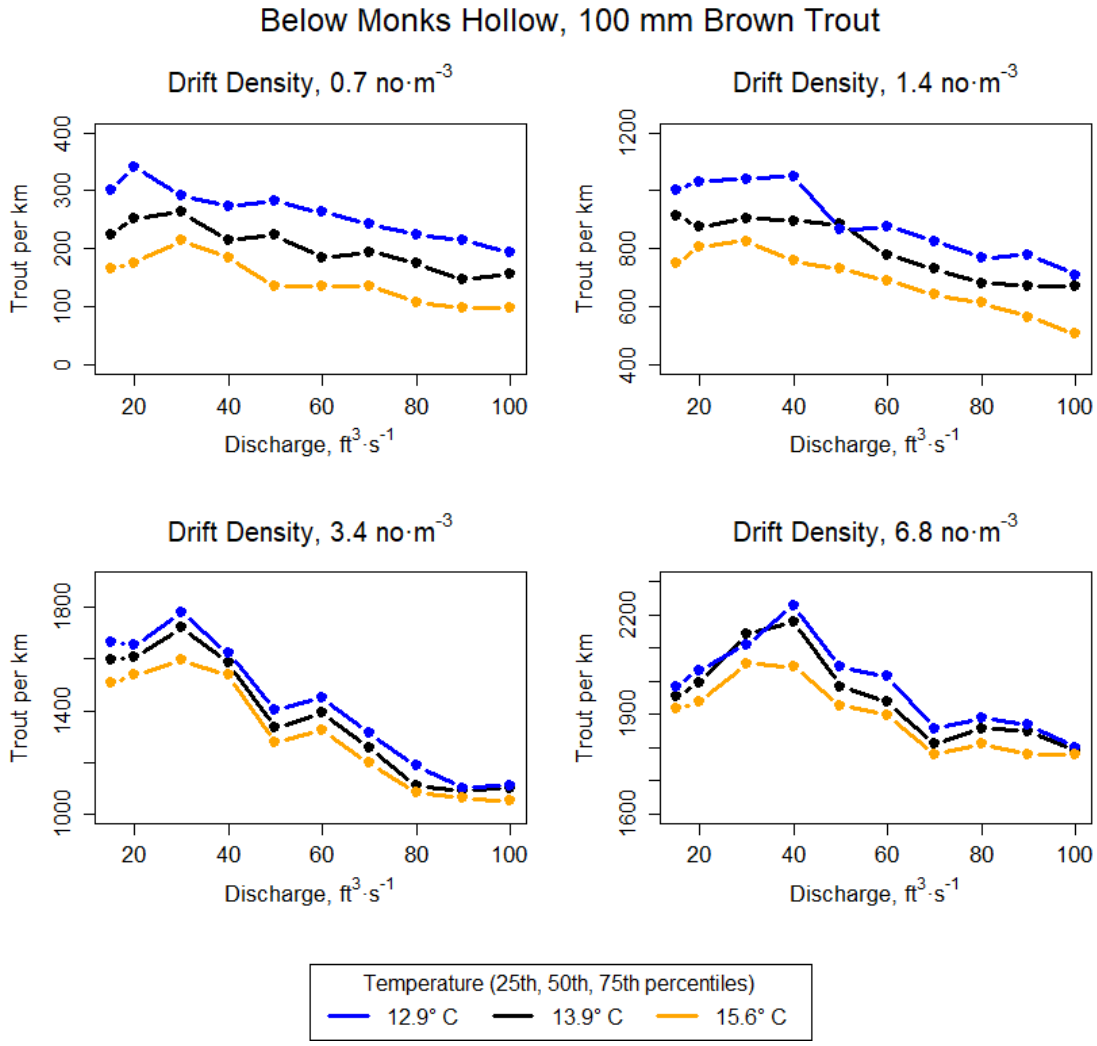

Figure A.1.4. Net rate of energy intake model results of 100 mm brown trout capacity in Diamond Fork Creek given August 2016 (0.7 no/m3), 2x August 2016 (1.4 no/m3), 5x August 2016 (3.4 no/m3), and 10x August 2016 (6.8 no/m3), given 25th, 50th, and 75th percentile temperatures from August and September 2016 and 2017.

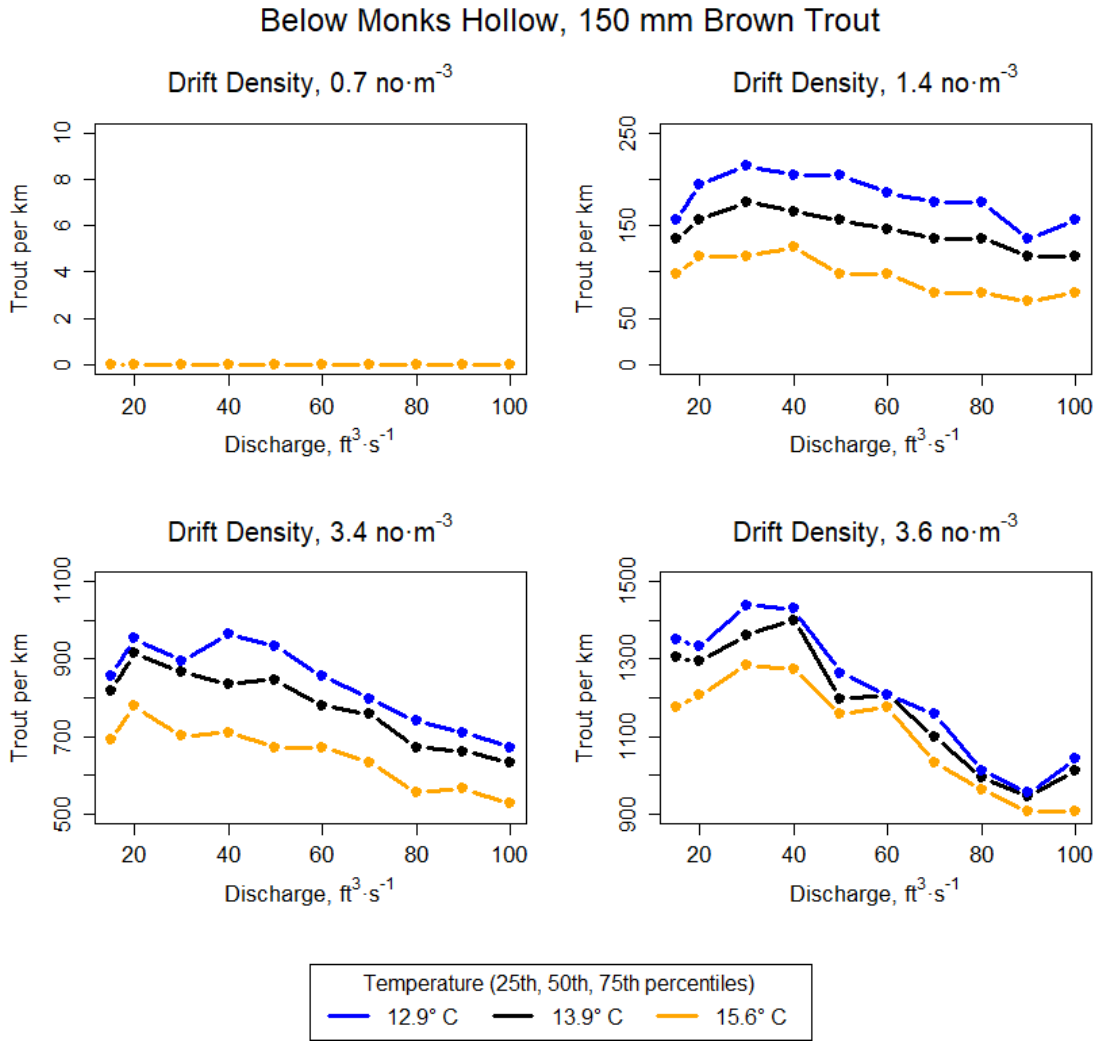

Figure A.1.5 Net rate of energy intake model results of 150 mm brown trout capacity in Diamond Fork Creek given August 2016 (0.7 no/m3), 2x August 2016 (1.4 no/m3), 5x August 2016 (3.4 no/m3), and 10x August 2016 (6.8 no/m3), given 25th, 50th, and 75th percentile temperatures from August and September 2016 and 2017.

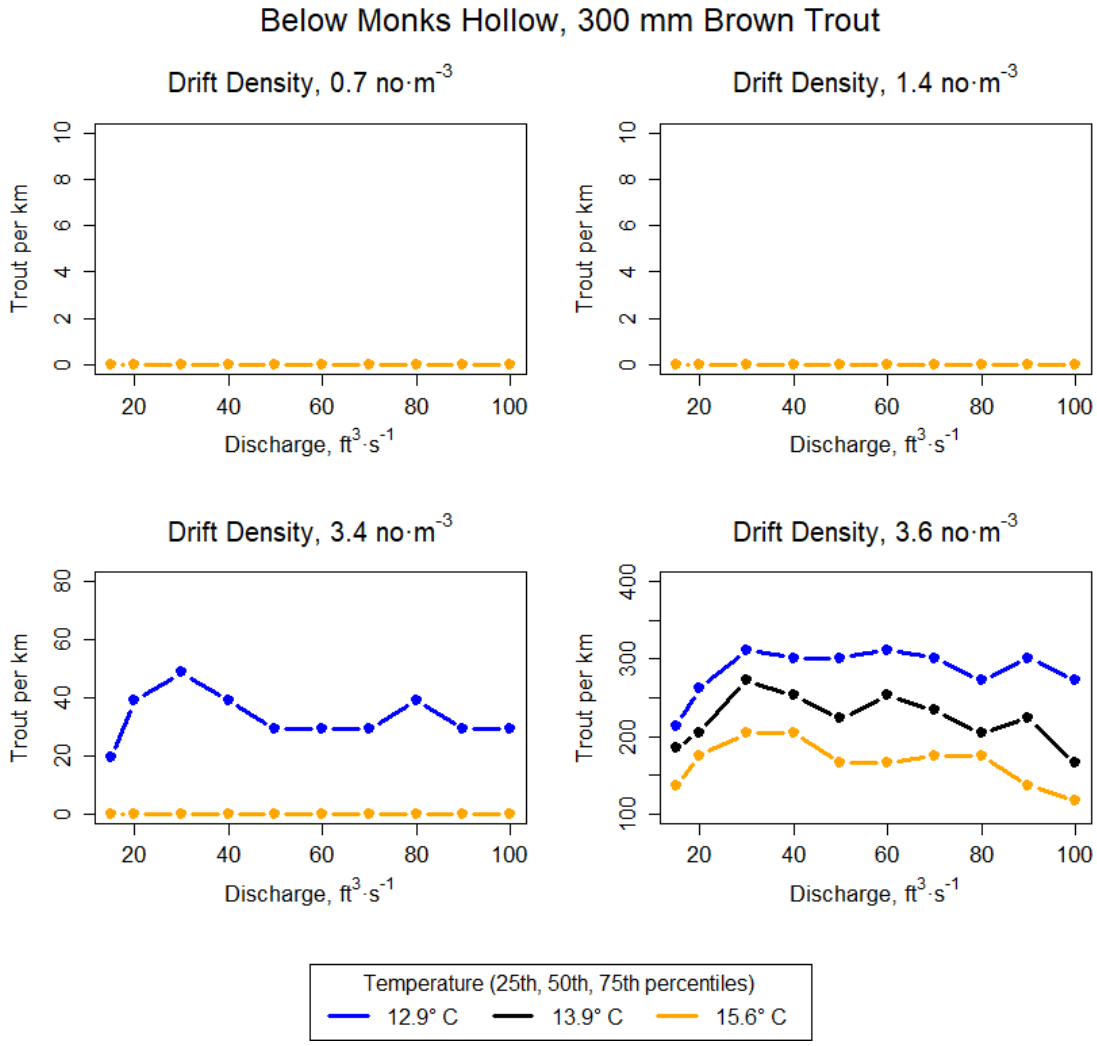

Figure A.1.6. Net rate of energy intake model results of 300 mm brown trout capacity in Diamond Fork Creek given August 2016 (0.7 no/m3), 2x August 2016 (1.4 no/m3), 5x August 2016 (3.4 no/m3), and 10x August 2016 (6.8 no/m3), given 25th, 50th, and 75th percentile temperatures from August and September 2016 and 2017.

APPENDIX 2

HYDROGRAPHS FOR INDIVIDUAL SITES ON THE DIAMOND FORK RIVER AND SIXTH WATER CREEK

A.2.1 Introduction

To improve the linkages between flow and sediment, fish, and macroinvertebrates, hydrographs were estimated for each of the 15 sampling sites throughout the Diamond Fork system (9 fish/macroinvertebrate sites, 8 sediment transport sites, 4 of which overlap). Discharge is measured at two U.S. Geological Survey (USGS) gage stations, Sixth Water Creek above Syar Tunnel (Station ID: 1014900) and Diamond Fork River Above Red Hollow (Station ID: 10149400). Known releases are recorded for Strawberry Tunnel, Syar Tunnel Outlet, and the Monks Hollow flow release structure. A stage height is recorded by the Strawberry Water Users Association (SWUA) gage located just upstream of Childs Bridge. Using the known discharges and flow releases, along with the construction of a rating curve for the SWUA gage, hydrographs are estimated using linear interpolation for the individual sites as a function of drainage area. Natural hydrographs for the USGS gaging stations were computed to by performing a mass balance and manually estimating discharge for dates where the mass balance became negative or overly unrealistic. These estimated natural hydrographs were used to estimate discharge for the non-augmented portion of the Diamond Fork River (above the 3 Forks area), and to estimate natural accretion between the Diamond Fork USGS gage and the SWUA gage in order to estimate discharge for dates prior to the beginning of the SWUA rating curve, 8/17/2016. Estimated discharge for all sites occur from 4/15/2004 to 11/30/2017.

A.2.2 Methods and Results

Flow release data for Strawberry Tunnel, Syar Tunnel Outlet, and the Monks Hollow flow release structure was obtained from the Central Utah Water Conservancy District and from the Utah Reclamation and Mitigation Commission. Data was reported as acre-feet per day from 1/1/2004 to 11/30/2017, and converted to a mean daily discharge in cubic feet per second (cfs). Discharge for Sixth Water Creek and the Diamond Fork River was retrieved from the USGS National Water Information System (NWIS) for the same time frame as mean daily discharge in cfs. The Sixth Water USGS gage was not in operation from 1/1/2004 till 4/15/2004, therefore all estimated discharges were made for dates when all flows and releases were known, constraining the estimation period from 4/15/2004 to 11/30/2017. Throughout these dates, a few of the Sixth Water USGS gage record was missing values. These values were estimated manually to based off of known post and prior mean daily discharge values.

Discharge was estimated as a function of drainage area. Using ArcGIS 10.3.1, the contributing drainage area for each site, gage station, and flow release location was derived using a 10 meter DEM from the National Elevation Dataset. Discharge for sites that were in close proximity to each other such as ARC and RCB were estimated using the same drainage area, assuming the relatively small change in drainage area between the two would have negligible effects.

A.2.2.1 Estimating Natural Hydrographs

Estimating the natural discharge for the system is crucial for some of the sites. Natural flow at Strawberry Tunnel is assumed to be 0, therefore any flow at that site is outflow from the tunnel. The increase of discharge between Strawberry Tunnel and the

Table A.2.1. All sites for which a synthetic hydrograph was created, including known flow release and measured discharge locations.

Site	**Code**	**Drainage Area, km^2**	**Type**	**Estimation Method**
Strawberry Tunnel	-	2	Flow Release	Known Release
Upper Sixth Water	USW	24	Sample Site	Interpolation by Drainage Area
Landslide	LS	26	Sample Site	Interpolation by Drainage Area
Rays Crossing	RCB, ARC	28	Sample Site	Interpolation by Drainage Area
Sixth Water above ST (USGS)	SW_{USGS}	40	Gage Station	Known Discharge
Syar Tunnel	-	40	Flow Release	Known Release
Below Syar Tunnel	BST	40	Sample Site	Interpolation by Drainage Area
Sixth Water 3 Forks	S3F	101	Sample Site	Interpolation by Drainage Area
Monks Hollow Flow Release Structure	-	251	Flow Release	Known Release
Diamond Fork above RH (USGS)	DF_{USGS}	251	Gage Station	Known Discharge
Below Monks Hollow	BMH	251	Sample Site	Same as DF_{USGS}
Monks Hollow Bridge	MHB	275	Sample Site	Interpolation by Drainage Area
Diamond Campground	DCG	339	Sample Site	Interpolation by Drainage Area
Brimhall Bridge	BB	361	Sample Site	Interpolation by Drainage Area
Motherload	MO	386	Sample Site	Interpolation by Drainage Area
Childs Bridge	CB	402	Sample Site	SWUA Rating Curve
Guard Station	GS	57	Sample Site	Extrapolation by Drainage Area
Diamond Fork 3 Forks	D3F	93	Sample Site	Relation with Natural DF flow

Sixth Water USGS gage therefore is due to natural accretion. The same principle applies for the Diamond Fork USGS gage and the three flow release locations. To calculate the natural hydrograph at these two gages was derived by performing a mass balance of the system where:

$$SWnatural = SW_{USGS} - \text{Strawberry Tunnel Releases.} \quad \text{(A.2.1)}$$

and

$$DFnatural = DF_{USGS} - \text{Strawberry Tunnel Releases} - \text{Syar Tunnel Releases} - \text{Monks Hollow Releases.} \quad \text{(A.2.2)}$$

There were dates throughout the period of record when the mass balance became negative, or did not appear to be feasible (i.e. unreasonably low values or sudden spikes). Sudden changes in flow releases often caused the mass balance to spike or become negative. Erroneous values were manually fixed by evaluating pre and post conditions and interpolating between stable values.

A.2.2.2 Estimating Discharge at Childs Bridge

The Diamond Fork USGS gage provides the last known discharge on the river until the next USGS gage located on the Spanish Fork River, several miles downstream of the confluence with the Diamond Fork. Luckily, there is an operating gage owned by SWUA located approximately 50 meters upstream of Childs Bridge. The SWUA gage, although functioning, does not have a rating curve associated with it and therefore only reports gage height (measurements assumed to be taken every 10 or 15 minutes). The data acquired however was reported as a mean daily gage height which could be translated into a mean daily discharge. Using the discharge measurements made while

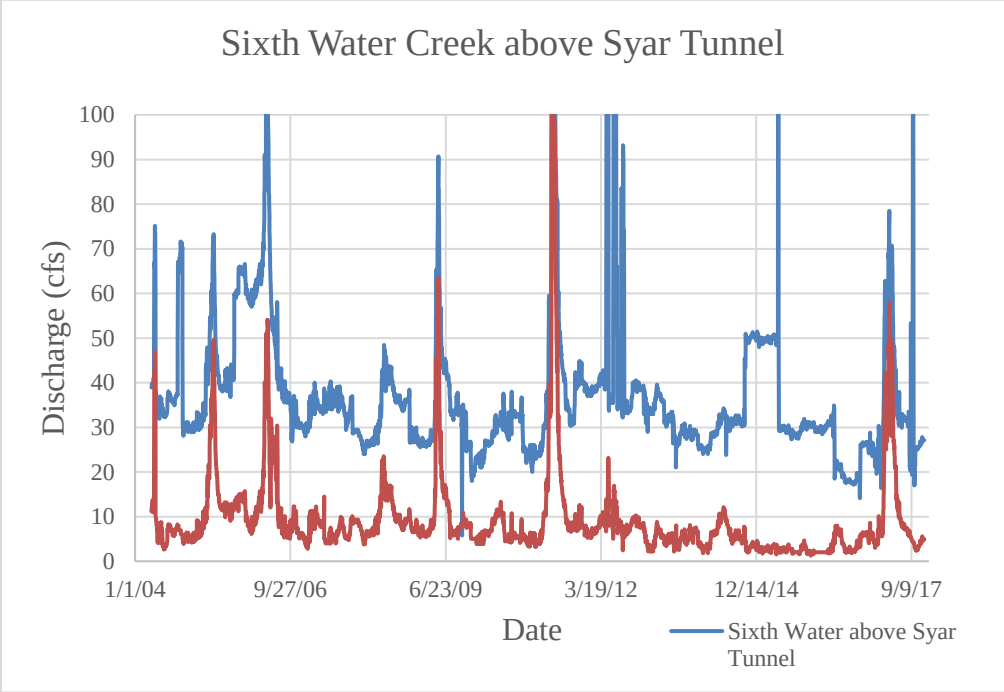

Figure A.2.1. Measured and estimated natural discharge at Sixth Water Creek above Syar Tunnel USGS gage (Station ID: 10149000).

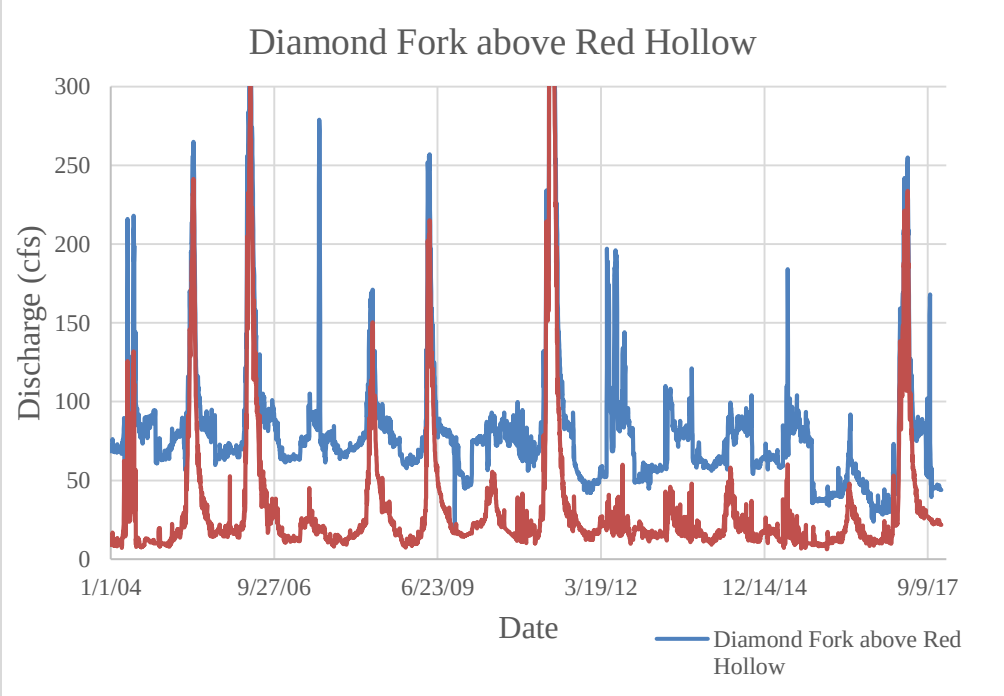

Figure A.2.2. Measured and estimated natural discharge at the Diamond Fork above Red Hollow USGS gage (Station ID: 10149400).

measuring sediment transport, a rating curve was developed for the time period between 8/17/2016 to 11/30/2017. A total of 14 discharge measurements were made ranging from 24.6 cfs to 313.9 cfs. Two measurements of 167.4 cfs and 162.8 cfs were excluded from the rating curve since they had gage heights much larger than gage heights associated with measurements made above 170 cfs. This made the rating curve more agreeable with larger discharge values and resulted in an R^2 value of 0.982. The rating curve developed for the SWUA gage is

$$Q_{SWUA} = 164.17*h^{1.5647} \quad \text{(A.2.3)}$$

where Q_{SWUA} is the estimated discharge and h is the recorded mean daily gage height. Creating the rating curve with gage height recordings made at the same time of the discharge measurements would increase the accuracy of the rating curve, but for our purposes and with the available data, the rating curve is satisfactory. This rating curve is most applicable from the dates of 8/17/2016 to 11/30/2017 and for discharges ranging from 12.3 cfs to 627.8 cfs (one half the smallest measured discharge and twice the largest measured discharge).

Using the rating curve, a hydrograph for the specified time period was created. Gage height adjustments were applied for necessary dates to improve accuracy and to account for times of scour and fill. Along with applying gage height corrections, a rule was applied that discharge cannot go below that of what is measured at the DF USGS gage.

To estimate the discharge record for dates prior to 8/17/2016, a relation between the natural flow accretion from the Diamond Fork USGS gage to Childs Bridge and the

natural flow at the DF USGS gage was made. Natural accretion of flow was computed by subtracting the DF USGS discharge from the SWUA discharge. Then the natural accretion of the flow could be added to the measured flow at the DF USGS gage. To increase accuracy with the rating curve, a multiplication factor of 1.05 was applied to estimated discharge for the SWUA gage. The multiplication factor was found by iteration until the slope of the estimated discharge and the rating curve estimates was equal to 1.0 (which also resulted in a R^2 value of 0.95). The equation for estimating discharge at the SWUA gage under conditions where the rating curve does not apply is therefore

$$Q_{SWUA} = 1.05*(Q_{DF\_USGS} + (0.4066*Q_{DFnatural} - 4.8556)) \quad (A.2.4)$$

where Q_{SWUA} is the estimated discharge for SWUA, Q_{DF_USGS} is the measured discharge at the DF USGS gage, and $Q_{DFnatural}$ is the estimated natural discharge at the DF USGS gage. This relation was applied from the dates of 4/15/2004 to 8/16/2016. This relation most likely overestimates discharge for some parts of the year, particularly during spring runoff when the change between the USGS gage and the SWUA gage is at times not that much. A more complicated hydrologic model would be needed to increase estimated discharge accuracy. However, using the equations 3 and 4 for the appropriate dates, an entire mean daily discharge record from 4/15/2004 to 11/30/2017 was constructed for the SWUA gage location.

A.2.2.3 Interpolating Discharge as a Function of Drainage Area

Discharge for the sites in between Strawberry Tunnel and the Sixth Water USGS gage station were estimated by linear interpolation, with flow being the dependent variable and drainage area being the independent variable. This was done using the

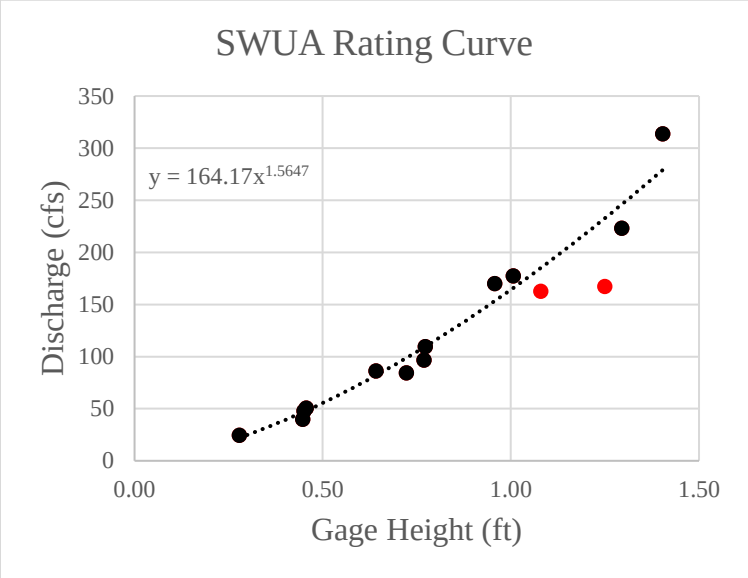

Figure A.2.3. SWUA rating curve used in estimating discharge for the Lower Diamond Fork sampling sites. Red points were excluded from the rating relation.

FORECAST() function in Microsoft Excel which uses linear regression to interpolate data. The same process for sites between the Sixth Water USGS gage and the Diamond Fork USGS gage was performed, except in this case, interpolation was performed between the measured discharge at the Sixth Water USGS gage plus the flow releases coming from the Syar Tunnel outlet, and the measured discharge at the Diamond Fork USGS gage minus the flow releases coming from the Monks Hollow Flow Release Structure. Discharge for sites between the DF USGS gage and the SWUA gage were also interpolated by drainage area. Methods for estimating discharge for the Diamond Fork 3 Forks and Guards Station sites are discussed below.

A.2.2.4 Estimating Discharge for Diamond Fork 3 Forks and Guard Station

To estimate the discharge at Diamond Fork 3 Forks, a relation was derived using measured discharge at Diamond Fork 3 Forks as the dependent variable (made during

sediment transport measurements, ranging from 4.5 cfs to 122.1 cfs) and the natural flow at the DF USGS gage as the independent variable. The relation was that

$$Q_{D3F} = 0.5099*Q_{DFnatural} -0.4856 \quad \text{(A.2.5)}$$

where Q_{D3F} is the discharge at Diamond Fork 3 Forks. To check the accuracy of this, a natural flow for Sixth Water 3 Forks was computed using linear interpolation based on drainage area. The two discharges were added to create a second estimated natural flow at the DF USGS gage. Only 20% of the time did the second estimated natural flow at the DF USGS gage exceed the first one by more than 10%. If the excess flow is divided equally between the three sites (Diamond Fork 3 Forks, Sixth Water 3 Forks, and the DF USGS gage), essentially meaning that each site is equally contributing to the error, then only 3% of the time does the second estimated natural flow exceed the first one by more than 10%. In both cases, the flow excess is only a few cfs in magnitude and only stands out during times of baseflow. Also, the problem only occurs in a few years, of which 2016 and 2017 are not minimally affected. Given the many complexities of estimating discharge and the simplicity of this method, equation 5 is a satisfactory for estimating mean daily discharge at the Diamond Fork 3 Forks site.

To estimate the discharge at Guard Station, the same FORECAST() function was used to extrapolate discharge as a function of drainage area using the estimated discharge at Diamond Fork 3 Forks, and the natural discharge at the DF USGS gage.